Deltares

Morphological models for IRM

Meuse 1D

Morphological models for IRM
Meuse 1D

Auteur(s)
Koen Berends
Roy Daggenvoorde
Kees Sloff

Morphological models for IRM
Meuse 1D

Client	Rijkswaterstaat Water, Verkeer en Leefomgeving
Contact	Dr. Ralph Schielen (ralph.schielen@rws.nl)
Reference	
Keywords	IRM, Meuse, Morphological modelling

Document control	
Version	1.2
Date	29-09-2020
Project nr.	11203684-015
Document ID	11203684-015-ZWS-0016
Pages	91
Status	definitief

Author(s)		
	Koen Berends	Kees Sloff
	Roy Daggenvoorde	

Doc. version	**Author**	**Reviewer**	**Approver**	**Publish**
1.2	Koen Berends	Jurjen de Jong	Gerard Blom	
		Anke Becker		

Summary

Within the context of Integraal Riviermanagement (IRM), Rijkswaterstaat (RWS) aims to create a one-dimensional morphodynamic model of the Meuse River between Eijsden and Keizersveer. This report describes the setup and calibration of this model. The purpose of the model is to simulate the long-term morphological development of the Meuse river bed both in response to human intervention and resulting from boundary forcing. The model is set up in the new D-HYDRO software suite (dflow1d).

Three models were built: representing the state of the river system in 1995 (j95), 2011 (j11) and 2019 (j19). All models were derived from the current 5th generation hydrodynamic SOBEK models but were simplified to allow for stable and fast morphological simulation. The conversion steps and choices are described in detail in this report.

The models were tested in two steps. First, the flow velocity, discharge distribution between main channel and floodplain, and water levels were compared with 2D model simulations. The 1D model main channel flow velocities compared favourably to 2D main channel flow velocities – which is most important for morphological simulation – using a uniform constant roughness value of 0.035 sm$^{-1/3}$. Water levels are generally overestimated by the 1D model compared to the 2D model.

Second, the morphological models are tested on annual sediment transport rates, bed level change over a period of 17 years, and celerity of bed disturbances. The ground truth data for these comparisons are based on a review of literature and available sounding data. Because the ground truth data was found to exhibit significant uncertainty, the morphological models were tested on their ability to simulate overall trends and correct orders of magnitude. We found that a combination of two sediment transport formulas (Meyer Peter Muller for coarse material; Engelund-Hansen for fine material) resulted in the best results. Both the annual sediment transport-load as well as the celerity of bed disturbances were found to be simulated within bounds suggested by literature. The overall trends in bed level change compare favourably with data.

Contents

1 Introduction

Within the context of Integraal Riviermanagement (IRM), Rijkswaterstaat (RWS) aims to create a one-dimensional morphodynamic model of the Meuse River between Eijsden and Keizersveer to assess the impact of human intervention as well as changes in external forcing (for example, water discharge, sediment load, or sea level rise) on the morphological development of the river bed. The immediate use of the model is for the PlanMER phase of the IRM program, where interventions are tested and evaluated for policy decisions regarding erosion and sedimentation of the river bed and discharge capacity of the river. The time scale of these developments is in the order of 30 years (until 2050), considering spatial scale in the order of several or tens of kilometres. The model is only meant for morphodynamics of the main channel of the Maas.

The model is developed in the D-HYDRO Suite. During the development of this model, D-HYDRO supported one-dimensional morphology as an ‘alpha-stage’ functionality. . This means that not all features are fully supported yet. The two major limitations encountered in this project were an unintended energy loss in curved bends and an incorrect effect of so-called storage areas. For both of these work-arounds have been found (see section 2.1.4) and recommendations are given for future improvements of the model following improvements to the software (section 5.2). Although the content of this report is written in English to provide access for both national and international researchers and stakeholders, we have used the Dutch names “Maas” (Meuse River), and sections “Grensmaas” (also named “Common Meuse” or “Gemeenschappelijk Maas”) and “Zandmaas”.

1.1 New models developed within this project

This report covers the construction and test results of the following models:

- dflow1d_dmor-maas-j19-v1
- dflow1d_dmor-maas-j11-v1
- dflow1d_dmor-maas-j95-v1

The naming convention is <software system>-<region>-<schematisation>-<version>:

- **dflow1d_dmor**: The models are constructed using the 1D component of D-HYDRO, with the D-MOR plugin enabled.
- **Maas**: The river system for which they are developed.
- **j19, j11, j95:** Each model is built using the geometry describing the state of the river system in the high-water season of a certain year. E.g. j19 refers to the high-water season 2019-2020.The exception is j95 which refers to the geometry during the high discharge in January/February 1995.
- **v1:** This is the first version of the models. Subsequent changes to the model will be given a new version number. Changes to the previous version will be documented separately.

1.2 Application disclaimer

Each of these models are developed for simulation of long-term morphological evolution of the channel bed, which includes the simulation of sediment transport, erosional and depositional trends with a length scale of more than a few kilometres. Accuracy of simulation results is strictly limited to the conditions and data-accuracy under which the model was tested, or can be reasonably expected, as described in this report.

The models are not developed for hydraulic applications (flow routing, water depths, water levels), detailed local morphological studies (scale in the order of hundred meters or less) or floodplain sedimentation. Please see section 1.3 for more information on related models.

1.3 Relation to other models

Below follows a list of related models which have been developed for Rijkswaterstaat, for a variety of purposes. The models developed within this project are grouped under '6th generation dflow1d_dmor'.

Table 1.1 Overview of the various models developed for Rijkswaterstaat (status mid 2020)

Model	Description
5th generation 2D (WAQUA)	Current hydraulic 2D models. These models will be replaced by the sixth generation within the *KPP Hydraulica Modelschematisaties* project
6th generation 2D (dflow2d_flow)	New hydraulic 2D models in D-HYDRO 2D. Under active development within *KPP Hydraulica Modelschematisaties*
6th generation 2D (dflow2d_dmor)	Adaptation of the hydraulic 2D models for small- to medium-scale morphological simulations. Development takes place within *KPP Rivierkunde*
5th generation 1D (SOBEK)	Current operational 1D hydraulic models. Maintenance and development within *KPP Hydraulica Modelschematisaties*
6th generation 1D (SOBEK)	Newly developed models based on 6th generation 2D models. Pilot project currently takes place for the Meuse within *KPP Hydraulica Modelschematisaties* and *KPP Hydraulica Software*
6th generation 1D (dflow1d_dmor)	Newly developed models based on 5th generation 1D models with D-HYDRO 1D. Development within *KPP BOA Rivieren*. Subject of this report

1.4 Project team

The project team of Deltares consisted of:

Name	Role
Dr. Aukje Spruyt	Project leader IRM model development
Dr. ir. Koen Berends	Project leader Meuse 1D
Ir. Roy Daggenvoorde (HKV Consultants)	Adviser
Drs. Carlijn Eijsberg - Bak	Adviser
Dr. ir. Kees Sloff	Expert adviser
Dr. Willem Ottevanger	Expert adviser
Ir. Jurjen de Jong	Reviewer
Dipl.-Ing. Anke Becker	Reviewer

The client was represented by dr. Ralph Schielen (Rijkswaterstaat WVL).

We are very grateful for the helpful assistance and advice of dr. Roy Frings and ir. Siebolt Folkertsma (Rijkswaterstaat Zuid-Nederland) as well as ir. Herm-Jan Barneveld (HKV Consultants, Wageningen University & Research).

1.5 Software

The new Maas morphology models are developed in the D-HYDRO 1D software system.

Previous 1D morphology models for the Maas were developed about 20 years ago (Sloff and Stolker, 2000, Berkhout, 2003) and used the SOBEK-RE (River-Estuary) modelling system. SOBEK-RE is not to be confused with the similarly named SOBEK-RUR software systems, which have been further developed for hydrodynamic simulations over the past decades ultimately resulting in SOBEK-3. A key difference between SOBEK-RE and SOBEK-RUR (and by extension SOBEK-3 and D-HYDRO 1D) is that the numerical scheme of SOBEK-RE allowed for a faster and more accurate morphological module. While SOBEK-3 does not have the advanced morphological module of SOBEK-RE, SOBEK-RE lacks in almost every other aspect compared to the modern software modules of SOBEK-3, Delft3D-4 and D-HYDRO 1D and 2D.

At present (2020), all 1D, 2D and 3D modelling tools at Deltares are migrated to a single software system D-HYDRO, which will contain identical solvers and GUI for the 1D as well as for the 2D/3D software. All operational models of Rijkswaterstaat will operate in D-HYDRO software in the future. The morphology module of this 1D modelling system (dflow1d) is identical to that of Delft3D-4 and dflow2d, with a much more extensive functionality than SOBEK-RE. However, during this project the support for the morphology module was in 'alpha status', and much development has been done concurrently.

In Appendix G1, an overview is given of the various models that are developed concurrently with the models described in this report. In Appendix G2, an overview is given of the various software development issues that were worked on concurrently with this project. Table 1.2 provides an overview of all software versions used in this project.

Table 1.2 Overview of software versions used

Name	Version
D-HYDRO 1D (Dflow 1d)	Dflowfm 1.2.100.66357M, DIMR_EXE Version 2.00.00.66357M
SIMONA	2017
SOBEK	Multiple versions, detailed in report
'convert_to_dflowfm' script (script to convert SOBEK flow models to dflow1d flow models)	1.22

1.6 Data sources considered in this project

The following sources of data have been used during the project:

- Hydraulic data:
  - Time series of discharges (10 minutes interval) at Borgharen Dorp, period 1996-2019, obtained from Rijkswaterstaat (waterinfo website).
  - Flow velocities and water levels derived from WAQUA simulations (see section 2.2).
- Topographic data:
  - Bed topography schematisations are converted directly from the SOBEK schematisations (5th generation, SOBEK-3) that have been transferred from Baseline and WAQUA, using WAQ2PROF. Years 1995, 2011 and 2019.
  - Bed-levels, average for main channel, per kilometre, for period 1889-2017, owned by RWS-ZN, in Excel <Maasbodem 1889-2017_v2.xlsx>, and referred to in this document as Kragten (2018).
  - Information on morphological developments.

- Bed composition data:
  - Grain-size distribution for the Grensmaas obtained from the studies of Berkhout (2003) and de Jong (2005) and previously implemented in older versions of the SOBEK-RE model for the Grensmaas.
  - Grain-size distribution for the Zandmaas obtained from the SOBEK-RE model of Sloff and Stolker (2000), which is based on measurements (‘trilflips’ to max. 5 m depth, and ‘Akkerman/Steek/pulsboringen’ to max. 7 m deep, at intervals of 400 m, and seismic profiles along 5 longitudinal profiles) in the period of 1996 to 1999.
  - Analyses of bed material samples of, amongst others, Duizendstra (1999) and Murillo-Muñoz (1996).
- Sediment transport:
  - Estimated annual sediment loads derived from studies based on field measurements and data processing (dune-tracking), reported by Gerretsen (1968), Duizendstra (1999), Wilbers (1996).

2 Methodology

2.1 Model setup

2.1.1 Reference models & general approach

The following 5th generation hydraulic models (see also Table 1.1) form the basis of the morphological 1D models:

- Sobek-maas-j19_5-v2
- Sobek-maas-j11_5-v3
- Sobek-maas-j95_5-v2

These models were made available by Rijkswaterstaat through Helpdesk Water for the purpose of this project. The general approach of model construction and testing of the IRM 1D models is shown in Figure 2.1. The various steps are described in the following paragraphs.

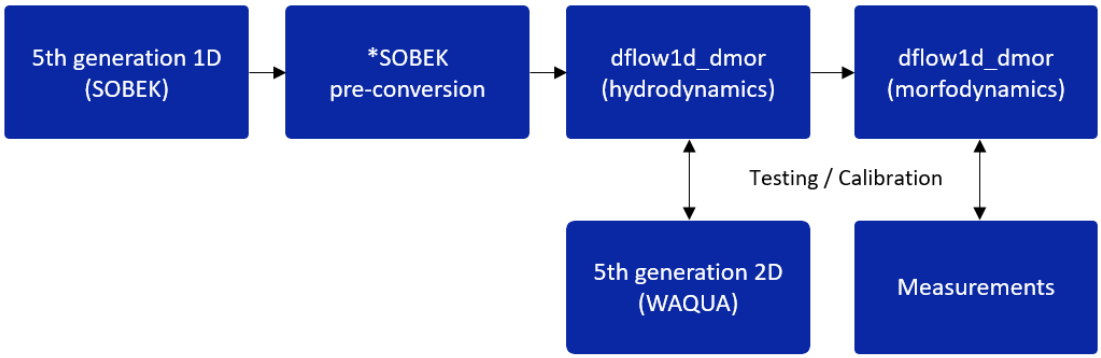

Figure 2.1 Overview of the general approach of model development

2.1.2 Conversion from official SOBEK versions to pre-conversion models

Various changes to the official SOBEK versions are required before conversion from SOBEK to dflow1d can be carried out. These changes include:

- Conversion to SOBEK version 3.19.39355.
- Removal of features that are not supported in dflow1d, such as river weirs, extra resistances and laterals with a Q(h) condition[1].

Some other changes were carried out to align and simplify three models. These were found to be necessary to be able to produce a stable morphological simulation. The major changes are:

- Using a simplified & unified real-time control (RTC) model for weir operation for all three models.
- Removal of regional systems (Dieze, Drongelens Kanaal).
- Removal of all side and backwater channels (Roer, Lateraalkanaal, Julianakanaal, Oude Maas, Afgedamde Maas).
- Removal of all retention areas.

[1] Discharge-stage (Q(h)) laterals were used to simulate shortened travel paths by flow crossing over floodplains ('shortcuts'). This solution improves flow routing but is not beneficial for morphological simulation.

The removal of retention areas reduces the storage in the river system during flood peaks, thereby leading to a small increase of peak flow, which may lead to an overestimation of sediment transport during extreme flood events. However, as the long-term morphological development is less dependent on the dynamics of these rare events, and more on general trends in discharge (e.g. a wet year versus a dry year), we believe the impact on model results is minor. The removal of the regional systems is compensated by the addition of two new laterals: Dieze and Drongelens Kanaal. The side and backwater systems do not contribute significantly to the flow through the system. As most sediment transport occurs after weir operation has ceased, the simplification of the RTC is not expected to affect model output significantly.

For the sake of clarity, we refer to this adapted 5th generation SOBEK model as the 'pre-conversion model'. A full list of changes can be found in the Appendix A.

2.1.3 Conversion from pre-conversion SOBEK to dflow1d

SOBEK-3 and dflow1d are two different modelling systems with different numerical solvers and different input format files. Figure 2.2 specifies how this conversion takes place.

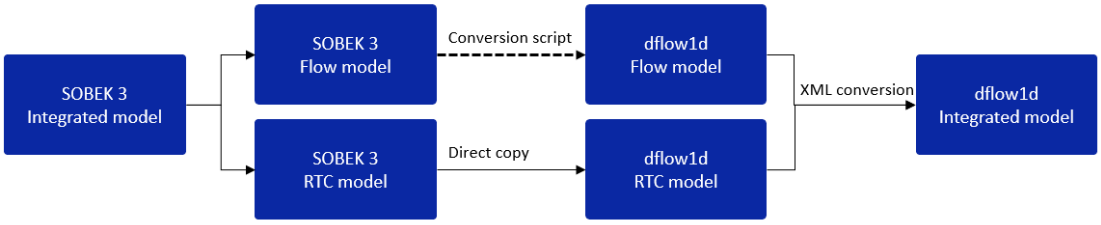

Figure 2.2 Overview of the conversion steps from SOBEK-3 to dflow1d

Both the SOBEK-3 and dflow1d models are *integrated models*, which means that what we commonly refer to as 'the model' (as specified in section 1.1) is a combined product of multiple (sub-)models. The user may be unaware of this distinction, as the models generally communicate during runtime without user interference. However, the distinction is important for the conversion, as each sub-model requires a different approach.

The flow model contains all cross-sections, geometry, structures and so on, for hydraulic and morphodynamical computations. The flow model is converted using the *convert_to_dflowfm* conversion script, version 1.22[2], followed by a manual check[3].

In the 5th generation 1D models, an RTC model governs the operation of the various weirs, locks and retention areas. As both SOBEK-3 and D-HYDRO use RTC TOOLS as the computational back-end, the RTC models can be directly copied without any change necessary.

The integration of the RTC and flow model is achieved using a single XML file, which governs the communication between the flow and RTC models during runtime. As some naming conventions have changed, the XML is based on the 5th generation XML file but requires manual changes. At this point, no generalized conversion script is available.

---

[2] This software can be found on Open Earth:
https://svn.oss.deltares.nl/repos/openearthtools/trunk/python/applications/delft3dfm/convert_to_dflowfm

[3] Most manual changes required after running the conversion script were included in the conversion script during and resulting from this project. A final check, which is recommended to all users, is the sign of the discharge at the downstream boundary condition. In SOBEK, the sign is related to the direction of the branch. In dflow1d, the sign is related to whether the water is flowing into or out of the system. An incorrect sign may lead to unwanted behavior in simulation but will likely not make the model crash.

2.1.4 Enabling morphology

Morphological simulation puts different requirements on the numerical model than a purely hydraulic simulation. Some specific model choices – such as shortcuts, local resistances and sudden changes in calibrated roughness – can improve the accuracy of simulated water levels but have adverse effect on morphological accuracy. These changes are listed here.

Apart from the changes in the category detailed above, some extra steps were taken to specifically to improve morphological simulation. These are listed below.

- **Model straightening**. The current version of dflow1d does not have a dedicated 1D solver. Instead, the same solver is used both for 2D as 1D. The benefits of this approach will not be discussed here in detail, but a disadvantageous side effect is that it results in energy loss in curved bends. This is not desired behaviour for 1D morphological models, as it could lead to non-physical sedimentation in bends. Therefore, we manually straighten the domain – meaning that all branches are now perfectly straight while keeping the same length. A custom coordinate system is used. It is expected that this step will not be necessary in future versions of dflow1d.
- **Uniform roughness field**. The roughness field of the main channel of the 5th generation 1D model varies spatially as well as with discharge, resulting from a calibration on water levels. Because roughness directly affects sediment transport through modifying the bed shear stresses, non-physical (calibrated) roughness fields are undesirable. Therefore, we imposed a spatially uniform field, i.e. one single (Manning *n*) roughness coefficient for the entire model. The value is determined during testing (section 3.1).
- **Widening of the main channel section**. Channel sections determine which roughness field is used for which part of the cross-section. In the 5th generation, there are two roughness fields: one for the main channel and another for the floodplains. However, the main channel section serves an additional purpose: it bounds the width over which the sediment transport and morphological change[4] are calculated in the 'tabulated cross section' type. These means that only the deeper levels with widths less than the width of the main channel section will erode or accrete. If the main channel accretes past (above) the bed level at the boundary of the main section, dflow1d will abruptly and prematurely terminate the simulation. To prevent this, the main channel sections are widened where they are deemed too narrow. Note that does not change the cross-section shape, hence it is not a widening of the cross-section itself (only of the width over which the main-channel roughness is applied and over which sediment is transported). Appendix B specifies the procedure in detail.
- **Removal of the storage area**. In the current alpha-status of dflow1d there are still some inconsistencies that occur when cross-sections have a significant storage area (storage width), which is expected to adversely affect morphological results. Based on experiences with the original SOBEK-RE models (using a quasi-steady approach) the storage areas are considered less relevant for morphodynamics than for hydrodynamics. In hydrodynamic simulations the storage width in the cross sections, e.g. stagnant areas in inundated flood plains and lakes, are contributing to attenuation of the flood wave and reduction of its propagation celerity. However, as long as the flood peaks are not too sharp, this effect is not relevant for morphology. Therefore, the storage area of the cross-section was removed. The effect of reduced attenuation is considered less severe than the misrepresentation of storage area in the software. In Annex C the results of an analysis have been presented to evaluate this effect in more detail, using the original SOBEK-RE model schematisations (with and without accounting for the storage width). The analysis shows that the impacts of eliminating the storage from the cross-section does indeed not create a noticeable error with relevance for morphology. The error in flood peak flow velocity is in the order of 1%, causing an error in sediment transport of about 4%. That is very well within the ranges of accuracy of the morphodynamic approach.

[4] A core assumption of dflow1d is that sediment transport – and therefore morphological change – takes place only in the main channel. Therefore, the sediment transport is based on the flow velocity in the main channel (not the mean flow velocity of the entire cross-section).

Note that this effect is only relevant in situations with a fully unsteady flow calculation (not for steady flow, or quasi-steady flow).

Enabling morphology requires a few additional input files determining the morphological settings, sediment transport parameters and initial bed composition. The most important morphological parameter is the morphological scaling factor (Morfac), which is set at 1 (no scaling). The sediment transport functions and parameters are subject to calibration (section 2.3). The initial bed composition is detailed in a separate section (section 2.1.5).

2.1.5 Initial bed composition

The sediment data for the morphodynamic model comes from SOBEK-RE-models of the Zandmaas (Sloff & Stolker, 2000) and Grensmaas (Berkhout, 2003, De Jong, 2005) which were based on borings. This data describes the sediment in 40 0.25 m thick layers, a total sediment layer of 10 m. The details of the conversion of sediment data between the SOBEK-RE formats and dflow1d formats are described in Appendix D. The composition of each layer is given by 10 volume fractions of different sediment sizes (Table 2.1).

Table 2.1 Overview of sediment fractions

Fraction	Lower bound (m)	Upper bound (m)	Fraction	Lower bound (m)	Upper bound (m)
1	0.00008	0.000125	**6**	0.004	0.016
2	0.000125	0.00025	**7**	0.016	0.0315
3	0.00025	0.001	**8**	0.0315	0.063
4	0.001	0.004	**9**	0.063	0.1
5	0.004	0.008	**10**	0.1	0.2

The spatial distribution of the sediment grain size is shown in Figure 2.3, Figure 2.4 and Figure 2.5, showing coarser material upstream and finer material downstream. Here we give a brief overview on how this bed composition compares to literature. In their study on sediment transport in the Meuse, Murrillo-Muñoz (1998), Duizendstra (1999) and Sloff and Stolker (2000) mapped the composition of the top layer. The characteristic gravel-sand transition of the Maas occurs between river kilometer 80-100 km, and coincides with a transition from a high-slope gravel bed river to a gentle slope sand bed river, which contributes to the process of downstream fining (cf. Figure 2.4, Figure 2.7). The general observation of downstream fining was made by Van Manen et al. (1994) in a separate study as well. The difference in typical grain-size distribution for Grensmaas and Zandmaas is well illustrated in Figure 2.6.

The most recent study of the substrate was performed by Arcadis (2011). Wegman (2019) summarized their study in a short communication on the thickness of the coarse layer along the Meuse. They report that the Maas up to river km 15 (i.e. geographically termed the *Kalkmaas*, or ‘limestone Meuse’) has no fine substrate. Instead, the gravel is lying directly on top of limestone. The rest of the Grensmaas does have pockets of fine material underneath the gravel top layers. The depth of the coarse layer is variable – in some locations more than 5 meters, while in others less than two. We observe a variable thickness of the coarse layer in Figure 2.3 as well. A more in-depth comparison between this substrate model and the more recent study by Arcadis (2011) is advisable for studies into the effect of top layer erosion and scouring of the fine substrate.

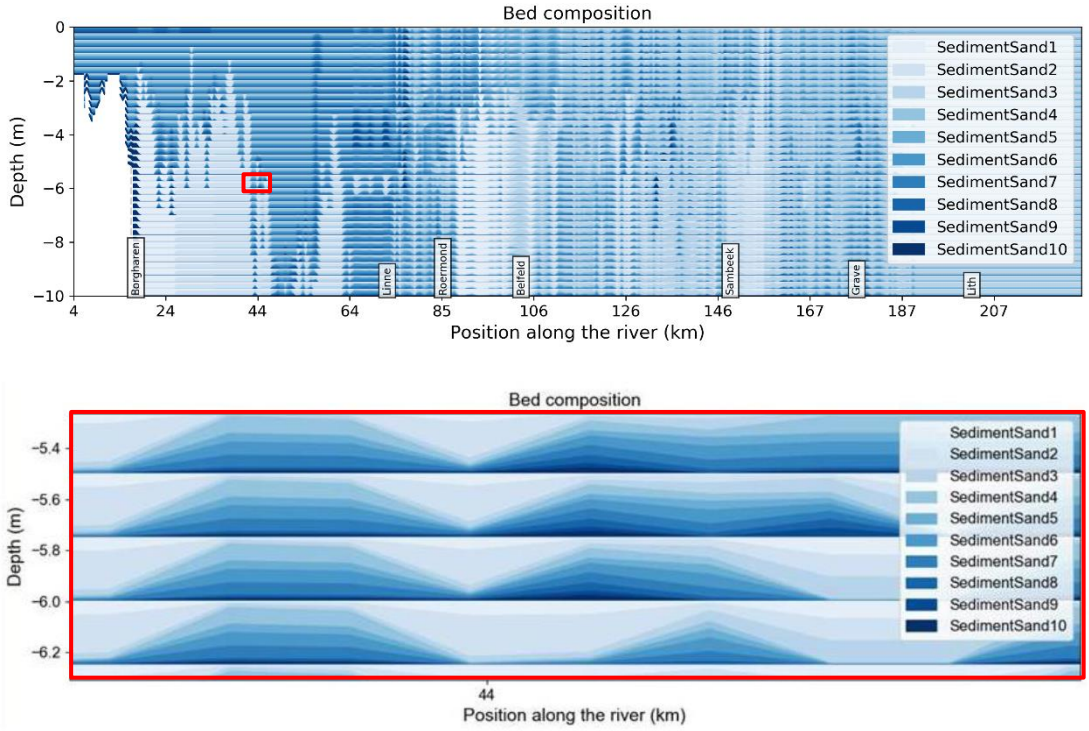

Figure 2.3 Composition of the bed and substrate layers in the dflow1d model (top).Within each of the 40 layers the sediment sizes are stacked, such that their height corresponds to the fraction. The figure below shows a detail with four layers, the red box in the top figure. Darker shades indicate higher grain sizes.

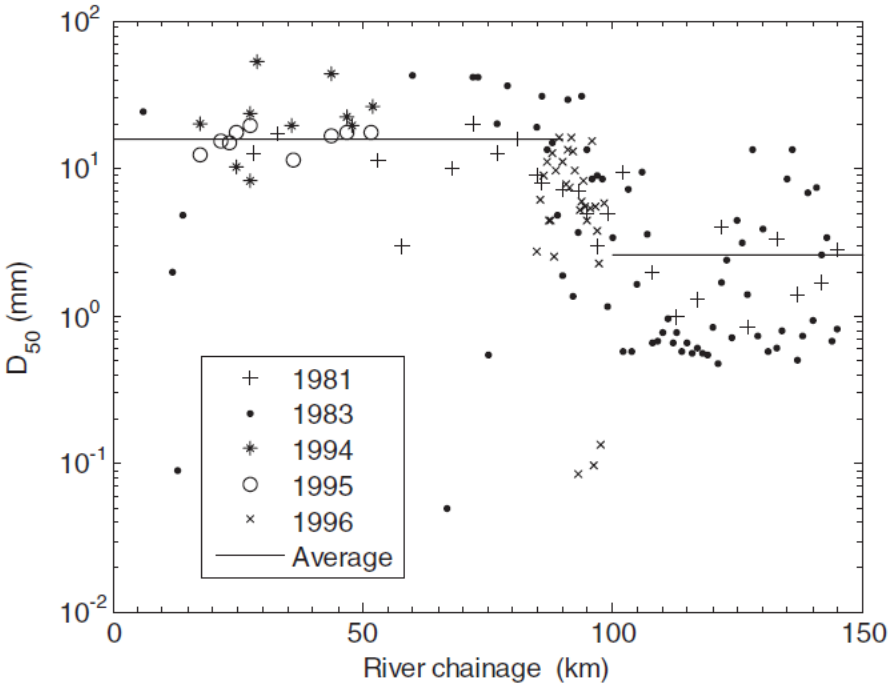

Figure 2.4 Median grain size (D50) in the top layer (Murillo-Muñoz, R. & Klaassen, G.J., 2006).

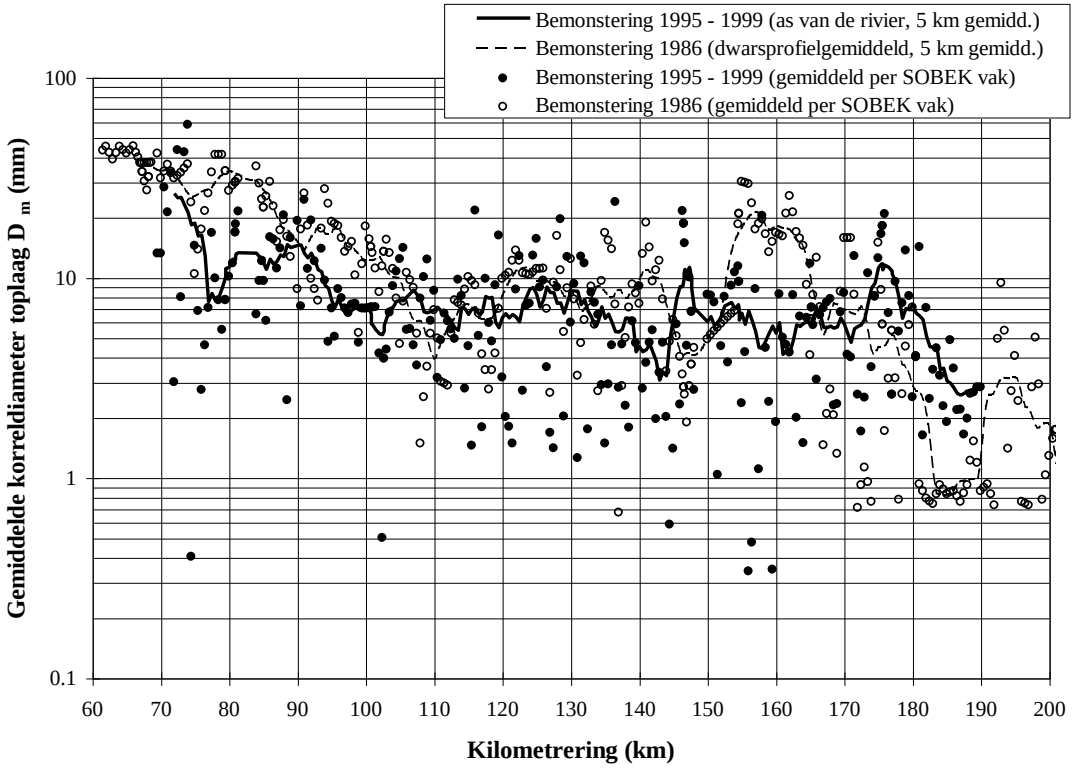

Figure 2.5 Mean grain size (D_m) in the top layer for the Zandmaas, as presented in Sloff and Stolker (2000)

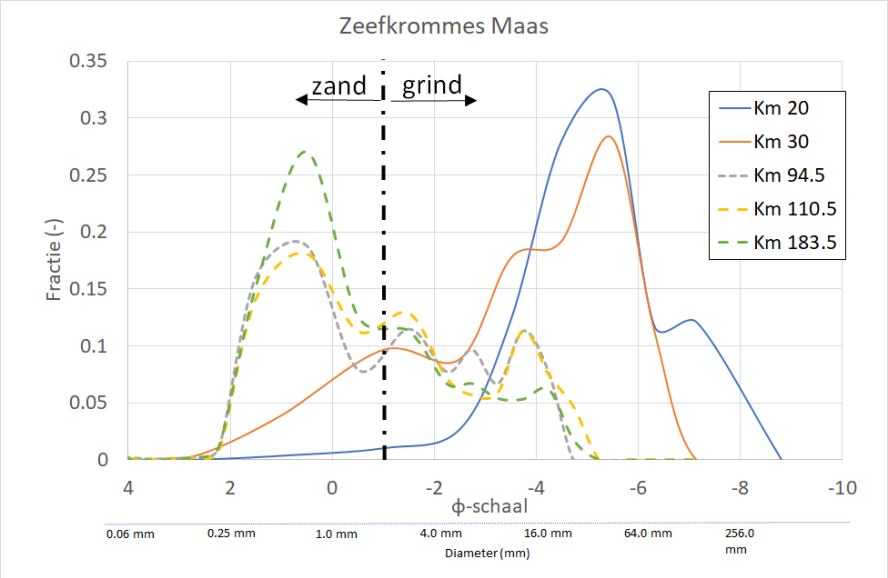

Figure 2.6 Sediment fractions used for the model, taken at a few locations in the Grensmaas (km 20 and 30) and in the Zandmaas (km 94.5, 110.5, 183.5)

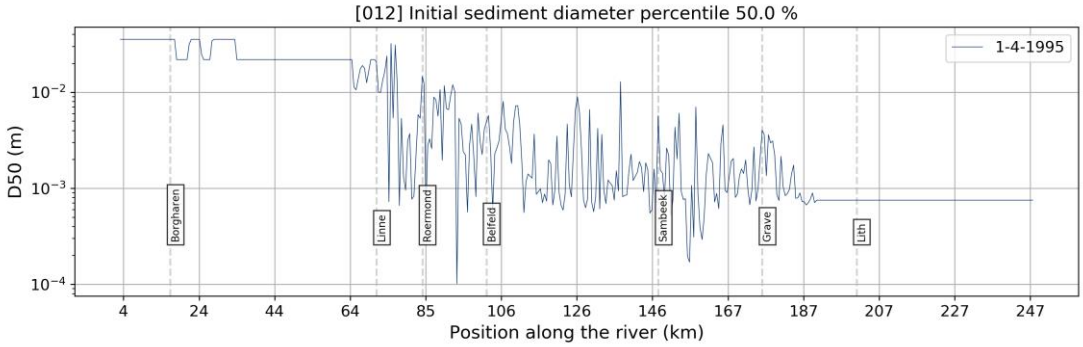

Figure 2.7 Median grain size (D50) in the top layer in the sediment layer model; showing a clear change in median grain size from Grensmaas to Zandmaas (around Linne) as shown in the measured data in the previous figures. Note that the D50 is model output, and is computed from the complete sediment composition model (shown in Figure 2.3)

2.1.6 General settings for the morphology module

Three models were constructed, representing the river states of 1995, 2011 and 2019. These models are identical, except for the floodplain roughness fields and (cross section) geometry. All models have an average grid size (Δx) of 500 meters. The timestep is variable based on a maximum CFL criterium for flow of 0.7 (fully implicit timestep reduction) and has a maximum of 10 minutes.

The morphological scale factor Morfac is set to 1, which means no scaling is performed. For Meyer-Peter and Müller (1948) type sediment-transport model the hiding and exposure is included using the Ashida & Michiue (1973) formulation. A 'hiding and exposure' parameter setting is not required for Engelund and Hansen transport model (1967), as it does not include this process, and also not required for Wilcock and Crowe transport model (2003) because it has its own hiding and exposure formulation. All simulations have been carried out with an active-layer thickness of 1 m (see section 2.3.3 for details).

The active layer thickness is chosen constant for the model, with a value of 1 m. The active layer thickness determines the speed of adjustment of bed composition (speed of mixing). The time of mixing scales linearly with the thickness. Thicker layers have a slower adaptation of grain sizes. Although the active-layer thickness is often associated to the height of bed forms, it is known from experience that in 1D simulations a higher value is needed than strictly based on average dune height (i.e. more than the proposed 0.5 * dune height). For example, the SOBEK-RE model of the Zandmaas used an active layer a few decimetres. In the present model the value has not been varied.

2.1.7 Boundary conditions for the morphodynamic simulations

The hydraulic downstream open boundary is forced using the 5th generation j15 stage-discharge relationship. The upstream hydraulic boundary condition and most lateral inflows are defined by a discharge time series generated using the *Randvoorwaarden Generator Watermodellen Maas* (RGWM) software. As input for this software we used the discharge series at Borgharen, obtained from https://waterinfo.rws.nl, for the period October 1995 to 2019. For the period of April 1995 to October 1995 – which was not available from waterinfo at the time of this study – the discharge series was extended using an earlier record.

The RGWM software does not generate lateral inflows for the Dieze and Drongelen Kanaal that discharge the Aa-Dommel regional system. Instead, RGWM generated discharge series for the regional rivers (i.e. Aa, Dommel and Zandleij), which eventually discharge on the Meuse through the Dieze River and Drongelen Canal. Since this regional system was cut from the morphological model, the 5th generation 1D model was run to determine the inflows from this regional system[5].

The morphological boundary conditions are unconstrained regarding the bed level. The upstream boundary condition is defined as a zero-sediment rate flux, i.e. no sediment from Belgium. Although there are little direct measurements of upstream sediment transports, it is commonly assumed that little to no sediment is coming in from Belgium (Duizendstra, 1999; van Looy, 2009). Downstream, no morphological boundary condition is needed because water always flows out of the model[6].

2.1.8 Morphodynamic simulation periods

Table 2.2 provides an overview of all simulation periods.

Table 2.2 Overview of simulation sets

Simulation	Forcing	Model
1	Steady 250 m^3s^{-1}	J95 (dflow1d) / WAQUA
2	Steady 800 m^3s^{-1}	J95 (dflow1d) / WAQUA
3	Steady 1500 m^3s^{-1}	J95 (dflow1d) / WAQUA
4	Steady 2260 m^3s^{-1}	J95 (dflow1d) / WAQUA
5	Hydrograph April 1995 - December 2010	J95
6	Hydrograph April 1995- December 2010	J11
7	Hydrograph January 2011 – December 2019	J11
8	Hydrograph January 2011 – December 2019	J19

Simulation sets 1 through 4 are used for hydrodynamic testing. Simulation sets 5 and 6 are used for calibration of morphological settings. Simulations 7 and 8 are used for validation of the calibrated model schematisation.

2.1.9 Initial bed topography

We use two sets of simulations with different initial bed topography for each period, to account for human intervention in the meantime. Human intervention implemented in the river within the simulation period (e.g. dredging works) is not directly simulated by the model. Therefore, the model simulation for 1995 will not be able to reproduce secondary effects (e.g. downstream migration of a dredged trench) of human interventions that were introduced in steps after 1995 (e.g., propagation of the channel deepening of the phase 1 project at Grave). In contrast to the 1995 model, the 2011 model has those human interventions from earlier years all available at the start of the simulation. Therefore, secondary effects are likely overestimated when using the 2011 schematisation as a replacement of the 1995 bed for calculating the morphological developments between 1995-2011 (see 2.3.1.2 for an overview). By simulating both models, it is possible to study to some extent the discrepancies between simulation and observation, due to these human interventions.

[5] Note that if this option is not available to future users, a distribution of 80% (Dieze) and 20% (Drongelens Kanaal) of the combined discharge of the Aa, Dommel and Zandleij may be acceptable (De Jong, 2020)

[6] no influence of tide due to the use of a stage discharge relation as hydrodynamic boundary condition

2.2 Hydrodynamic testing

For morphodynamic simulations the flow velocities and the distribution of flow between main channel and flood plain are the most relevant hydrodynamic feature. The purpose of hydrodynamic testing for this morphodynamic model is therefore to make sure that the simulated flow velocities are plausible. Since detailed flow measurements are not available - the 5th generation SOBEK models were calibrated on measured water levels instead – we turn to the 5th generation 2D (WAQUA) model to help determine what constitutes plausibility. Note, however, that the 2D model was only calibrated on water levels as well. Nonetheless, the more detailed representation of geometry and flows in the 2D model allow a more accurate hydraulic behaviour than the calibrated 1D models, or the limited number of flow-velocity measurements at 2 or 3 locations for rating curves.

The reason why we focus on flow velocity instead of water levels is because the sediment transport scales exponentially with flow velocity. For 1D specifically, it scales with the flow velocity in the main channel, as sediment transport and morphodynamic change is only computed in that section. Water levels are only of secondary importance – determining at what stage certain threshold features become important (e.g. weirs, floodplains, embankments etc.).

We compare dflow1d results with WAQUA along the river axis on the following model output: (1) flow velocity in the main channel, (2) discharge in the main channel and (3) water levels. These three variables are readily available as output from the dflow1d model[7]. They are obtained from the WAQUA models as follows:

- **Water levels** are available at water level stations. These stations are located on the river axis at every river kilometre.
- **Main channel flow velocities** and **discharge** are derived from the raw model output. Discharge and depth-averaged flow velocities are available on every grid line. To transform these gridline variables to main channel variables the following three steps are required.
  - Use the main channel shape from the Baseline database[8] to select all main channel gridlines. Note that due to widening of the main-channel section in the 1D model, the main-channel shape from Baseline is not necessarily similar to the width in the model. In the 1D model the effect of widening on flow velocity appeared to be small, and generally caused a slight increase in flow velocity at high discharge compared to the simulation with original main-channel width (due to a smaller contribution of the rough flood plains). The effect can be ignored compared to the uncertainties found in the comparison of 1D and 2D results.
  - Determine the streamwise position of the gridlines perpendicular to the river axis.
  - Average the flow velocities and sum the discharges per gridline to get main channel variables along the river.

Note that the Baseline channel shapes do not necessarily align well with the numerical grid. The result is that the number of numerical cells assigned to the ‘main channel’ or the ‘floodplain’ can change from location to location. The summation of the discharge through the main channel is especially sensitive to this, and even more so at lower discharges (see e.g. figure E.2).

Differences between dflowfm1d and WAQUA are expressed graphically using figures and quantitatively using the bias and standard deviation of residuals. A limited number of model runs is performed with different values of the uniform friction value between physically realistic bounds (0.025 $sm^{-1/3}$ and 0.050 $sm^{-1/3}$) and from these limited number of runs one value is selected based on comparison with ground-truth data. No further optimisation is performed.

[7] With the side note that main channel velocity & discharge are available only as output of the morphological module, i.e. morphology must be enabled to retrieve this output.

[8] That is all polygons within the ‘secties’ layer with attribute value SECTIE=1

2.3 Morphodynamic testing and optimisation

The purpose of morphodynamic testing is twofold: first to test whether the model produces plausible and stable results, and second to see which combination of morphodynamic settings (sediment transport formula, parameters) agrees best with the observations.

2.3.1 Observations

2.3.1.1 Sediment transport

Duizendstra (1999) studied sediment transport rates on the Grensmaas based on bedload transport measurements and bed level changes. Duizenstra hypothesized that before December 1993 no sediment transport took place up to 1200 m^3s^{-1} due to an armoured layer (*pleisterlaag*) of coarse material, but that the flood of December 1993 broke up the armoured layer. After this flood wave, bed load transport reportedly took place starting as low as 300 m^3s^{-1} as delayed mobilization of the exposed fine materials that were entrained from below the armoured bed during the 1993 flood and deposited in sand bars. Duizendstra estimated the annual average transport rates in the order of 20.000 m^3/y to 60.000 m^3/y. Wilbers (1996) estimated an annual transport of 55.000 m^3/y in the Grensmaas, and 40.000 m^3/y in the Zandmaas. Murillo-Muñoz & Klaassen (2006) report transport rates between 19.000 m^3/y to 70.000 m^3/y. Citing Duizendstra (1999), he noted that the mobilization of the armoured layer governs sediment transport in the Grensmaas at discharges higher than 1250 m^3s^{-1}.

In general, the number of primary sources (original research) on sediment transport rates is limited. The general assumptions are that on average the transport rates vary between 20.000 and 70.000 m^3 per year and that all sediment is sourced locally, i.e. either picked up upstream or brought into the channel by bank erosion or human intervention, and that no sediment is transported into the system upstream from Eijsden / Lixhe (Belgium).

Note that these values are based on a limited number of measurements, upscaled to yearly transports by way of discharge-sediment transport (Q-S) relations and other disputable assumptions. Therefore, these rates are not exact numbers – and no confident intervals are known. We therefore treat these ranges as ‘orders of magnitude’ or ‘ball park’, meaning that we will not strive to remain strictly within these ranges.

2.3.1.2 Bed level change 1995-2019

Various sources were considered as a basis for the bed level change that took place in the Maas over the years 1995 to 2019. First, a selected number of sources from literature were consulted on known trends and documented human intervention. Second, an analysis of sounding data by De Jong (2019) has been considered, and thirdly the analysis of sounding data by Kragten (2018) was studied. These analyses were not meant to be exhaustive but meant to highlight the major changes in the bed which can (or cannot) be reproduced by model simulations.

Human intervention and autonomous trends in bed morphology

Like most rivers, the Meuse river is not a natural river in the sense that it is unaltered by human intervention. In fact, the Meuse river is actively maintained to improve inland navigation, increase flood safety and improve the ecological status. Major works have recently been carried out in the *Maaswerken* program, which includes the subprojects *Grensmaasproject* (2008-2027) and *project Zandmaas* (2005-2015). Local projects carried out within this program were mostly variations on increasing the discharge conveyance capacity of the channel (Dutch: *rivierverruiming*), nature development (river banks) and improvement for navigability and upscaling for bigger ships (program Maasroute), such as channel deepening and channel widening.

According to Van Dongen & Meijer (2008), Asselman et al. (2018) and other sources, the major human interventions in the period 1995-2011 were:

- [1996-1997] Channel deepening Gennep-Grave, with 3 m deepening over a width of 50 m between km 155.7 – 164.2 and deepening of 1.5 m between km 166.3 – 174.2.
- [1999-2001] Channel widening from km 86.9-92.5.
- [2005-2007] Channel deepening Grave-Ravenstein from km 176-181 with 3 m.

And after 2011:

- [2010-2013] Channel deepening in weir section (Dutch: *stuwpand*) Grave between km 164 – 175.
- [around 2014] Channel deepening in weir section Sambeek, between km 109 – 121.

The channel deepening projects were carried out in various phases (pers. communication RWS-ZN). The channel deepening at Gennep-Grave (1996) was phase 1 of a pilot project. The second phase of the pilot (PP2), which extended the channel bed deepening downstream, was carried out between 2011 and 2014 as part of the Maaswerken programme and took place concurrently with another channel deepening at weir section Sambeek (as listed above).

In the Grensmaas, major human intervention has taken place from 2007/2008 onward, both in context of the Maaswerken project, project Boertien and project Vlaanderen (Van Looy, 2009). Individual projects include strengthening of river banks with coarse material, the construction of gravel sills (*grinddrempels*), and widening of channels, which may have contributed to local rise of the bed (Van Looy, 2009). As part of this program a lot of coarse sediment has been extracted (gravel mining). Still, a net effect of all these works, as well by manual adding (gravel sills) as by erosion of banks, is that a lot sediment is ‘brought into the main channel’ over this period. In personal communication with Rijkswaterstaat, these amounts have been estimated to be in the order of tens of thousands m^3.

The ‘autonomous’ trend in the river has been one of gradual erosion of the bed. Van Dongen & Meijer (2008) point to sand mining, supply limitation from upstream, and a general slope adjustment as likely explanations. Over the period 1995-2007 they computed an average erosion of about 0.02-0.03 m/y in the Maas from rkm 15 to 164.

Analysis of sounding data

This paragraph briefly reviews two analyses of sounding data. De Jong (2020) analysed bed soundings as part of the 6^{th} generation 2D model development and using processed data available in the Baseline database. Kragten (2018) processed bed soundings, while continuing work done by Meander (Meijer).

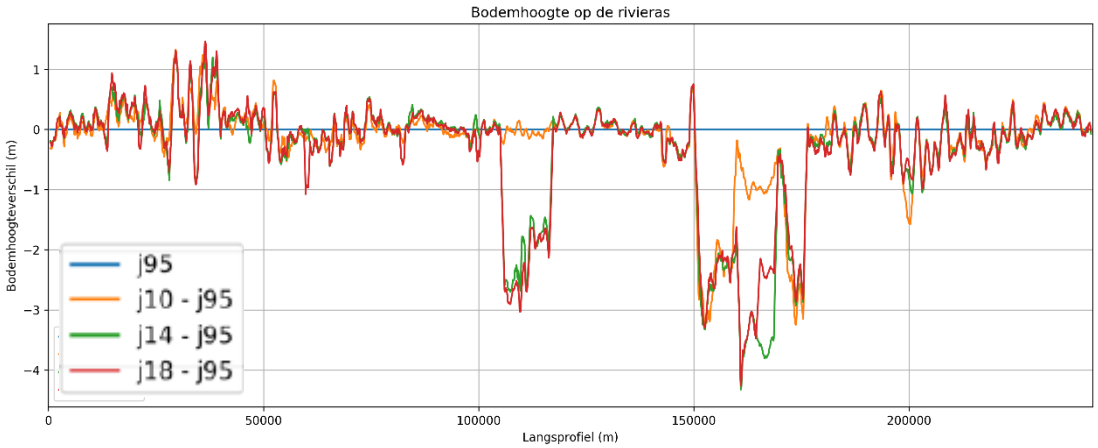

Figure 2.8 Changes to the river bed at the centre axis (moving average over 1 km). Adapted from De Jong (2019).

The analysis of De Jong (Figure 2.8) is based on the sounding data as processed in the Baseline database. It shows the change at the centre axis of the river since 1995. Overall, it (local) bed level increases since 1995 on the Grensmaas, which may be attributed to the construction of the gravel sills and (sediment) measures in the Maaswerken, Boertien and Vlaanderen projects. More downstream the bed level lowering projects at stuwpand Sambeek (~ 110 km) and the various phases of deepening between Grave and Ravenstein (~150 km to ~180 km) are clearly visible. Apart from the human interventions though, little large-scale autonomous changes are to be seen.

Compare to the analysis by De Jong (2019), the data by Meijer and Kragten (2018) provides a more detailed look at the years between 1995 and 2010. These data were analysed for large scale trends by averaging over the various geographical regions of the Meuse[9]. In addition, the changes that occurred due to large-scale channel deepening (between the consecutive years that these measures were implemented) have been removed from the time-averaging procedure. In establishing the processed region-averaged and time-averaged values, the effect of deepening is masked out. This is necessary because the model simulation has no human intervention incorporated within the simulation. A fair comparison between modelled bed-level changes and observed changes should therefore exclude the man-made changes (channel deepening) that are dominant in Figure 2.8. Note that the response of the river bed to these deepenings has not been considered in this way, but these are local impacts that are considered to have a small effect on the large-scale trends.

Results show a general erosional trend until 2004 (Figure 2.10). A (partial) explanation for the erosion, which was also described in other literature, is that the period between 1997 and 2004 saw a succession of flood seasons with a high peak discharge, followed by a period of low-discharge seasons from 2004 to 2011, as shown in Figure 2.9.

[9] The same averaging over geographical regions is used in the IRM quickscan studies. We adopted this approach to be aligned with these studies.

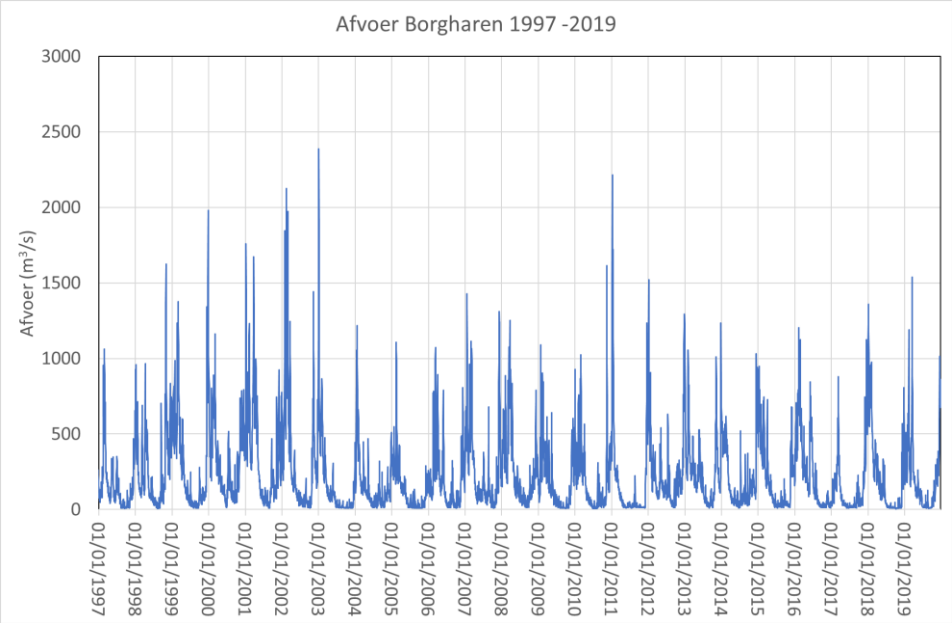

Figure 2.9 Discharge time series at Borgharen for period 1997-2019

Figure 2.10 shows that on the Grensmaas erosion has reduced significantly and has reversed even to a net deposition trend for the period of 2011-2017. Closer inspection of this data (Figure 2.11) revealed that much deposition in the Grensmaas appears to have taken place in in the period 2009-2010, and that from that period onward no the bed seems to be relatively stable. The sudden bed level increase between 2009 and 2010 is curious and cannot be satisfactorily explained yet. Considering that we assume no sediment is brought into the system from Belgium, this bed level increase must be either explained by human intervention (Maaswerken, construction of 'grinddrempels') or due to a measurement error (e.g. not only the 2007, but the 2008 and 2009 datasets must be rejected). This inconsistency is recommended to be studied in more detail.

In the period 2011-2017 we do see some large local changes along the entire Maas, but little overall morphological trends. This is in line with De Jong (2019). The sections over which the bed-level trends are averaged in Figure 2.10 are taken equal to those of Ten Brinke (2019) for comparison, The transition of Zandmaas to Bedijkte Maas is usually taken around km 165 instead of 155. There is insufficient data in the Bergsche Maas in Kragten (2018) to add the bed-level trends for that section.

However, a few remarks must be made regarding the Kragten (2018) dataset, partly based on personal communication with Rijkswaterstaat Zuid Nederland:

- Before 2004 soundings were single beam. After that, they are multibeam soundings. It is known that this switch in measuring technology introduces a bias. This bias is corrected in De Jong (2019), but possibly not in Kragten (2018).
- Although care is taken to mask out the effect of human intervention, the erosion in the period 1995-2011 in the Zandmaas may include secondary effects of human intervention. Therefore, the natural erosion processes may be overestimated in the averaging.
- Considering no sediment is assumed to be transported into the system from upstream, the most likely source of the sediment of the deposition is local pickup, human intervention and bank erosion.
- The sounding data of 2007 is considered to be unreliable by local authorities[10], as it was considered very unlikely that the river – which had before shown a modest erosional trend, had suddenly shown such large erosion in the order of 0.2 m. This significant deviation is for instance visible in Figure 2.11 for the average bed-level of the Grensmaas from 1995 to 2017.

[10] Internal meeting notes of Rijkswaterstaat Zuid Nederland, d.d. 16 april 2008, 'Presentatie data Grensmaas 2008'.

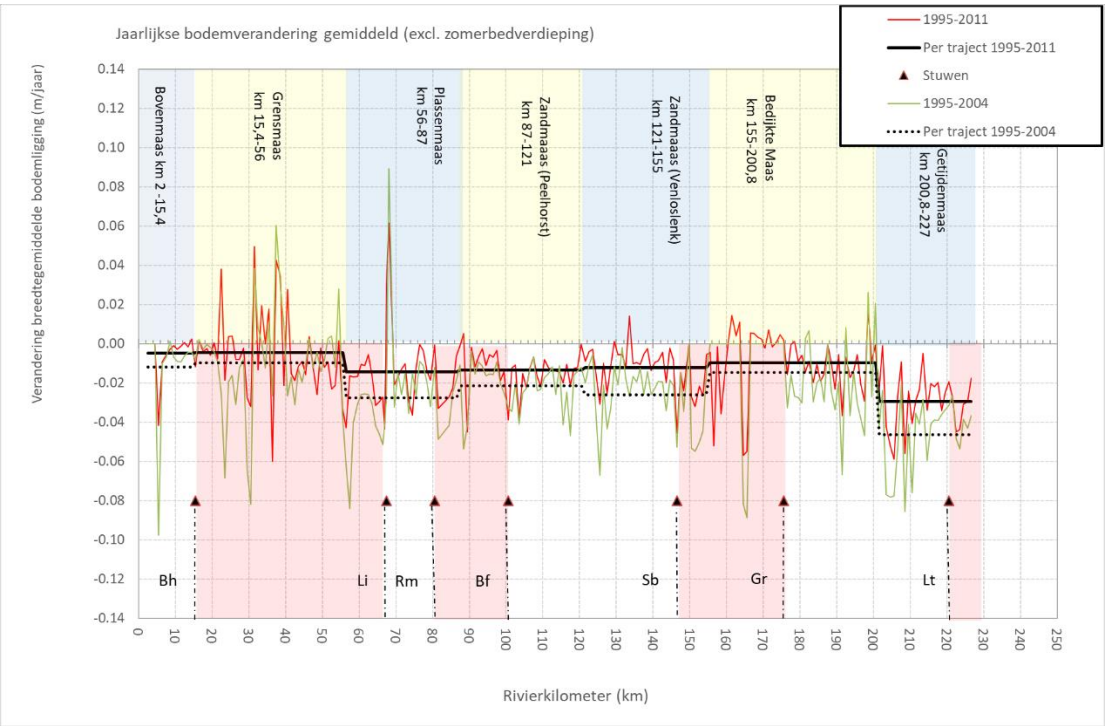

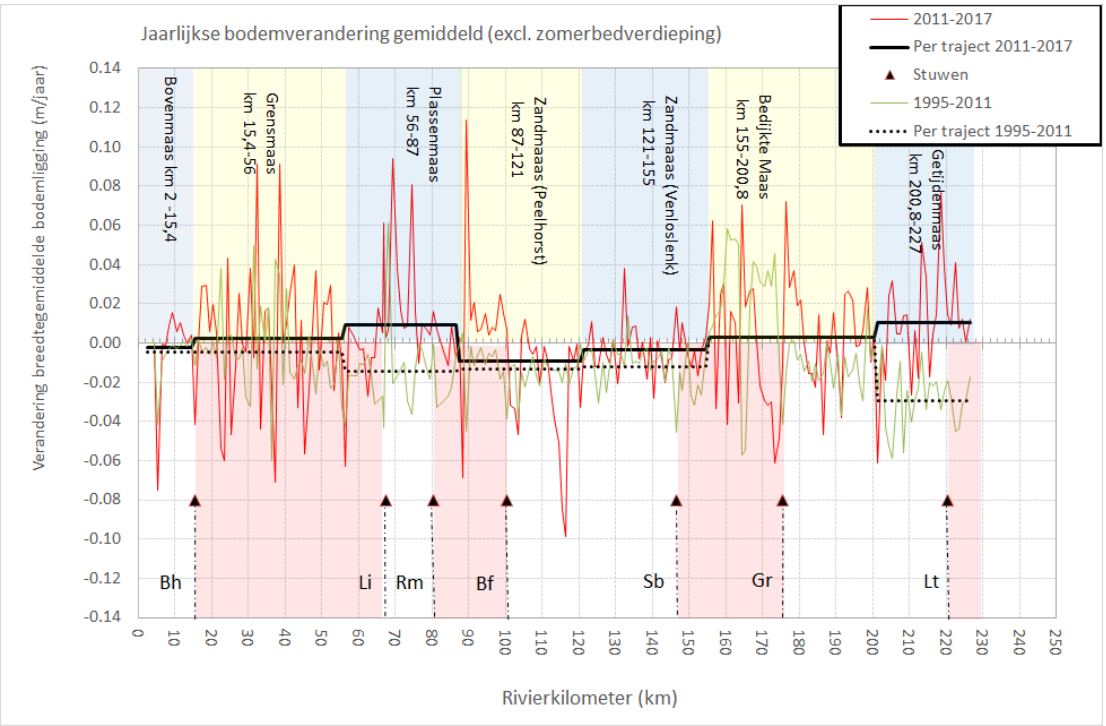

Figure 2.10 Changes in the river bed between 1995-2004 and 1995-2011(top) and 2011-2017 (bottom), averaged over geographical regions. The weirs are denoted by Borgharen (Bh), Linne (Li), Roermond (Rm), Belfeld (Bf), Sambeek (Sb), Grave (Gr) and Lith (Lt). The geographical regions are shown on the top. Based on data by Kragten (2018).

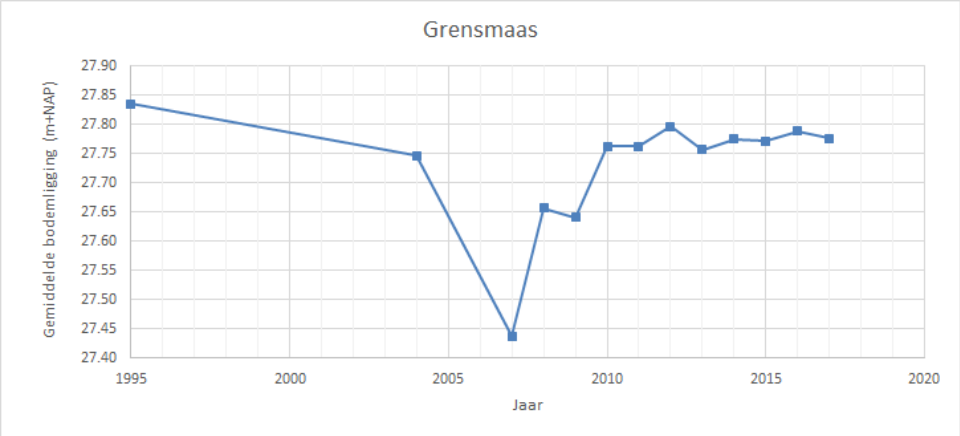

Figure 2.11 Development of section-average bed level of the Grensmaas (section between km 15 – 56) as function of time according to data reported by Kragten (2018). The data from 2007 was later rejected by local authorities and considered invalid. Based on data by Kragten (2018).

Summary of bed level change

Considering the various sources of literature, we consider that the following bed level changes should be reproducible by the morphological model:

- A general erosion between 1995 and 2011 (with uncertainty on trends between 2004-2011).
- Little change between 2011-2017.

The deposition in the Grensmaas after 2011 – whether entirely physical or not – will not be reproducible by the model because of supply limited conditions from upstream.

2.3.1.3 Celerity of bed disturbance

The purpose of simulating the celerity of bed disturbances is to estimate how fast human intervention in the river system such as channel bed deepening propagate downstream. This is important to estimate the life span of human interventions and maintenance planning. The celerity or propagation speed of morphological changes is in the order of 200-300 m/year in the Maas (Sieben, 2011), and therefore it is considered relevant for impacts on the scale of decades for which this model is designed (length scales of impacted sections in the order of several kilometres).

2.3.2 Model testing and calibration

An optimisation of morphological settings is carried out to improve agreement between simulation and observation (section 2.3.1). The morphological settings that are improved concern the type (equation) and parameters of the sediment transport formulation.

An important difference between the SOBEK-RE and D-HYDRO software should be pointed out at this point. In D-HYDRO, the type and parameters of the sediment transport formulae are defined globally per sediment fraction. Therefore, it is not possible – as it was in SOBEK-RE – to define a separate transport formulation per river branch (nevertheless, in turn SOBEK-RE did not allow a different sediment-transport model per size fraction).

Initially, sediment transport is computed following the non-uniform Meyer-Peter Müller (1948) formulation for bed load transport – which is expected to perform well in bed load dominated (e.g. gravel/sand) rivers. However, since the Meuse has both a gravel and sand dominated part, also the Engelund-Hansen (1967) equation has been considered for simulating transport of the finer fractions. The Engelund-Hansen formula was developed for total transport (i.e. bed-load plus suspended-load) and is expected to perform better in the downstream part of the system where part of the sediment may be transported in suspension. In addition, the Wilcock and Crowe (2003) sediment transport formula has been tested, which was developed more recently and was developed to deal with a range of sediment sizes on the sand-gravel scale and may therefore perform favourably on the Meuse.

3 Results

3.1 Hydrodynamic tests

3.1.1 Initial difference

Initial model runs were performed using simulation set 1 through 4 (Table 2.2), using an initial uniform roughness field with an initially low Manning coefficient value of 0.025 $sm^{-1/3}$. Initial results show that 1D flow velocities in the main channel are higher than those in the 2D model, both at 1500 m^3s^{-1} (Figure 3.1) and other steady discharges (Table 3.1). Water levels are generally lower, which contributes in combination with the widened main-channel section in the 1D model, to a higher main channel discharge as well (less flow in the flood plain). All these discrepancies are expected to be reduced by a higher uniform friction value. A full overview of figures is given in Appendix E.1.

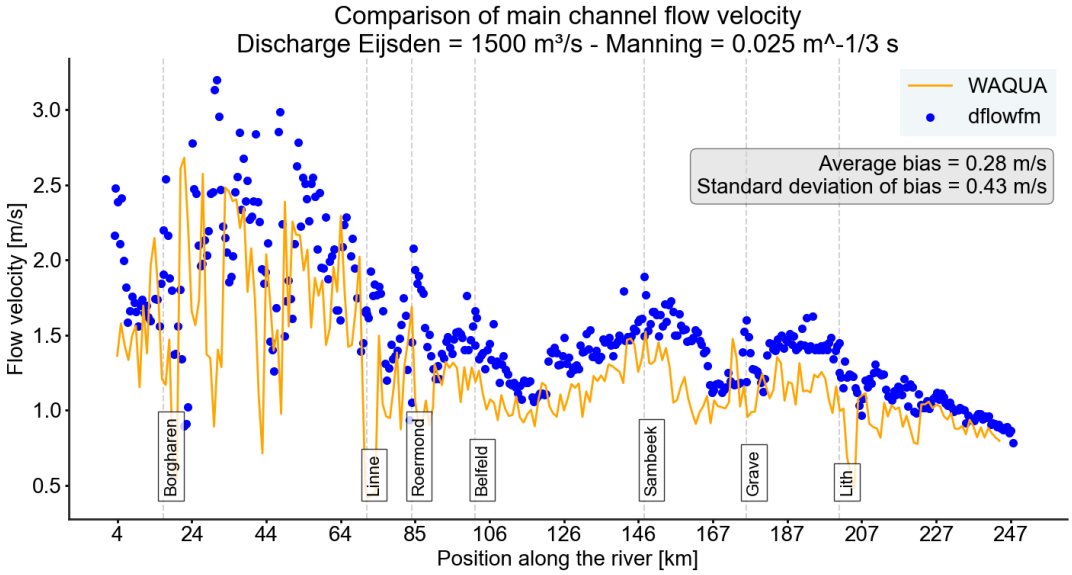

Figure 3.1 Initial difference between dflowfm (1d) and WAQUA at 1500 m^3s^{-1} with Manning's n=0.025 $sm^{-1/3}$.

Table 3.1 Bias and standard deviation (in parenthesis) for different discharges with Manning's n=0.025 $sm^{-1/3}$

Discharge at Eijsden (m^3s^{-1})	Bias and standard deviation in water level (m)	Bias and standard deviation in main channel discharge (m^3s^{-1})	Bias and standard deviation in main channel flow velocity (ms^{-1})
250	-0.10 (0.15)	8.14 (20.44)	0.08 (0.20)
800	-0.08 (0.31)	39.73 (100.91)	0.13 (0.31)
1500	-0.60 (0.42)	128.06 (222.14)	0.28 (0.43)
2260	-0.69 (0.36)	442.41 (442.81)	0.48 (0.54)

3.1.2 Sensitivity analysis

Next the value of the uniform roughness field was varied within steps to 0.050 $sm^{-1/3}$. The summarized results are shown Figure 3.2. From these results we concluded that, overall, 0.035 $sm^{-1/3}$ produces relatively good results for each variable (water level, main channel flow velocity and main channel discharge). For reproduction of water levels, a Manning value of 0.030 $sm^{-1/3}$ would be better. However, reproduction of flow velocities is more important for morphodynamic simulations (see section 2.2). Therefore, it was decided that no (further) optimisation of the Manning value was necessary.

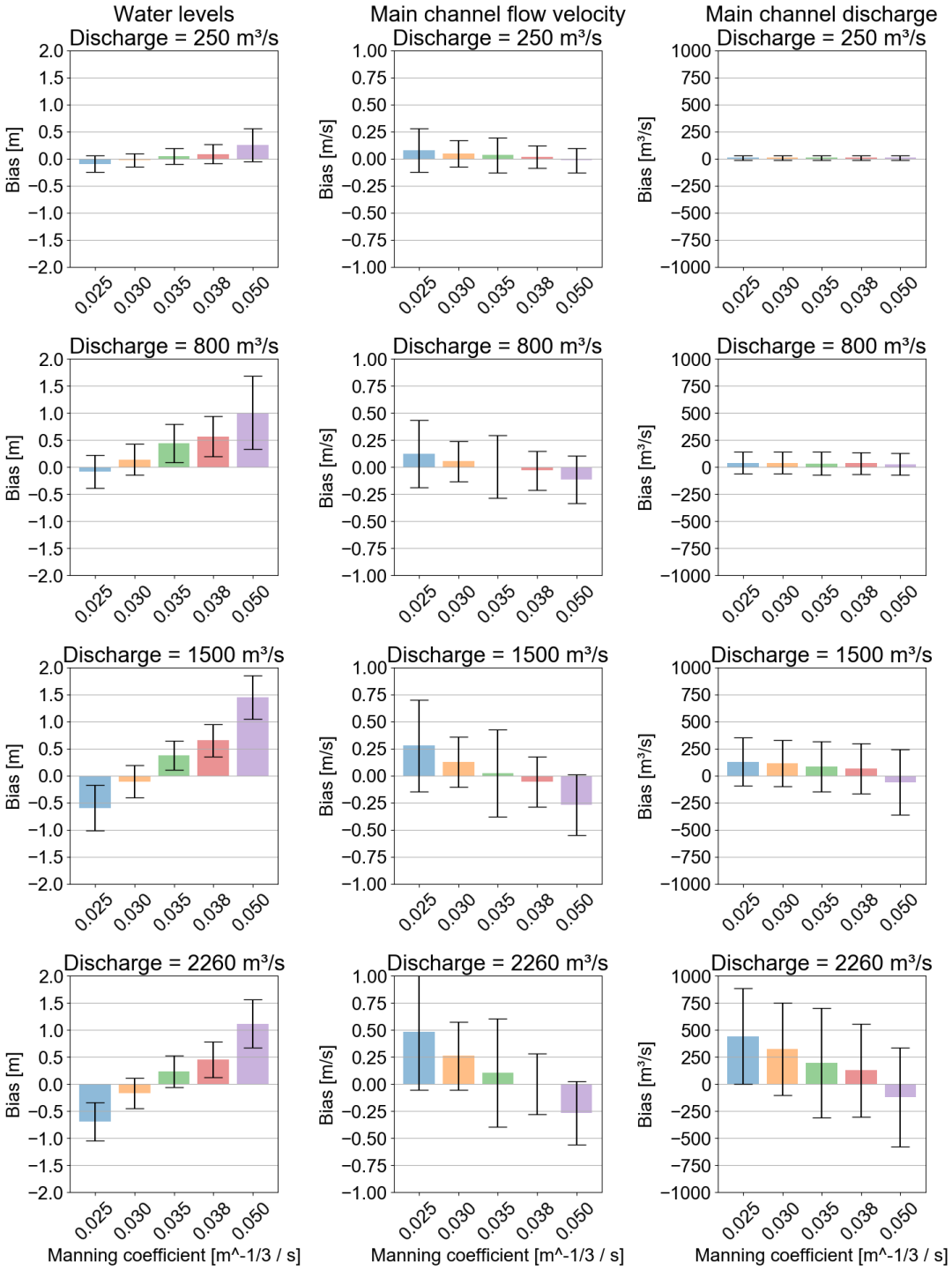

Figure 3.2 Boxplot of the biases for four different Manning values and four different discharge levels. The whisker bars depict the standard deviation of the error, while the boxes show the average error (bias).

The final comparison between dflow1d and WAQUA shows that the differences of the flow velocities in the main channel between dflow1d and WAQUA are relatively small and that large-scale variation along the river is well reproduced in 1D (Figure 3.3). The water levels in the 1D model are generally higher than in the 2D model results (Figure 3.4). Spatially the largest differences can be found in the upstream parts of the Meuse River (from 20 km till 100 km). These are the steepest parts of the river. Table 3.2 summarises the differences for all discharges. Appendix D.2 has all other figures.

Given the good agreement between 1D and 2D model results for flow velocities and considering that main channel flow velocities are the most important physical driver for sediment transport and morphological change, we continue a model-wide uniform Manning value of 0.035 $sm^{-1/3}$ was selected for further simulations.

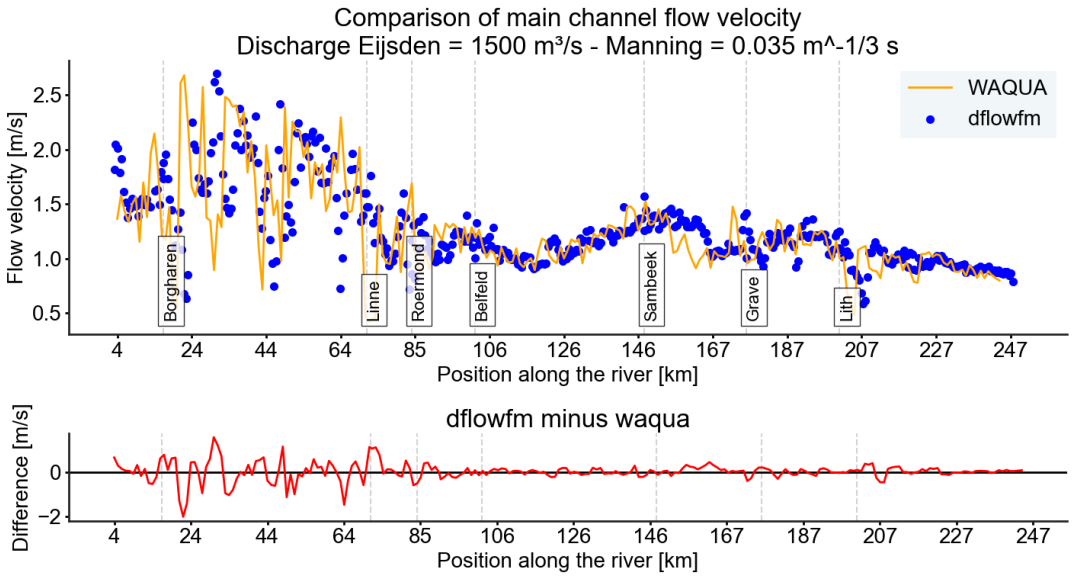

Figure 3.3 Final difference in main channel flow velocity at 1500 m^3s^{-1}

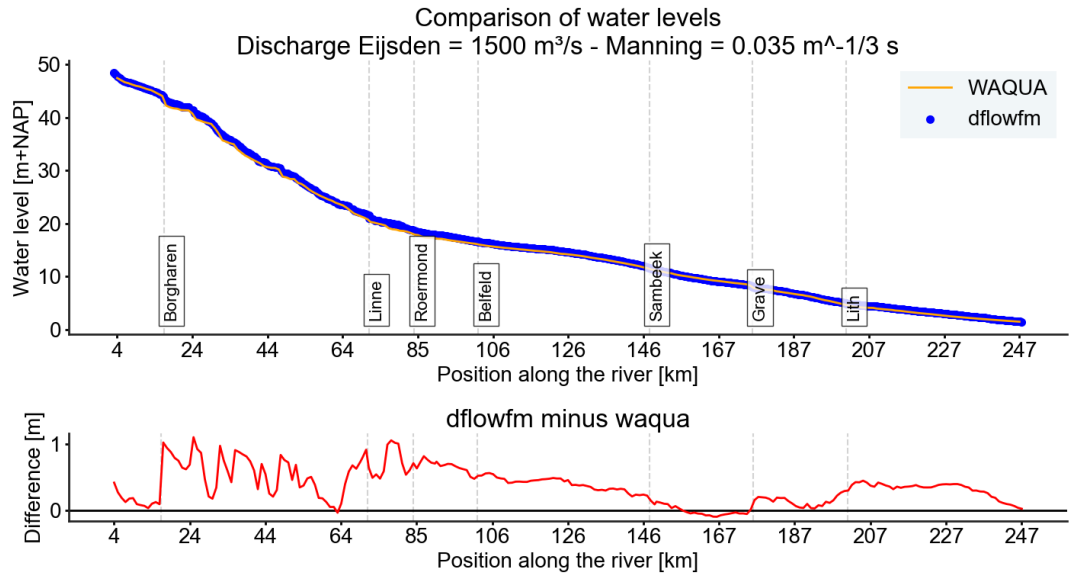

Figure 3.4 Final difference in computed water level at 1500 m^3s^{-1}

Table 3.2 Average bias (standard deviation) of the hydrodynamic model with (Manning) n=0.035 $sm^{-1/3}$

Discharge at Eijsden (m3/s)	Bias and standard deviation in water level (m)	Bias and standard deviation in main channel discharge (m3s-1)	Bias and standard deviation in main channel flow velocity (m/s)
250	0.04 (0.15)	8.09 (20.48)	0.03 (0.16)
800	0.44 (0.35)	34.24 (106.82)	0.00 (0.29)
1500	0.37 (0.27)	85.93 (232.03)	0.02 (0.40)
2260	0.24 (0.29)	197.96 (505.00)	0.10 (0.50)

3.2 Morphodynamic tests

3.2.1 Morphodynamic calibration

Especially in the upper reach of the Maas the bed is characterised by cobbles and pebbles (gravel range). In the start of the morphology phase, the experiences from earlier work indicated that because of the grain-size distribution, sorting and 'hiding and exposure' processes are governing the upper reaches of the model. This requires Meyer-Peter Müller or similar formula per size fraction with a critical Shields value and 'hiding and exposure' applied to it. This allows for simulation of armouring during low flows, which is characteristic for the Grensmaas.

After initial morphodynamic testing with various settings, we decided on the following three general scenarios: (1) Meyer-Peter Müller for all sediment fractions, (2) Wilcock-Crowe for all sediment fractions and (3) a combination of Meyer-Peter Müller for coarse material, Engelund-Hansen for fine material (< 1 mm). Below a summary of the major findings is presented. Full results can be found in Appendix E.

3.2.1.1 Meyer-Peter Müller (1948) for non-uniform sediment (MPM)

Settings used:

- TraFrm = 4 (selected transport formula: General Formula[11]), ACAL=8.0 (pre-factor for calibration. 8.0 is the default value for the MPM formula), RipFac = 1.0 (Ripple factor), ThetaC = 0.047 (critical shear stress), IHidExp = 3 (hiding and exposure according to Ashida and Michiue, 1973).
- Thresh = 1 m (threshold for fixed layers), ThTrLyr = 1.0 m (thickness of active layer, constant), MxNULyr = 40 (number of under layers), ThUnLyr = 0.50 (maximum thickness of each under layer).

Simulations with MPM showed a relatively low sediment transport rate (Figure 3.5), below the estimated average ranges of 20.000 m^3/year to 70.000 m^3/year, which led to relatively small changes in the morphology. Especially given the drop in sediment transport after km 60, which coincides with a sudden fining of the top layer sediment (Figure 2.7), indicates that sediment transport of finer material is underestimated. In the SOBEK-RE model for the Zandmaas (Sloff and Stolker, 2000) the transport rates were reasonably reproduced with similar settings (MPM, ThetaC = 0.047 N/m^2, ripple factor = 0.9, and ACAL = 6.4), but with a smaller active-layer thickness (0.15 m). A reduction of ThetaC , or a change in ripple factor were found to worsen the results. However, the computations with the new model for the full river (including the Grensmaas) show that even with further adjustment of the parameters, the difference between too high loads on the Grensmaas and too low loads on the Zandmaas cannot be eliminated. Since this inconsistent behaviour occurs at the gravel-sand transition, it is assumed that hiding and exposure may play a relevant role here.

[11] This formula is a Meyer-Peter and Müller type of formula, but with parameters that can be modified by the user

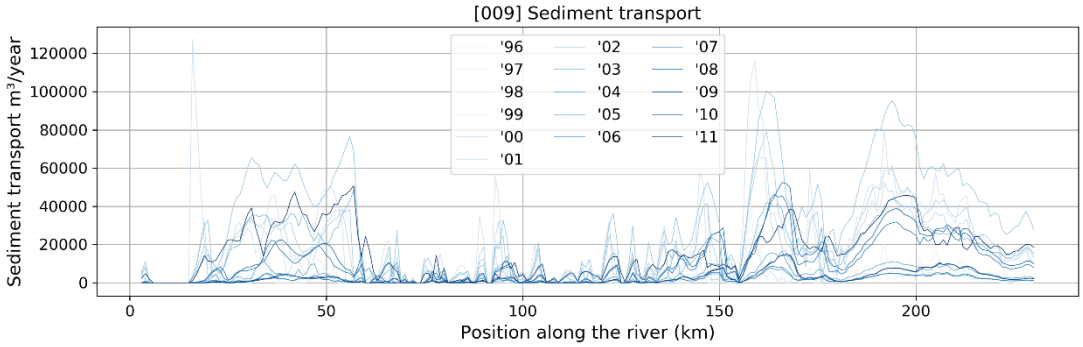

Figure 3.5 Sediment transport for simulation set 5 (j95, 1995-2011) with MPM

3.2.1.2 Wilcock and Crowe (2003) (W&C)

Settings used:

- Trafrm = 16 (selected transport formula: Wilcock & Crowe), ACAL = 1.0 (pre-factor for calibration).
- Thresh = 1 m (threshold for fixed layers), ThTrLyr = 1.0 m (thickness of active layer, constant), MxNULyr = 40 (number of under layers), ThUnLyr = 0.50 (maximum thickness of each under layer).

Note that W&C has its own hiding and exposure integrated in the formula. Simulations with W&C show very high transport rates (Figure 3.6), especially on the Grensmaas, and high gradients. This results in large, but overall quite unrealistic morphological change, with extreme erosion after Borgharen and high sedimentation around Linne (km 60-85). The model seems to perform reasonably well for the Zandmaas, but because it does not allow further fine-tuning, the W&C model cannot be applied to the full model. The model seems to perform even worse than the MPM simulation presented in the previous section. The change in behaviour of the model coincides with the transition from gravel to sand. It is known that the W&C model contains a switch that is determined by the ratio between shear stress acting on bed particles (τ) and the reference shear stress for particle size fraction i (τ_{ri}). This reference shear stress acts as a kind of critical shear stress but has a dependence on the amount of sand on the bed surface (F_s). It is expected that this dependence and intrinsic switch plays an important role in the poor performance of this model over the entire length of the Maas. The amount of sand (F_s) in the bed shows a significant jump through the transition as shown in Figure 2.6.

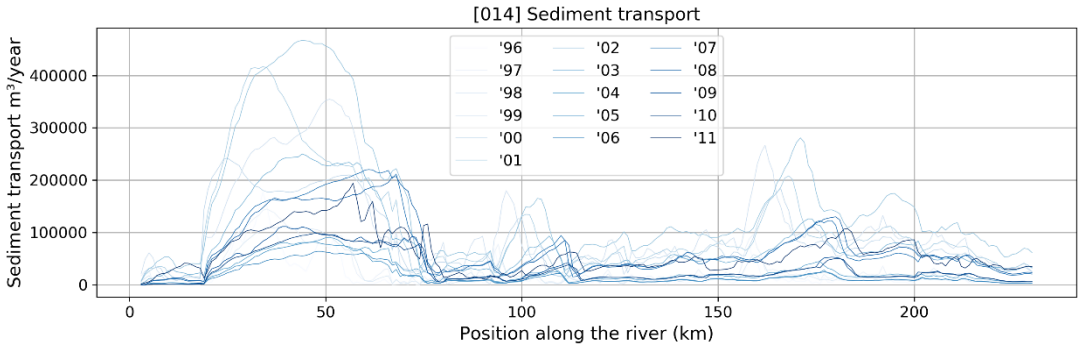

Figure 3.6 Sediment transport for simulation set 5 (j95, 1995-2011) with Wilcock &Crowe

3.2.1.3 Combination of Meyer-Peter Müller and Engelund-Hansen (MPM+EH)

Settings used:

- Fractions Di < 1 mm
  - Trafrm = 1 (selected transport formula: Engelund and Hansen), ACAL = 1.0 (pre-factor for calibration).
- Fractions Di > 1mm
  - TraFrm = 4 (selected transport formula: General Formula[12]), ACAL=8.0 (pre-factor for calibration), RipFac = 1.0 (Ripple factor), ThetaC = 0.047 (critical shear stress), IHidExp = 3 (hiding and exposure according to Ashida and Michiue, 1973).
- Thresh = 1 m (threshold for fixed layers), ThTrLyr = 1.0 m (thickness of active layer, constant), MxNULyr = 40 (number of under layers), ThUnLyr = 0.50 (maximum thickness of each under layer).

In the MPM and W&C simulations a strong division occurs between bed development and sediment load in Grensmaas and Zandmaas, which can be attributed to the properties of these transport formulas. In the Maas the majority of sediment movement occurs during flood condition. Figure 2.6 shows that the bed surface of the Grensmaas contains mostly gravel in the range of 16 to 64 mm with little sand (less than 15%), while the bed surface of the Zandmaas contains more than 50% of a mixture of sand mixed with gravel fractions of gravel smaller than 16 mm. In the previously considered formulas (W&C and MPM with AM hiding and exposure) the transport of gravel fractions is overestimated, while the transport of sand fractions in the Zandmaas are underestimated. It is expected that the combined influence of non-linearity (at high Shields values) and hiding and exposure determines this. Considering that only MPM for all fractions (and hiding and exposure with Ashida and Michiue) results in too low sediment transport rates for fine material, we decided to adopt the Engelund-Hansen formulation for fine material (< 1mm) and keep the MPM formulation for coarse material. Hiding and exposure is still used, but only affects the mobility of coarse fractions. As the very fine fractions are modelled with Engelund Hansen this process is not included (Engelund and Hansen does not include a critical shear stress to which this effect is applied). For high shear stresses (floods) this seems to be a justified assumption, as under these conditions the fine sand will be partially suspended and highly mobile. Results show that the sediment transport shows less abrupt gradients than MPM and overall higher sediment load (Figure 3.7). Although the annual sediment transport is somewhat higher than previously expected – especially during years with a high peak discharge (< 2004, shown as lighter colours) – the order of magnitude is generally in the right range.

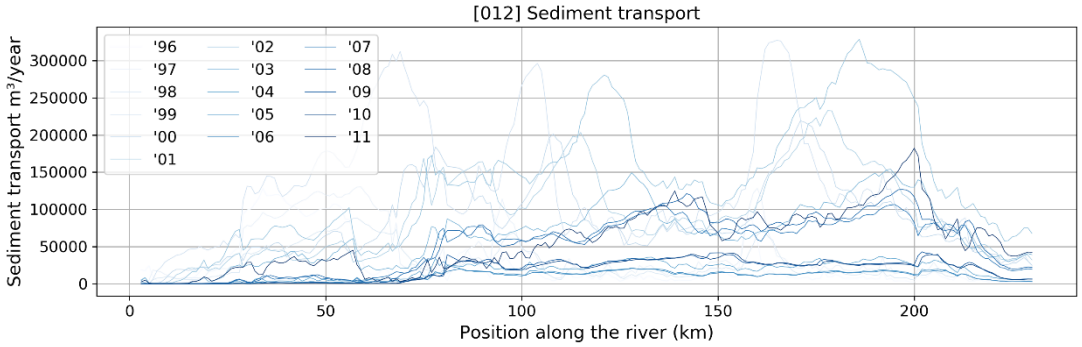

Figure 3.7 Sediment transport for simulation set 5 (j95, 1995-2011) with MPM+EH

[12] This formula is a Meyer-Peter and Müller type of formula, but with parameters that can be modified by the user

The bed level change over the period 1995-2011 shows (Figure 3.8) that the model simulations produce an erosional trend upstream from Roermond, while showing little change downstream. This is generally in line with expectations (section 2.3.1.2), although the erosional trends downstream from Roermond are not reproduced. However, we note that none of the simulations across all formulas and variations in settings were able to reproduce a general erosional trend across the entire Meuse. Both the sediment transport and the bed level changes show comparable results with the simulation set 6 (j11, 1995-2011), which points to little secondary effect of human intervention.

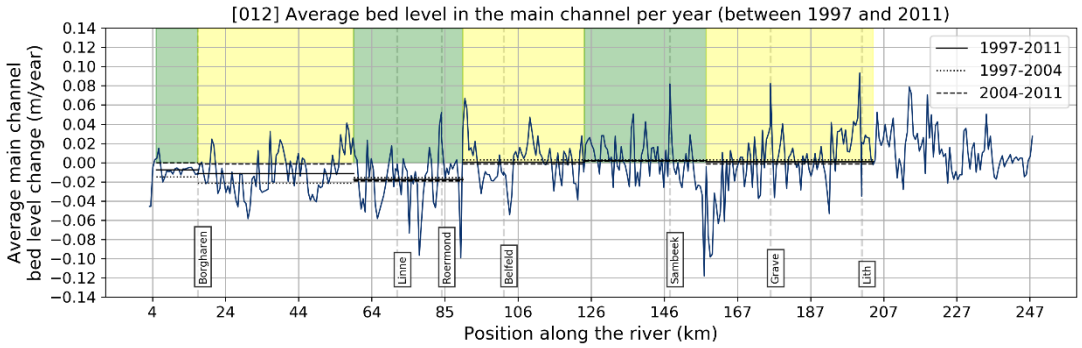

Figure 3.8 Average bed level change for simulation set 5 (j95, 1995-2011) with MPM+EH

Given the favourable results for sediment transport loads and bed level changes, we proceeded to test the celerity of bed level disturbances. To this end, we constructed five different artificial trenches and ran a simulation from 1995 to 2011 to test the propagation of these trenches, see figure 3.9.

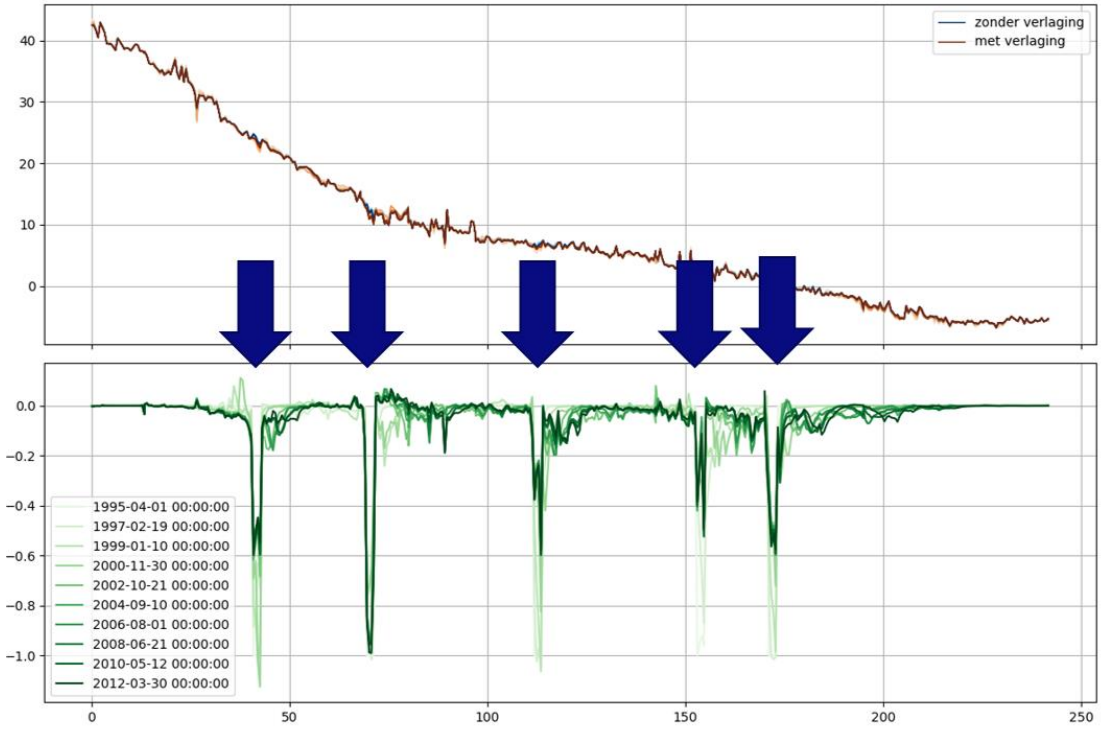

Figure 3.9 The location of the five trenches. Each trench was 2 km long and 1 meter deep.

The bed level celerity was best observed at the centre one of these five trenches. A closer look at one of the trenches (Figure 3.10) shows that the front propagates with approximately 10 km over a period of 17 years, which corresponds to a celerity of 500-600 m/year. This is higher, but within the same order of magnitude, as the 200-300 m/year estimated by Sieben (2011).

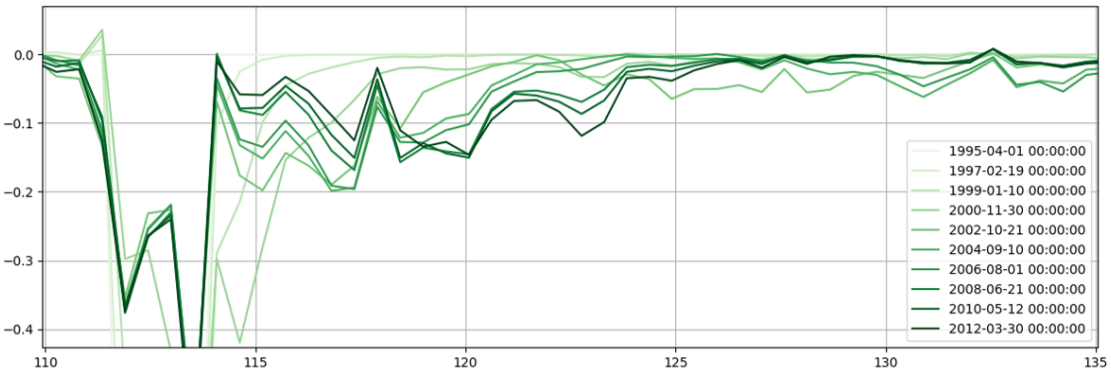

Figure 3.10 Close look at the erosion front of the middle trench.

Given the relatively high sediment transport rates, simulations with MPM+EH using lower values for the calibration factor (A_{cal}) and various values for the ripple factor were performed as well. None of those combinations were found to improve on the results for sediment transport and propagation speed above.

3.2.2 Morphodynamic validation

The MPM+EH combination was performed on the period 2011-2019 as well (simulation sets 7 and 8). Results show that the sediment transport rates are well within expected bounds (Figure 3.11), which further reinforces the idea that transport rates (and morphological changes) were so pronounced in the period 1995-2004 because of a sequence of years with a relatively high peak flood discharge. The morphological change in this period (Figure 3.12) generally shows the same trends as the calibration period – which suggest that an erosional trend is still being simulated upstream from Roermond – although a no erosion was expected in the Grensmaas (Figure 2.10, bottom panel). The same computation was performed with the j19 model. Although the j19 model shows overall more deposition (most notably on the Plassenmaas), the general trends are comparable to the j11 model. Full results can be found in Appendix F.2.

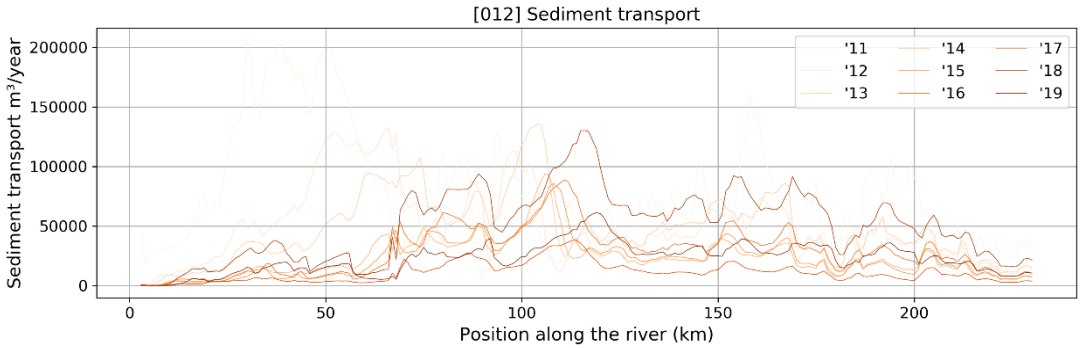

Figure 3.11 Sediment transport rates in the validation period with simulation set 7 (j11, 2011-2019)

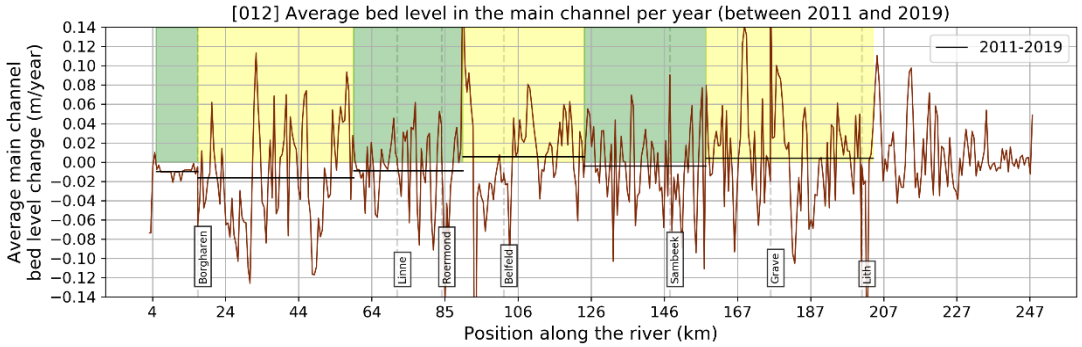

Figure 3.12 Morphological change in the validation period with simulation set 7 (j11, 2011-2019)

4 Discussion

4.1 Notes for model users

Comparing the results of morphological models with observations is challenging, not in the least because, to a far greater extent than hydraulic modelling, observations are very uncertain. This extends not only to transport rates but also to bed level measurements and the celerity of bed disturbances. In this study, we tried to find a balance between observations, how uncertain they might be, and what should be expected based on our understanding of the physical processes, to determine how well the models reproduce the physical system. This carries through to our notes for model users (section 4.2), which contains some provisions to the limitations inherent in morphodynamical modelling.

The model results are, overall, plausible with regard to available measurements and in line with our understanding of the physical system. However, users are advised to observe the same provisions we took while developing the model, and augment model results with expert judgement.

4.2 Use cases and notes for model users

The 1D models developed within this project were constructed for studies into large scale changes and propagation of human intervention. The results shown in this report show that the propagation celerity of bed disturbances is within expected order of magnitude and that large-scale morphological changes are within expected bounds. Therefore, it can be reasonably expected that the model can be used for these purposes, within the scope, accuracy and provisions reported in this document.

There are a few use cases that these models are emphatically not suited for:

- detailed morphological studies on the scale of less than a few kilometres, e.g. to support the detailed design of human intervention. For these kinds of studies, a 2D model is being developed. The outcomes of the 1D model for scales of a few kilometres (a few grid cells) are only indicative with respect to their amplitude.
- hydrodynamic studies, for which we refer to the set of hydrodynamic models, both 1D and 2D, available for the Meuse. Details of the official available models for hydrodynamics are found for instance in “Factsheet Maas Generatie 5” (Rijkswaterstaat, 2018).

This is not an exhaustive list.

5 Conclusions & disclaimers

5.1 Conclusions

This report described the development of a 1D morphological model for the Meuse. The model was derived from the 5th generation SOBEK models and converted to D-HYDRO following a number of documented steps. The D-HYDRO results were compared to WAQUA (2D) results and showed favourable comparison with (morphologically important) main channel velocity, although water levels are generally higher (0-1 m) than in the 2D model.

A morphological setup was selected with a 40 layer sediment model consisting of the top layer and 39 substrate layers, and 10 sediment fractions varying from gravel to sand. The sediment composition model compares favourably to literature on the composition of the top layer and more recent research into the substrate layers.

The Meyer-Peter Müller formula is used for coarse fractions (>1 mm) and the Engelund-Hansen formula for the finer fractions. Results show overall sediment transport within expected bounds (20.000 m^3/year to 70.000 m^3/year), with higher annual loads in years with relatively high flood peaks. Simulations show erosive trends in the upper part of the Meuse, and little movement on the downstream part, which largely compares well with observations. A numerical experiment with the propagation of trenches shows that the celerity of bed disturbances (~500-600 m/year) is within the expected order of magnitude.

5.2 Recommendation for future model development and analysis

The models delivered with this report are marked as ‘version 1’. While these models were built with care, it is quite conceivable that future research leads to further improvements. We highly recommend adopting a version control system on future versions of these models, such that future improvements are well documented.

We see a few major points of improvement for future study. First, a better insight into the sediment balance of the Meuse could benefit improving the interpretation of morphological models tremendously. Second, a closer look into the changes in the Grensmaas after 2004, i.e. the rate of deposition that may or may not have reversed the erosional trend, would help interpret the result of our validation, which shows an erosional trend even after 2011.

Other technical improvement which may be considered for future work are:

- **Using a curved model.** In the current version of dflow1d it was necessary to straighten the model, in order to prevent non-physical energy loss in curved bends (section 2.1.4). The disadvantage of this approach is that it is not straightforward to plot georeferenced model results on a map. It is expected that a future version of the software eliminates the need for this work-around.
- **Bank erosion and human intervention.** River banks and human intervention can be a source (and sink) for sediment. Actively bringing in sediment to simulate bank erosion, or taking out sediment to simulate dredging works, may help improve comparison with measurements. As reference we refer to the testing of the pilot project 1 (PP1) evaluated by Sloff and Stolker (2000).
- **Active layer thickness.** In this model an active layer thickness of 1 m was used. An additional study with smaller active layer thickness – between 0.1 m and 1 m – is recommended. The active-layer thickness is associated to small-scale perturbations of the bed (e.g. bed forms, groyne flames) and the value of 1 m is considered the upper side of the range of possible

values. There are no data-analyses that can provide sufficient support to the choice of this value and the implications to the bed level and bed composition. Additional analysis is recommended.
- Size fractions. Along the length of the model a wide range of particle sizes can be observed, from pebbles to silt. In the model some fractions in the quite common sand/gravel range between 250 µm - 8 mm are represented only by a limited number of classes (clusters of sieve sizes). This is assumed to have impacts on the sorting processes in the bed. It is therefore recommended to investigate the effect of subdividing these large classes in smaller ones, using the original (boring) data sets.
- **Including storage areas.** Eliminating the storage areas was necessary for the proper functioning of the present version of D-HYDRO 1D. We expect that future versions of D-HYDRO 1D will have full support for storage areas. After improvement of this functionality, the storage can be reintroduced. This is expected to improve the diffusivity of shape of the discharge wave as it travels downstream, because storage areas model (temporary) retention in backwaters that do not contribute to conveyance of discharge
- **Steady state solver for hydrodynamics.** To reduce computation time, the use of a steady-state solver allows application of a quasi-steady approach. In the past it has been shown that this can significantly reduce the computation time (order of 100 times faster)

5.3 Recommendation for data collection & data analysis

In this project we encountered various limitations on (readily) available data, as well as opportunities for future improvement:

- A careful analysis of the celerity of bed disturbances following the various human interventions carried out in the period 1995-2019 (see section 2.3.1.2), to further corroborate the findings of Sieben (2011).
- Accurate simulation of flow velocities is a basic condition for accurate simulation of sediment transport. Lacking measurements, we based our hydrodynamic testing on 2D simulations of the flow field. However, the 2D model itself is not validated for accurate flow velocities. More measurements of flow velocities in main channel and flood plains will greatly contribute to the confidence of both the 2D as the 1D morphological models.
- The construction of a new sediment composition model based on all available data, including the report by Arcadis (2011).

References

Arcadis (2011) Inventarisatie en interpretatie ondergrondgegevens Maas. Opdrachtgever: Rijkswaterstaat Limburg, C03021.910426.0100.

Ashida, K., Michiue, M. (1973) Study on bedload transport rate in open channel flows. In: International Symposium on River Mechanics, pp. 1–12.

Asselman, A., Barneveld H.J., Klijn, F., van Winden, A., Postma, R. (2018) Het verhaal van de Maas. Publicatie Platform Rivierkunde van Rijkswaterstaat.

Berkhout, W.A. (2003) Modelling of large-scale morphological processes in sand-gravel rivers. Analytical and numerical analysis of graded morphological processes in the River Meuse. M. Sc. Thesis Universiteit Twente. No.2003.034x. February 2003

De Jong, J. (2019) Ontwikkeling zesde-generatie Maas model. Deltares rapport 11200569-003-ZWS-0014 versie 0.8. Concept. December 2019.

De Jong, J. (2020) Toepassing van RGWM in RWsOS – Pilot D-HYDRO Maas, Deltares memo 11205258-002-ZWS-0006, 7 mei 2020

De Jong, W. (2005) Onzekerheidsanalyse bodemverandering Grensmaas: Een onderzoek naar de onzekerheid in de met SOBEK-graded gemodelleerde bodemverandering van de Grensmaas ten gevolge van de variatie in de afvoer. Royal Haskoning technisch rapport R0002/R/WDJ/Nij, MSc thesis Universiteit Twente, Augustus 2005.

Duizendstra, D. (1999) Sedimenttransport in de Grensmaas: Transportcapaciteit en aanbod van sediment. Rijkswaterstaat RIZA werkdocument 99.158X, Nov. 1999

Engelund, F., and E. Hansen (1967), A Monograph on Sediment Transport in Alluvial Streams, 62 pp., Teknisk Frolag, Tech. Univ. of Denmark, Copenhagen.

Gerretsen, J.H. (1968) Materiaaltransport door de Maas. Rijkswaterstaat, directie Limburg, Nota 68.8

Kragten (2018) Analyse Bodempeilingen Maas. Handleiding. Opdrachtgever: Rijkswaterstaat Zuid-Nederland. GDV083-0001

Meyer-Peter, E., and R. Müller (1948) Formulas for bed-load transport, in Proceedings of the 2nd Meeting of the International Association of Hydraulic Structures Research, pp. 39–64, Int. Assoc. of Hydraul. Res., Madrid.

Murillo-Muñoz, R.E. (1998) Downstream fining of sediments in the Meuse River. UNESCO-IHE, M.Sc. Thesis.

Murillo-Muñoz, R. & Klaassen, G.J. (2006) Downstream fining of sediments in the Meuse River. Proceedings of River Flow 2006, Ferreira, Alves, Leal & Cardoso (eds), p. 895.

Rijkswaterstaat (2018) Factsheet Maas Generatie 5, versie 2018_2, URL: www.helpdeskwater.nl/publish/pages/132741/factsheet-maas-generatie_5-v2018_2.pdf

Schropp, M.H. (2000) Evaluatie zomerbedverdieping Gennep – Grave. Rijkswaterstaat RIZA Rapport 2000.017, April 2000.

Sieben, I.J. (2011) Methodiek inschatting morfologische effecten in het zomerbed door lokale rivieringrepen: Update December 2011. Rijkswaterstaat Memo, d.d. 12 november 2010

Sloff, C.J. & Barneveld, H.J. (1996) Morfologisch model Zandmaas: MAASMOR 1995. WL | Delft Hydraulics rapport Q2066

Sloff, C.J. & Stolker, C. (2000) Calibratie SOBEK-Gegradeerd Zandmaas. WL | Delft Hydraulics rapport Q2589, Mei 2000

Van Dongen, B. & Meijer, D. (2008) Zomerbedveranderingen van de Maas (1889 – 2007). Meander rapport 10314 / 4500103893

Van Looy, K. (2009) Sedimentbeheerplan Gemeenschappelijke Maas. Rapporten van het Instituut voor Natuur- en Bosonderzoek 2009 (INBO.R.2009.15). Instituut voor Natuur- en Bosonderzoek, Brussel.

Van Manen, G.R., Onneweer, J.G., van den Berg, J.H. (1994) Ruimtelijke variatie van de sedimentaire structuur en textuur van de bedding van de Grensmaas (stuw Borgharen, km 15.5 – Maaseik, km. 52.7).

Wegman, C. (2019) Dikte Afdeklaag fijne zanden – Maas. HKV memo PR4107.11

Wilbers, A. (1996) The Border Meuse over the years. A study into the morphological changes of the bed of the Meuse River in the period 1978 through Faculteit Ruimtelijke Wetenschappen, Vakgroep Fysische Geografie, Universiteit Utrecht. Nederland (in Dutch)

Wilcock, P. R., and J. C. Crowe (2003) Surface-based transport model for mixed-size sediment, J. Hydraul. Eng., 129, 120–128, doi:10.1061/(ASCE)0733-9429(2003)129:2(120

Wolters, A.F. (1998) Morfologische ontwikkeling van de maas tussen Gennep en Grave - ten gevolge van baggerwerkzaamheden, RIZA rapport 98.060, 6 november 1998.

A Model build logs

A.1 J19 model

SOBEK models

Work version	Notes
W1	Original sobek-maas-j19_5-v2 model. SOBEK software version 3.17.45036
W2	Updated to SOBEK-3.19.47018
W3	All river weirs converted to simple weirs (river weirs not supported in dflow1d)
W4	Extra resistances removed. Cross-section BBN4 removed (in same location as BBN3, which is not allowed in dflow1d)
W5	Simplified RTC. Removed all FEWS specific nodes. All gated weirs/orifices converted to general structures (RTC for orifices have only limited support in dflow1d)
W6	Further simplified RTC.
W7	Changed boundary conditions to steady-state simulation and run time to January 2000 (every model will use 01-01-2000 as reference date)
W8	Removed Q(h) laterals & shortcut RTC: Shortcut 'Linne' (rkm 70-73) Shortcut 'Maasplassen1' (rkm 77-81) Shortcut 'Maasplassen2' (rkm 77-79)
W9	Removed regional systems, schutverlies RTC, retention area (RTC + branches), julianaknaal, lateraalkanaal, Maas-waal kanaal, afgedamde maas, roer, oude maas. Changed Sluis Borgharen PID input from Borgh-Julianakanaal LMW station to 15.00_MA (LMW station no longer exists in model). Changed Sluis Linne PID input from Heel_boven to 67.00_MA_Z. (Heel_boven station no longer exists in model). *w9 is the final SOBEK version*

Dflowfm models

Work version	Notes
W0	Converted flow model from Sobek w9. Does not run.
W1	Manually fixed to the flow model. Runs successfully
W2	Added RTC, fixed integrated model xml. *This model version is compared with SOBEK w9*
W3	Enable morphology to output main channel velocities (*this is output from the morphological module and can only be output if morphology is enabled).* Composition and bed level update is disabled.
W4	Straightening of the model domain Changed levee transition height to 0.75 m
W5	Uniform roughness field
W6	Main channel width fix
W7	Continued main channel width fix, after comparing the methodology with the Rhine project the main channel width is adjusted further. *This is the model which is used for calibration with WAQUA*
W8	*Model W3 with morphological parameters. This model is made in order to have a morphological simulation with the real (non-straightened) sediment data. The output of this simulation is used to convert de morphological data coordinates to the straightened grid.*
W9	*Model W7 with morphological data. The coordinates of the morphology are converted using a conversion table with real and straight coordinates. In this version the sedimentdata from the Zandmaas is partly replaced by dummy data, since the fractions in the Zandmaas and Grensmaas were different*
W10	*Morphological model with the correct sediment data for the Zandmaas.*
W11	*Total width is set equal to the flow width, storage area is removed.*

Work version	Notes
W12	*Main channel roughness to manning 0.035 $m^{1/3}/s$* *This is the final model used for morphodynamic calibration*

A.2 J11 model

SOBEK models

Work version	Notes
W1	Original sobek-maas-j11_5-v3 model. SOBEK software version 3.4
W2	Updated to SOBEK-3.5.7 • No error during import • Validation flow ok • Validation rtc not ok. Stuw Linne not connected, fixed manually

W3	Updates to SOBEK-3.9
	• No error during import
	• Renamed model from 'maas_2011' to flow model
	• Validation flow error;
	  ○ In some cross-sections floodplain 2 roughness section is used, but floodplain 1 is empty. This is not allowed anymore. Fixed manually by converting those to floodplain 1. Affected cross-sections: 1731__1m 1731__2, etc. en Kraaijenbersche Plas retention.
	  ○ The maximum flow width is larger than the total flow width in some cross-sections. This is not allowed anymore. Used auto-fix provided by DeltaShell.
	• Validation RTC error:
	  ○ "PID set points not a multiple of the model timestep". Some lines in PID table are invalid. All offending lines are manually fixed.

W4	Update to 3.7.13 • No conversion error • Flow model validation ok • RTC model validation not ok ○
W5	Update to 3.7.19 • No conversion error • Validation ok • Export to DIMR ok
W6	Conversion of weirs to simple weirs
W7	Removal of extra resistances
W8	Conversion of orifices to general structures. Removed cross-sections which were in the same location with another cross-section: DB_AA_23b, DB_AA_22b, DB_AA_193b. Changed crest level of Heelpl1 and Heelpl2 to 20.75 (from 20.70), because surrounding cross-sections are located at 20.75
W9	Copied the unified RTC model. Renamed observation points such that name is identical to id.
W10	Changed boundary conditions to QH (downstream) and steady discharge (upstream), time settings to 2000/01/01. Initial depth & flow to zero.
W11	Removed Dommel/Aa system Removed all 'schutverliezen' Removed retention areas Removed Julianakanaal Removed Lateraalkanaal Removed Maas-Waalkanal Removed sluis Huemen, Roer Balgstuw, Removed Oude Maas, Afgedamde Maas and Geleenbeek
W12	Copied RTC and XML from j19

Dflowfm models

Work version	Notes
W0	Converted flow model from Sobek w9. Does not run.
W1	Manually fixed to the flow model. Runs successfully
W2	Added RTC, fixed integrated model xml. *This model version is compared with SOBEK w9*
W3	Enable morphology to output main channel velocities (*this is output from the morphological module, and can only be output if morphology is enabled).* Composition and bed level update is disabled.

Work version	Notes
W4	Straightening of the model domain Changed levee transition height to 0.75 m
W5	Uniform roughness field
W6	Main channel width fix *This is the model which is used for calibration with WAQUA*
W12	*Main channel roughness to manning 0.035 $m^{1/3}/s$* *This is the final model used for morphodynamic calibration*

A.3 J95 model

SOBEK models

Work version	Notes
W1	Original sobek-maas-j11_5-v3 model. SOBEK software version 3.4
W2	Updated to SOBEK-3.5.7 • No error during import • Validation flow ok • Validation rtc not ok. Stuw Linne not connected, fixed manually

W3	Updates to SOBEK-3.9
	• No error during import
	• Renamed model from 'maas_2011' to flow model
	• Validation flow error;
	  ○ In some cross-sections floodplain 2 roughness section is used, but floodplain 1 is empty. This is not allowed anymore. Fixed manually by converting those to floodplain 1. Affected cross-sections: 1731__1m 1731__2, etc. en Kraaijenbersche Plas retention.
	  ○ The maximum flow width is larger than the total flow width in some cross-sections. This is not allowed anymore. Used auto-fix provided by DeltaShell.
	• Validation RTC error:
	  ○ "PID set points not a multiple of the model timestep". Some lines in PID table are invalid. All offending lines are manually fixed.

W4	Update to 3.7.13 • No conversion error • Flow model validation ok • RTC model validation not ok ○
W5	Update to 3.7.19 • No conversion error • Validation ok Export to DIMR ok
W6	Conversion of weirs to simple weirs
W7	Removal of extra resistances
W8	Conversion of orifices to general structures. Removed cross-sections which were in the same location with another cross-section: DB_AA_23b, DB_AA_22b, DB_AA_193b. Changed crest level of Heelpl1 and Heelpl2 to 20.75 (from 20.70), because surrounding cross-sections are located at 20.75
W9	Copied the unified RTC model. Renamed observation points such that name is identical to id.
W10	Changed boundary conditions to QH (downstream) and steady discharge (upstream), time settings to 2000/01/01. Initial depth & flow to zero.
W11	Removed Dommel/Aa system Removed all 'schutverliezen' Removed retention areas Removed Julianakanaal Removed Lateraalkanaal Removed Maas-Waalkanal Removed sluis Huemen, Roer Balgstuw, Removed Oude Maas, Afgedamde Maas and Geleenbeek
W12	Copied RTC and XML from j19 Model runs in about 15 sec for 20 days.

Dflowfm models

Work version	Notes
W0	Converted flow model from Sobek w9. Does not run.
W1	Manually fixed to the flow model. Runs successfully
W2	Added RTC, fixed integrated model xml. *This model version is compared with SOBEK w9*
W3	Enable morphology to output main channel velocities (*this is output from the morphological module, and can only be output if morphology is enabled).* Composition and bed level update is disabled.
W4	Straightening of the model domain Changed levee transition height to 0.75 m
W5	Uniform roughness field
W6	Main channel width fix *This is the model which is used for calibration with WAQUA*
W12	*Main channel roughness to manning 0.035 $m^{1/3}/s$* *This is the final model used for morphodynamic calibration*

B Main channel width adjustments

Heavy accretion of the main channel section can lead to higher bed levels in the main channel than the floodplain. This is not allowed and will lead to premature termination of the simulation. Widening of the main channel, increases the lowest point in the floodplain and therefor increases the maximum accretion before the premature termination.

Figure B. 2 shows the procedure to adjust the main channel width. The main elements are the detection of the “knikpunt” (break of slope) and the manual adjustment if the main channel is too narrow.

The “knikpunt” is the location where flow width of the cross-section (red line in Figure B. 1) changes from convex to concave. The upper figure in Figure B. 1 shows the original cross-section, the lower figure shows the adjusted cross-section. The dashed line shows the height of the main channel and the background colours depict the main channel and floodplain width.

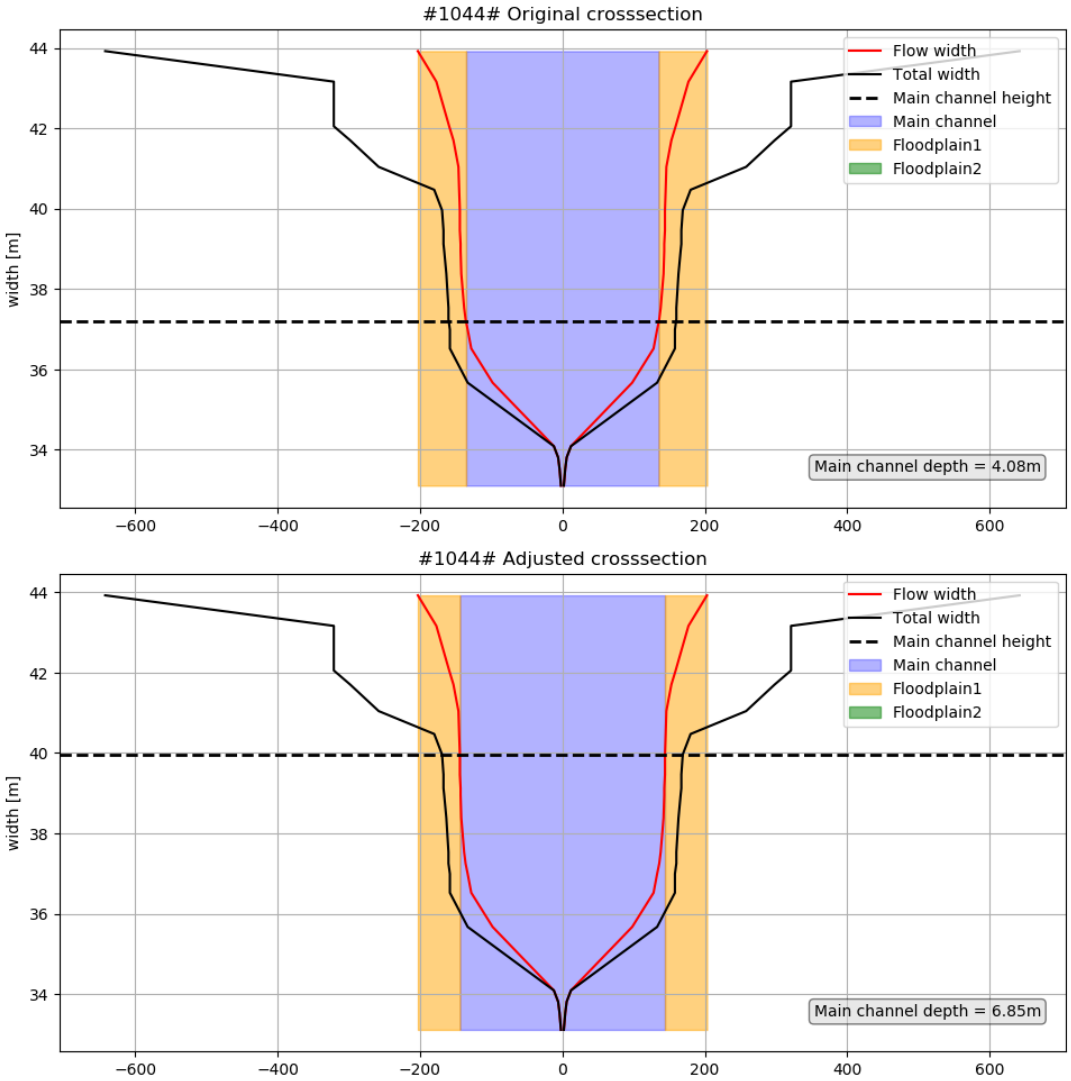

Figure B. 1 Example of automatic main channel width adjustment

If the main channel depth is smaller than 5 meter after the automatic adjustment manual adjustment is required. This is mostly the case when the automatic adjustment fails to find the “knikpunt”. In the manual adjustment the width is set to the first “knikpunt” in the total width of the cross-section. The manually adjusted main channel widths are stored in a spreadsheet in order to be able to reproduce the results.

The entire procedure for main channel adjustment is shown in the flowchart in Figure B. 2.

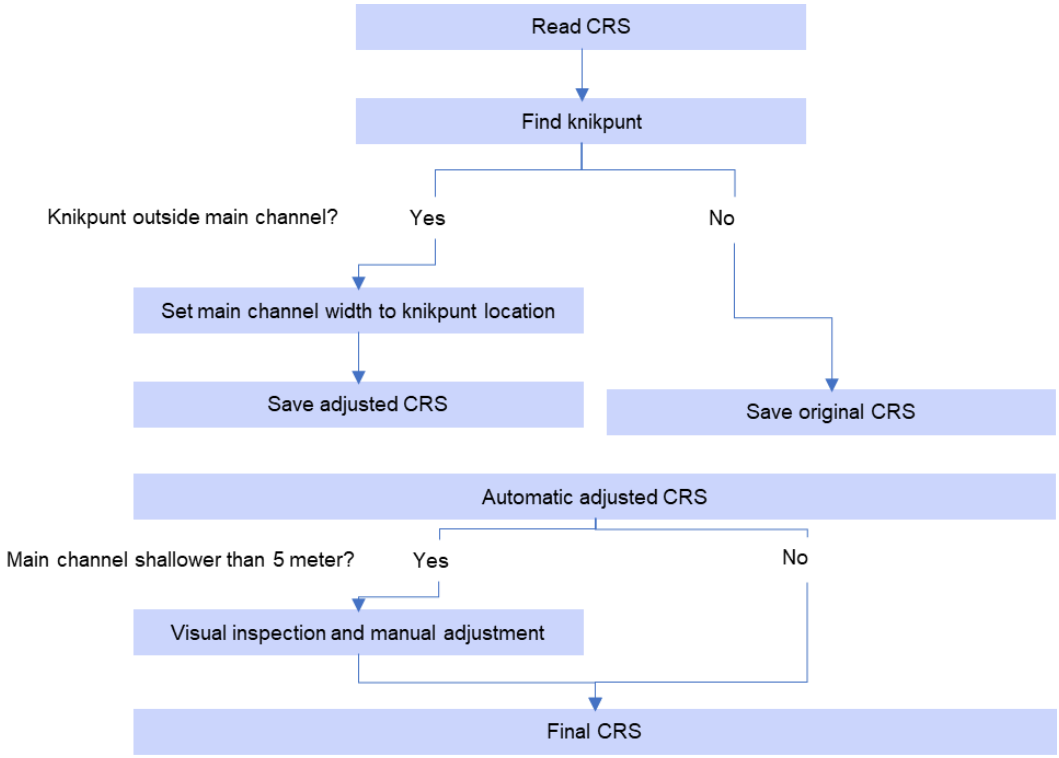

Figure B. 2 Main channel width adjustment per cross section (CRS)

C Removal of storage width

To convert the model to dflow1d, and subsequently to run it for morphodynamics, the storage parts have been removed from the schematisation. This is necessary to prevent undesired numerical behaviour that has been observed with including the storage terms in the numerical solution. Storage can relevant for damping and propagation of unsteady flows (flood waves). This Annex presents an analysis to estimate the errors that are made in hydraulics and morphology by removing the storage width.

It is relevant to mention that the exclusion of storage terms has various relevant benefits for morphological simulations in case speeding-up of simulations is desired. Storage has therefore been removed (or ignored) in all previous morphodynamic simulations for the Rijntakken and Maas. These used SOBEK-RE with a quasi-steady approach, in which storage does not have any relevance. The main advantages of applying such a quasi-steady approach are:

- Behaviour of other models with quasi-steady morphology (including 2D DVR) is similar;
- The use of large morphological factors is less problematic;
- Numerical solutions are consistent and accurate.

The propagation speed of a flood wave is roughly estimated (for a model with Manning friction and wide rectangular cross-section):

$$c = \frac{5}{3}\frac{B_f}{B}u$$

With B_f = flow width, and B is the total width at the water surface (including storage width). For B=B_f it can be found that the speed of the flood wave is 5/3·u, and is therefore faster than the flow velocity u. For B_f<3/5·B the flood wave will move slower than the flow velocity. For a situation with tabulated cross section with flood plain the following relation can be used.

$$c = \frac{5}{3}\frac{1}{B}\left(B_{f,m}u_m + B_{f,w}u_w\right)$$

Here index m relates to main channel, and index w relates to flood plain (winterbed).
Damping of the wave can be roughly estimated as (sine-shaped wave in rectangular channel):

$$\frac{dQ\max}{ds} = -5.8\frac{\left(B/B_f\right)^2}{C^2 S_0^2}\cdot\frac{a_0}{T^2} \quad [m^3/s/m]$$

Where a_0 is the amplitude, C is the Chézy coefficient for hydraulic roughness, S_0 is the slope, and T is the period. It shows that with increasing B/B_f (more storage) the damping also increases. Also, an increasing roughness (decreasing C) or reduced bed slope will provide more damping. Finally, also for a high amplitude or a shorter wave, a stronger damping will occur.
For example, in the Meuse the ratio B_f/B is approximately 0.8 for the width at high flows. In this example we consider the reduction of the discharge peak (and the associated water level difference) between the Stevensweert/Maasbracht km 61.25 and Heerewaarden km 202.3 (distance about 140 km).

The numbers corresponding to the damping of a 1600 m^3/s flood peak and a period T=8 days (a typical duration for the Meuse) are shown below:

B_f/B	0.8	0.9	1
C	45	45	45
S_0	0.0001	0.0001	0.0001
a_0	1600	1600	1600
T	691200	691200	691200
dQmax/ds	-0.00150	-0.00118	-0.00096
ΔQ over 140 km	-209.8	-165.8	-134.3
ΔQ over 140 km (%)	-13.1%	-10.4%	-8.4%

These estimates have been compared to outcomes of simulations with a SOBEK-RE model for the Zandmaas, Figure C. 1 to Figure C. 3 below. When computed with B_f/B = 1 (no storage, including removal of weirs) the damping of the flood peak released at Maasbracht (inflow boundary) is expected to be in the order of 162 m^3/s. Effectively this corresponds to the damping for B_f/B = 0.9, which is explained since only the storage from the tabulated cross-sections were removed in the model, but not the storage areas of the summer-dike sections. If storage is fully eliminated, the damping of the initially released flood wave is reduced from -210 m^3/s (B_f/B =0.75, confirmed in the table and in the figure) to -134 m^3/s. This means 76 m^3/s less damping on a flood peak of 1600 m^3/s.

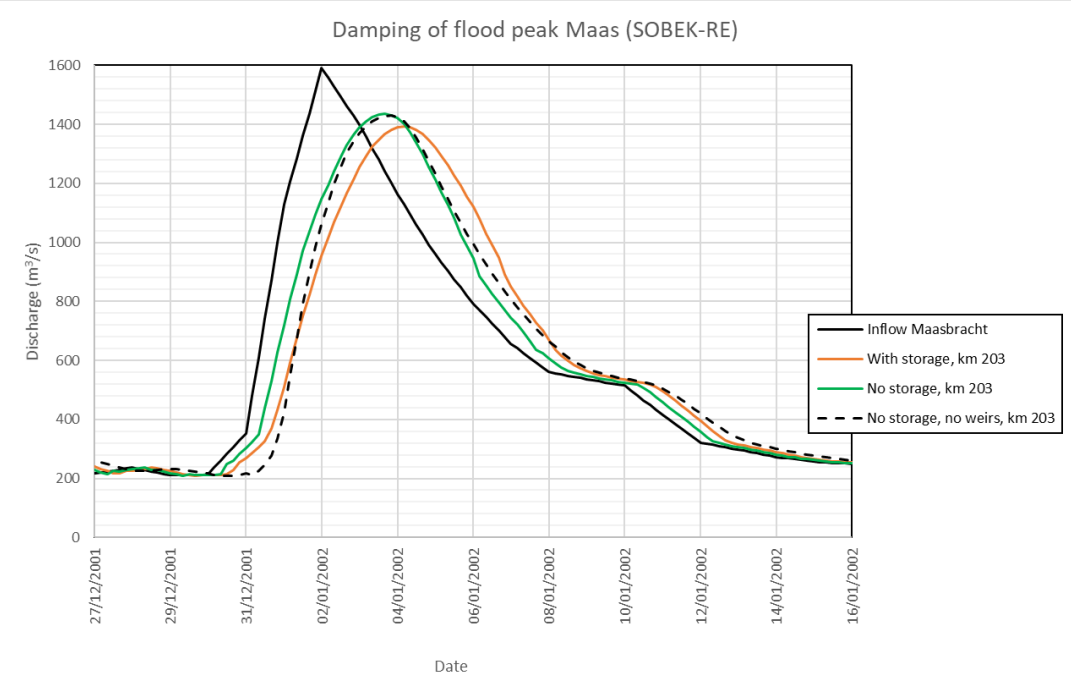

Figure C. 1 Computed discharge as function of time for a flood peak, at Maasbracht and at Lith (km 202.5), for simulations with storage, without storage, and without storage and weirs.

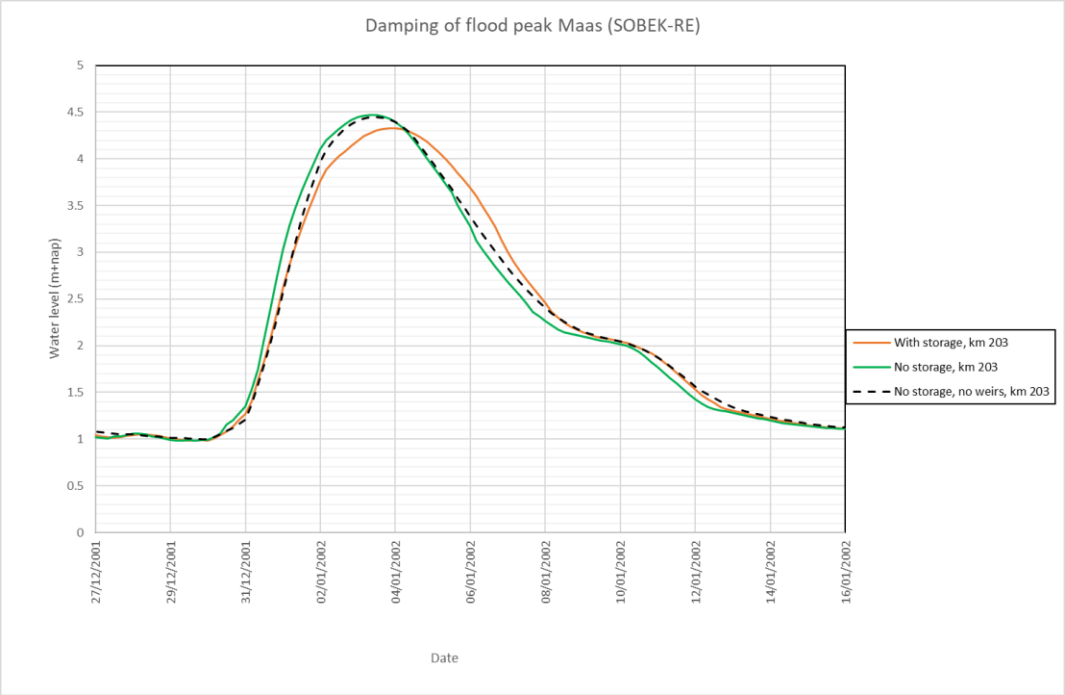

Figure C. 2 Computed water level as function of time for a flood peak, at Maasbracht and at Lith (km 202.5), for simulations with storage, without storage, and without storage and weirs.

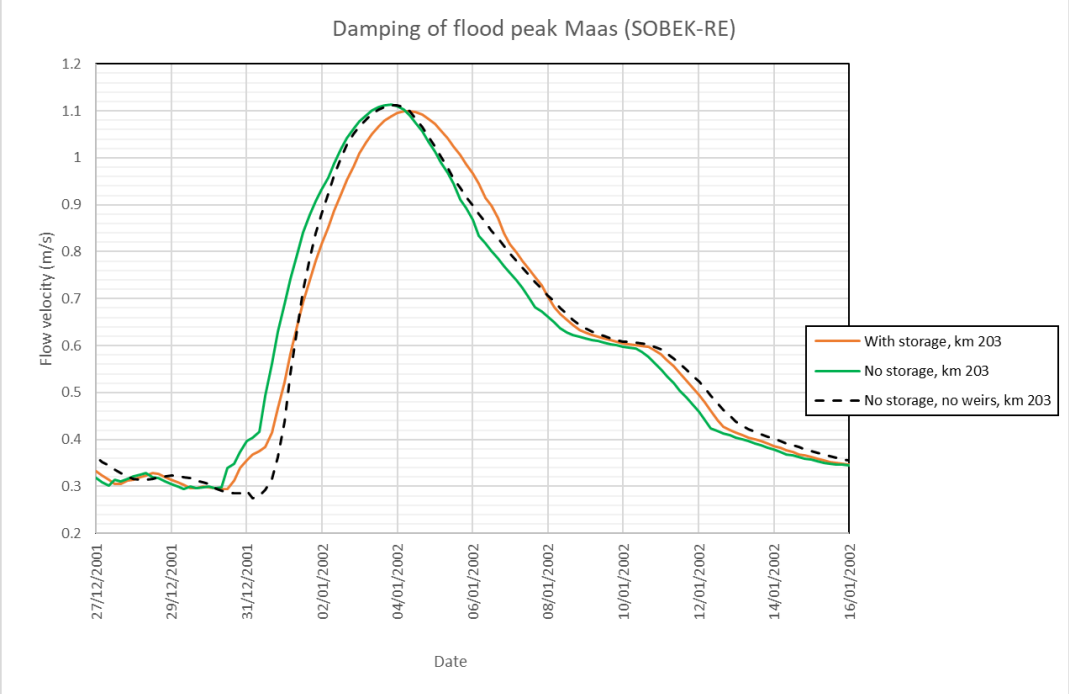

Figure C. 3 Computed flow velocity as function of time for a flood peak, at Maasbracht and at Lith (km 202.5), for simulations with storage, without storage, and without storage and weirs.

The theoretical formula for speed of the flood wave seems to overpredict the celerity with roughly 50% compared to the SOBEK simulation. In simulations without storage the flood peak arrives about 12 hours earlier at Heerewaarden. The flood level at the peak is about 15 cm lower when the storage is included. In these simulations the peak flow-velocity in the main channel is reduced from 1.11 m/s to 1.10 m/s (difference of 0.01 m/s, i.e. 1%) when storage is included.

The analysis shows that the impacts of eliminating the storage from the cross-section does not create a noticeable error with relevance for morphology. The error in flood peak flow velocity is in the order of 1%, causing an error in sediment-transport calculation of about 4%. That is very well within the ranges of accuracy of the morphodynamic approach.

D Sediment data conversion

The sediment data for the dflow1d-model comes from SOBEK-RE. To convert the sediment data from the SOBEK-RE-format to dflow1d the steps in Figure D. 1.

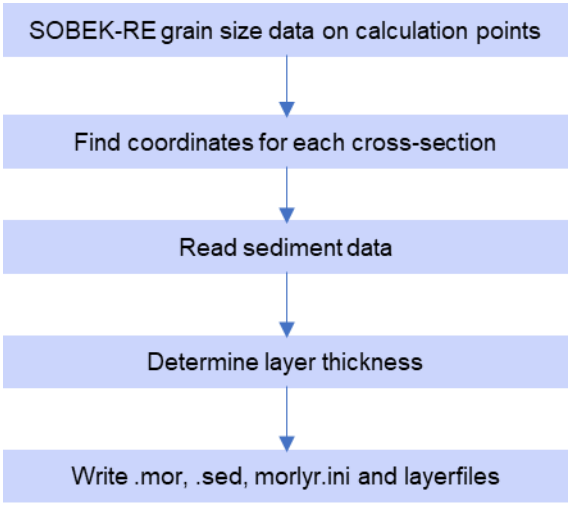

Figure D. 1 Sediment data conversion

Read SOBEK-RE-data

In SOBEK-RE sediment data is available at each combination of branch and chainage. The sediment data for the Meuse consists of 40 layers of 0.25 meter with 10 different sediment fractions (Table D. 1).

Table D. 1 Sediment fractions

Fraction	Lower bound (m)	Upper bound (m)	Fraction	Lower bound (m)	Upper bound (m)
1	0.00008	0.000125	6	0.004	0.016
2	0.000125	0.00025	7	0.016	0.0315
3	0.00025	0.001	8	0.0315	0.063
4	0.001	0.004	9	0.063	0.1
5	0.004	0.008	10	0.1	0.2

Coordinates

The branch-chainage combinations in SOBEK-RE do not have corresponding coordinates. In order to be able to use the data in dflow1d each branch and chainage needs to be converted to coordinates. With the following procedure branch and chainage combinations are translated to the coordinates of the straightened model.

1 Use the file “0gridsobek.prn” to convert SOBEK-RE branch-chainage to rivierkilometers
2 Use “hectometerpunten.shp” to convert the rivierkilometers to XY
3 Run both a curved and a straightened dflow1d-model
4 The order of the nodes are the same in both models, so the coordinates of these nodes can be used as a conversion table for real coordinates to straightened coordinates.

Determine layer thickness

The layer thickness is the total thickness of the morphologically active sediment. In SOBEK-RE the fixed underlayer is described by a layer where all sediment is of the largest fraction. The number of layers above this layer times 0.25 meter is the layer thickness for dflow1d.

Write dflowfm1d-files

The SOBEK-RE sediment-data is written to the following files:

- *.sed-file*: This files contains the data on all sediments, the characteristics of the 10 fractions are in this file.
- Per layer: (all these files are .xyz-files, on each row the coordinates and the corresponding value)
  - *Thickness file*: This file gives for each layer the thickness, if the layer is below the fixed layer from SOBEK-RE the value is 0 m, else the value is 0.25 m.
  - *Volume fractions per fraction*: values between 0 and 1 describing the amount of sediment from the fraction present at each location.

NB: In SOBEK-RE layer number 40 is the upmost layer, in dflow1d this is the other way around.

E Results hydrodynamic testing

E.1 Initial differences – manning = 0.025 $sm^{-1/3}$

E.1.1 Discharge Eijsden 250 m^3/s

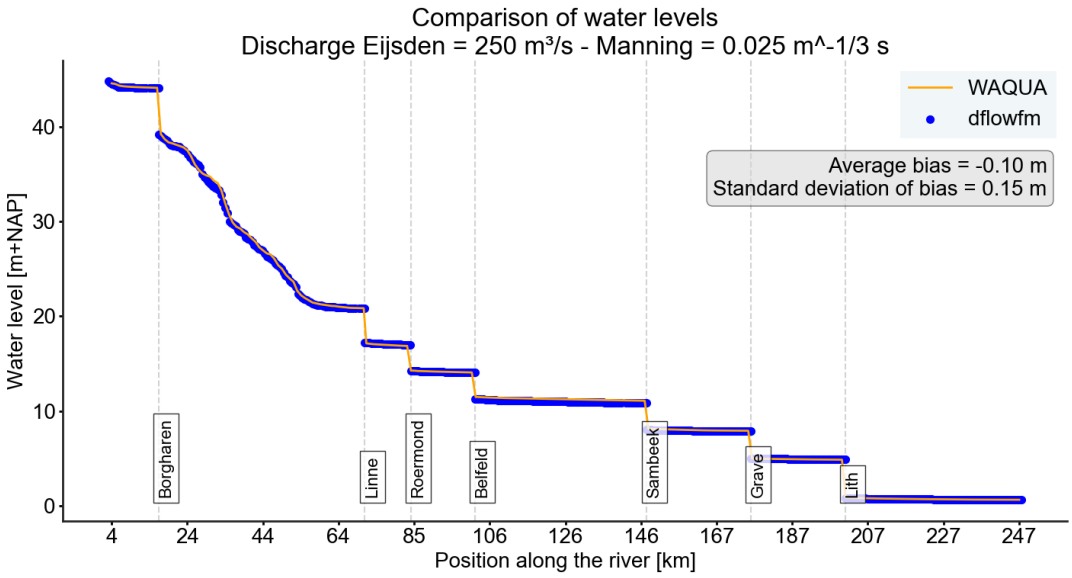

Figure E. 1 Initial comparison of main channel flow discharge $Q_{Eijsden}$ = 250 m^3/s

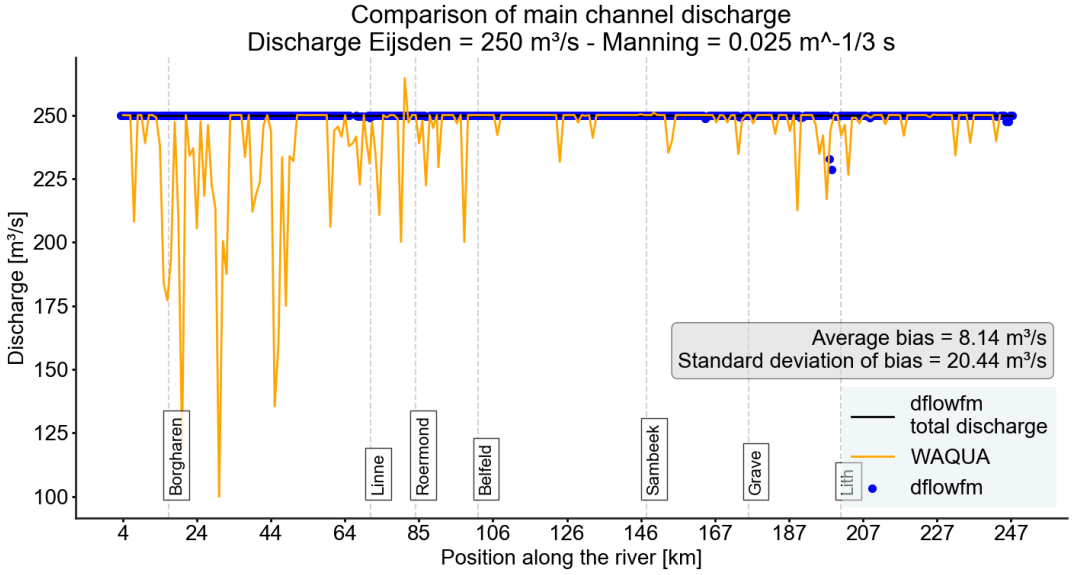

Figure E. 2 Initial comparison of main channel flow discharge $Q_{Eijsden}$ = 250 m^3/s. The apparent variation in 2D is an artefact of how the main channel discharge is computed; see section 2.2.

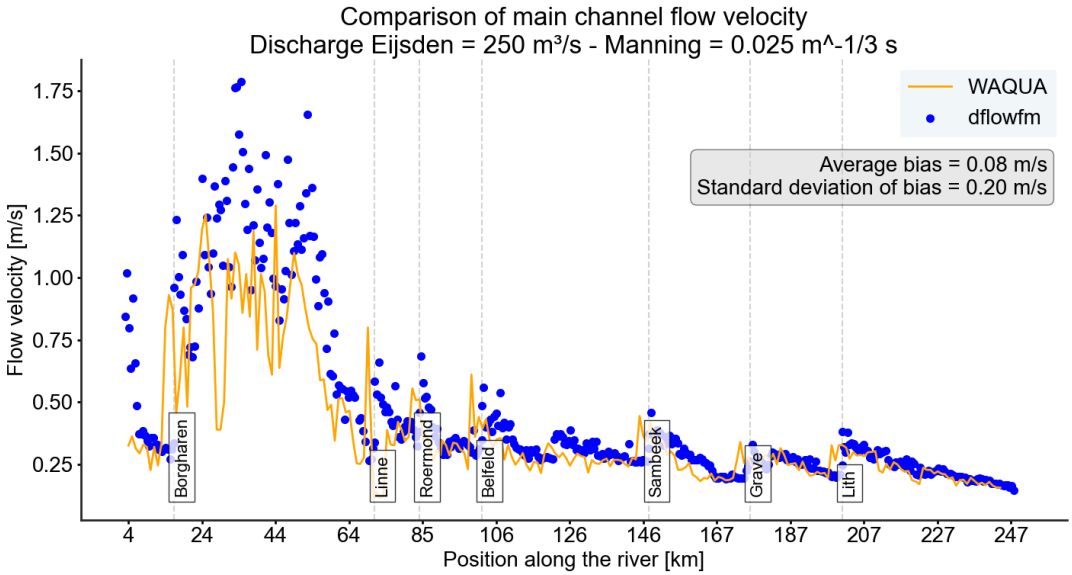

Figure E. 3 Initial comparison of main channel flow velocity $Q_{Eijsden}$ = 250 m³/s

E.1.2 Discharge Eijsden 800 m³/s

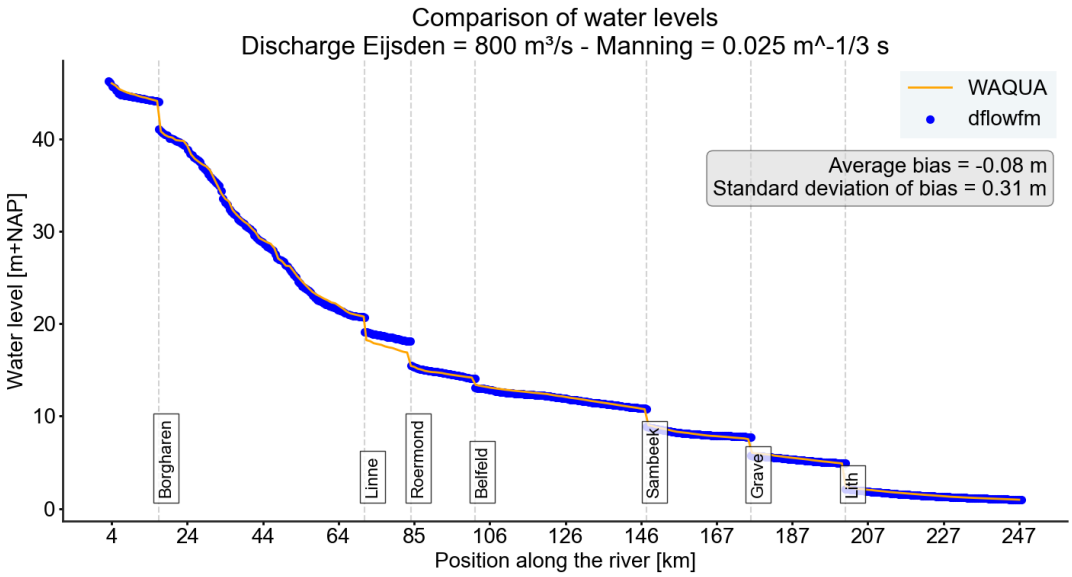

Figure E. 4 Initial comparison of main channel flow discharge $Q_{Eijsden}$ = 800 m³/s

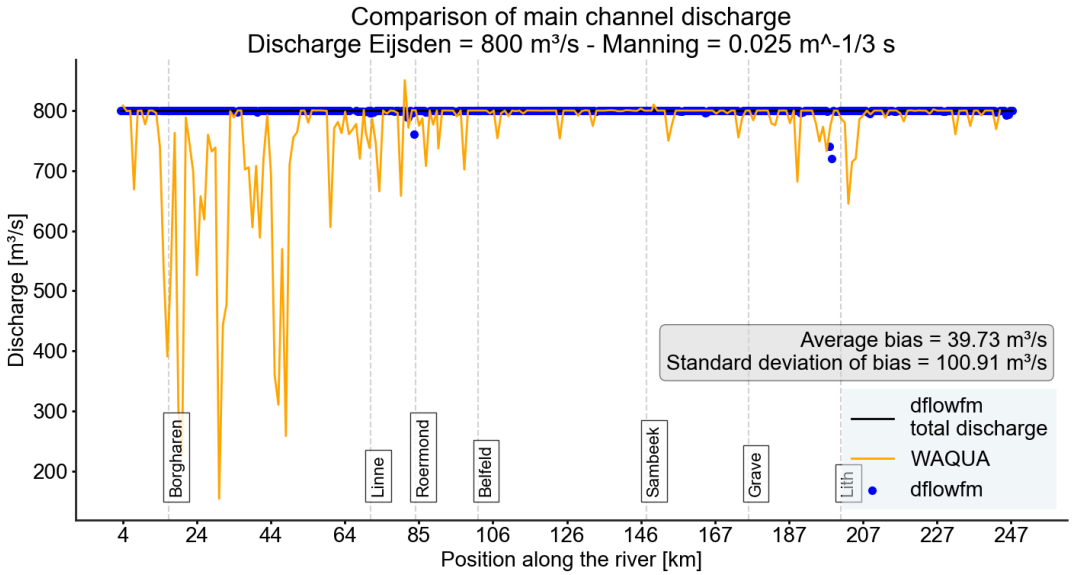

Figure E. 5 Initial comparison of main channel flow discharge $Q_{Eijsden}$ = 800 m³/s. The apparent variation in 2D is an artefact of how the main channel discharge is computed; see section 2.2.

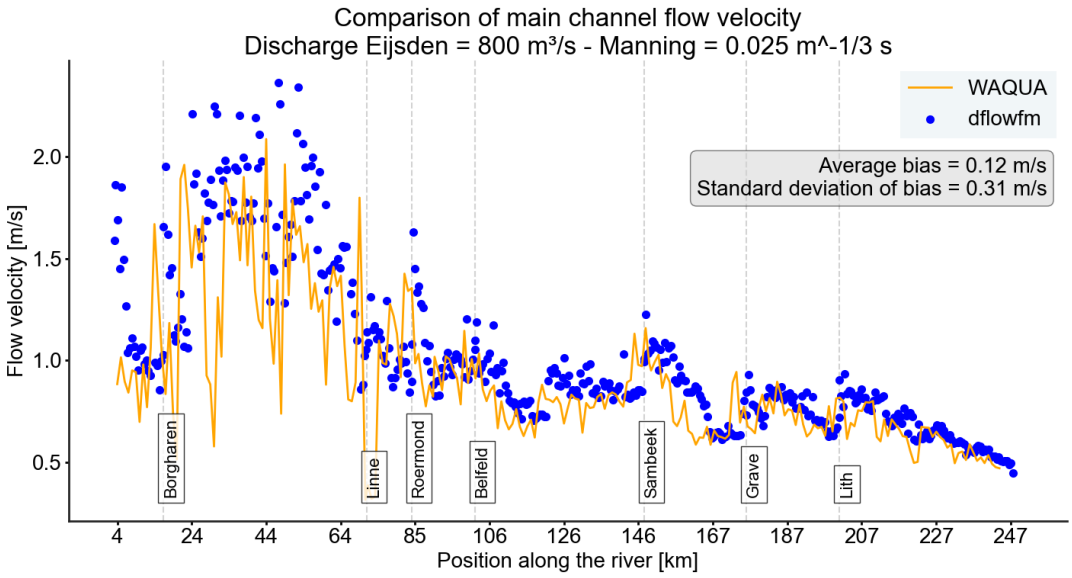

Figure E. 6 Initial comparison of main channel flow velocity $Q_{Eijsden}$ = 800 m³/s

E.1.3 Discharge Eijsden 1500 m³/s

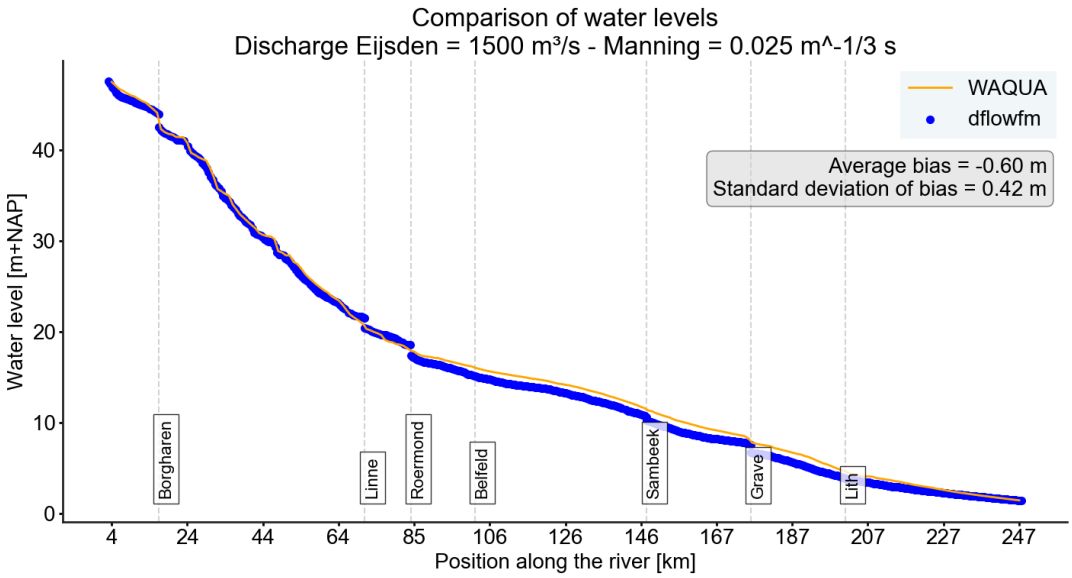

Figure E. 7 Initial comparison of main channel flow discharge $Q_{Eijsden}$ = 1500 m³/s

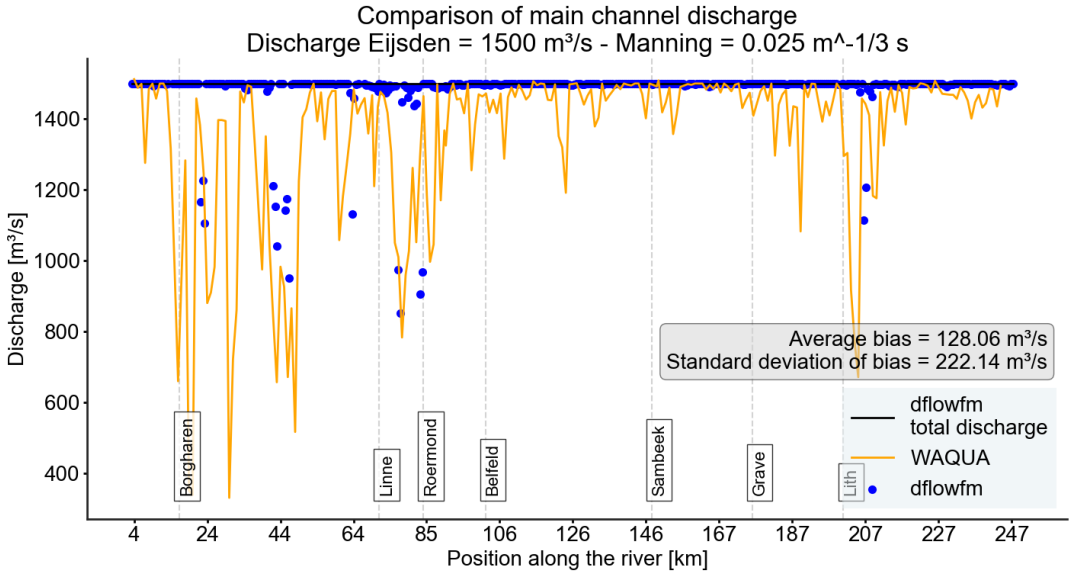

Figure E. 8 Initial comparison of main channel flow discharge $Q_{Eijsden}$ = 1500 m³/s. The apparent variation in 2D is an artefact of how the main channel discharge is computed; see section 2.2.

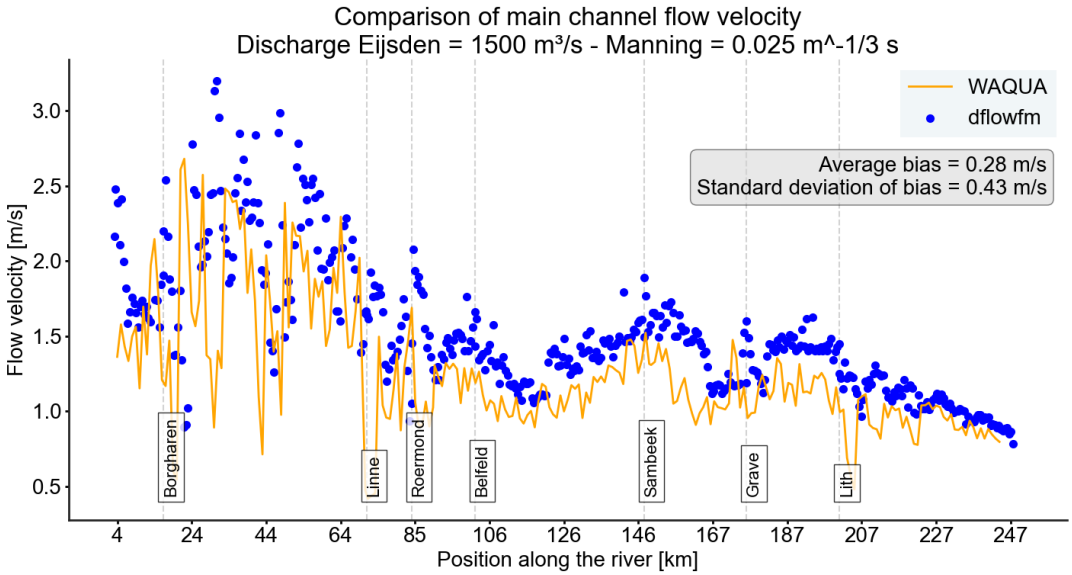

Figure E. 9 Initial comparison of main channel flow velocity $Q_{Eijsden}$ = 1500 m³/s

E.1.4 Discharge Eijsden 2260 m³/s

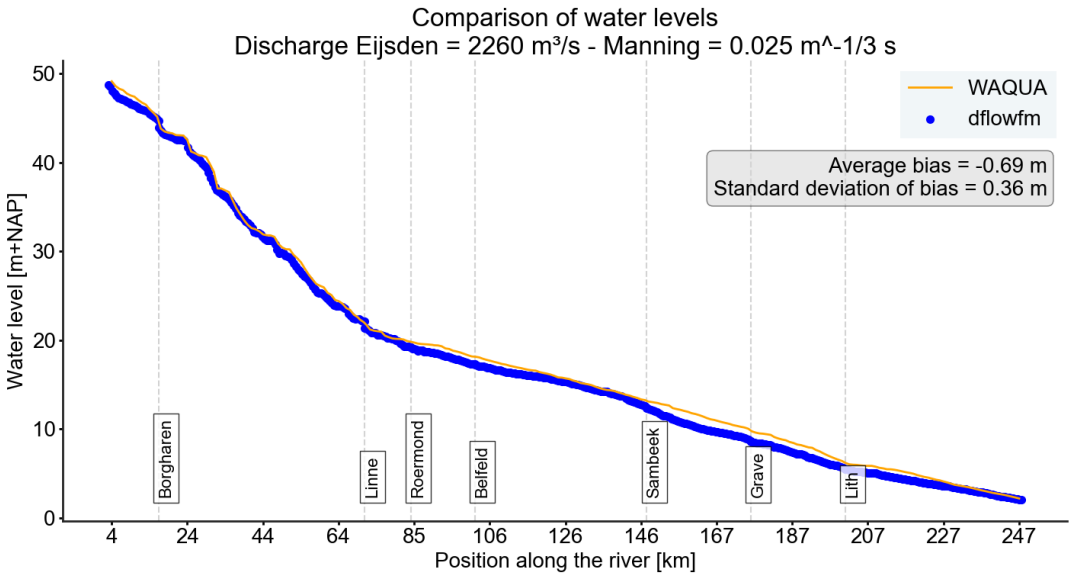

Figure E. 10 Initial comparison of main channel flow discharge $Q_{Eijsden}$ = 2260 m³/s

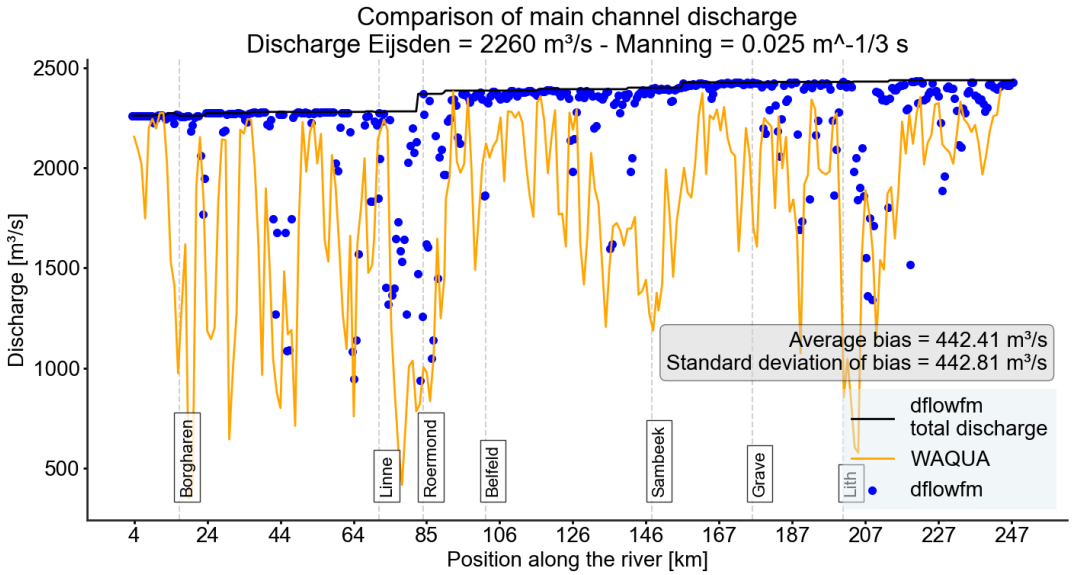

Figure E. 11 Initial comparison of main channel flow discharge $Q_{Eijsden}$ = 2260 m³/s. The apparent variation in 2D is an artefact of how the main channel discharge is computed; see section 2.2.

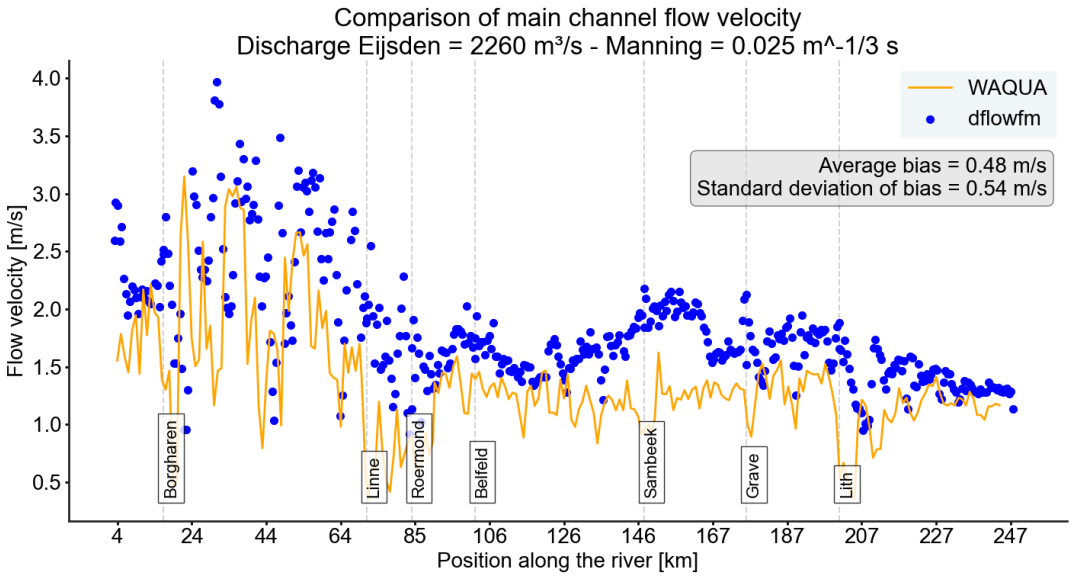

Figure E. 12 Initial comparison of main channel flow velocity $Q_{Eijsden}$ = 2260 m³/s

E.2 Calibrated differences – manning = 0.035 $sm^{-1/3}$

E.2.1 Discharge Eijsden 250 m^3/s

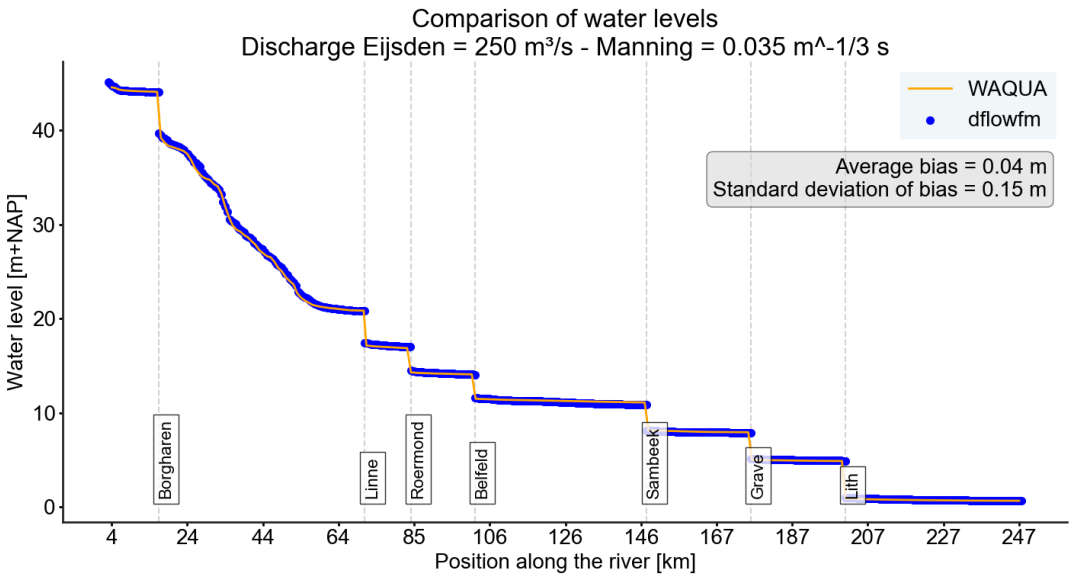

Figure E. 13 Final comparison of main channel flow discharge $Q_{Eijsden}$ = 250 m^3/s

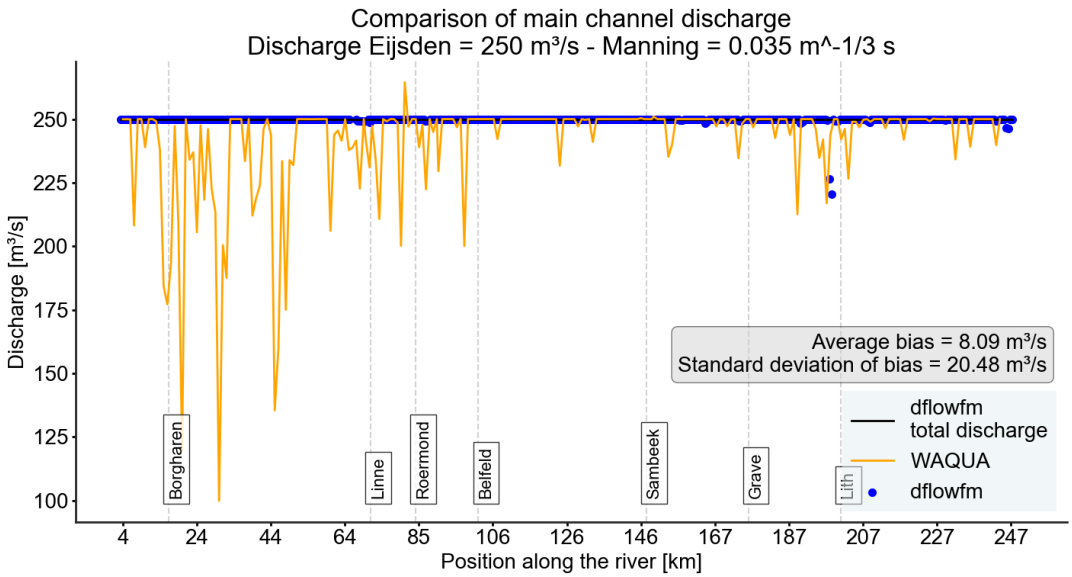

Figure E. 14 Final comparison of main channel flow discharge $Q_{Eijsden}$ = 250 m^3/s. The apparent variation in 2D is an artefact of how the main channel discharge is computed; see section 2.2.

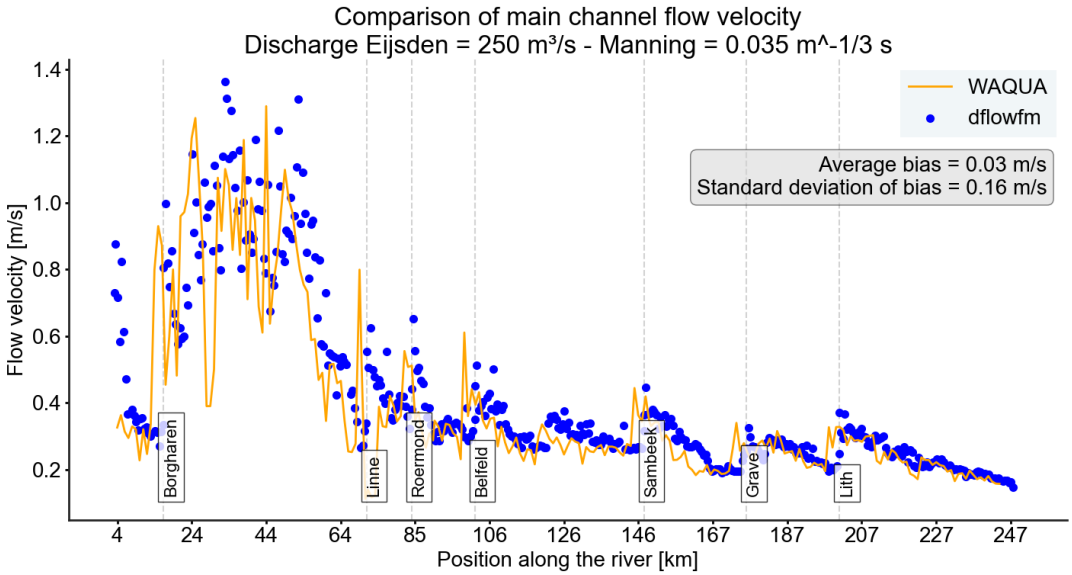

Figure E. 15 Final comparison of main channel flow velocity $Q_{Eijsden}$ = 250 m³/s

E.2.2 Discharge Eijsden 800 m³/s

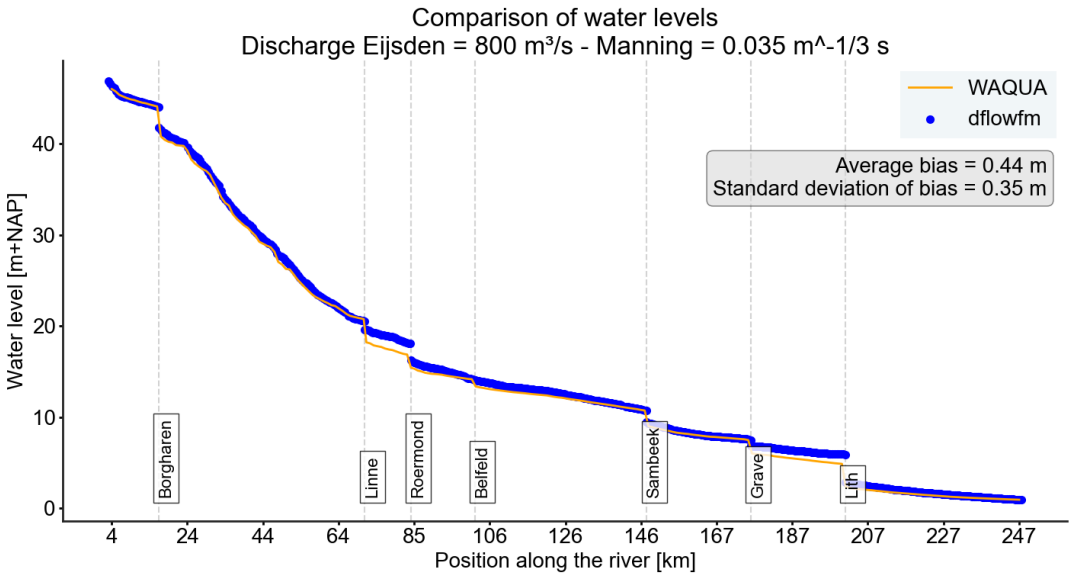

Figure E. 16 Final comparison of main channel flow discharge $Q_{Eijsden}$ = 800 m³/s

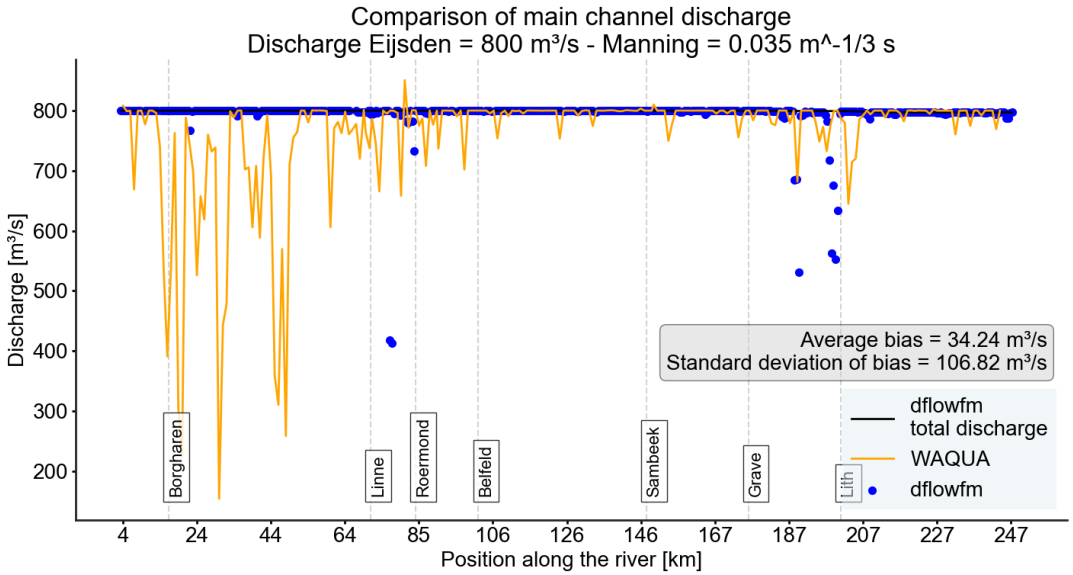

Figure E. 17 Final comparison of main channel flow discharge $Q_{Eijsden}$ = 800 m³/s. The apparent variation in 2D is an artefact of how the main channel discharge is computed; see section 2.2.

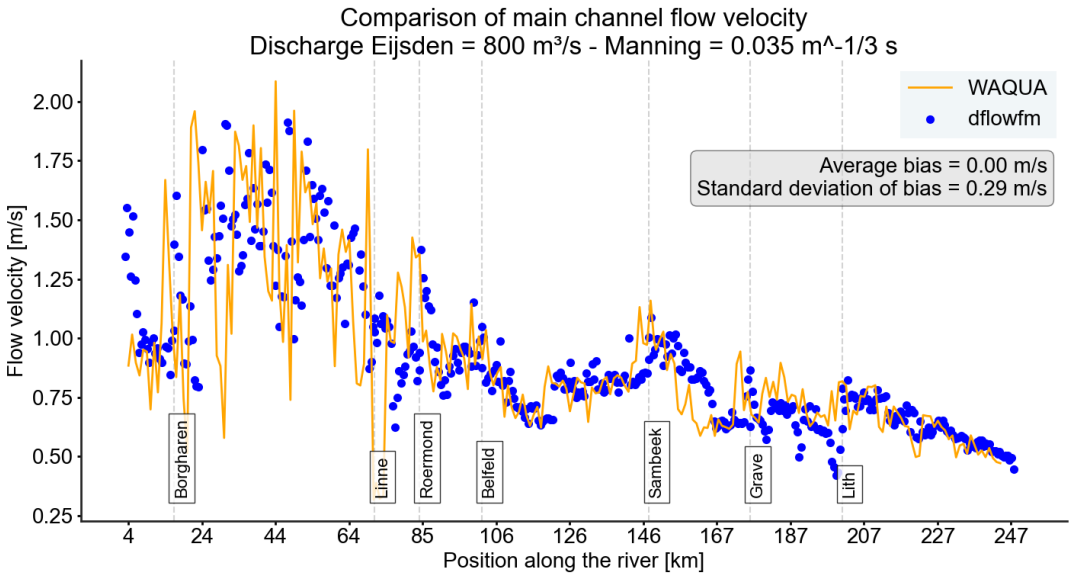

Figure E. 18 Final comparison of main channel flow velocity $Q_{Eijsden}$ = 800 m³/s

E.2.3 Discharge Eijsden 1500 m³/s

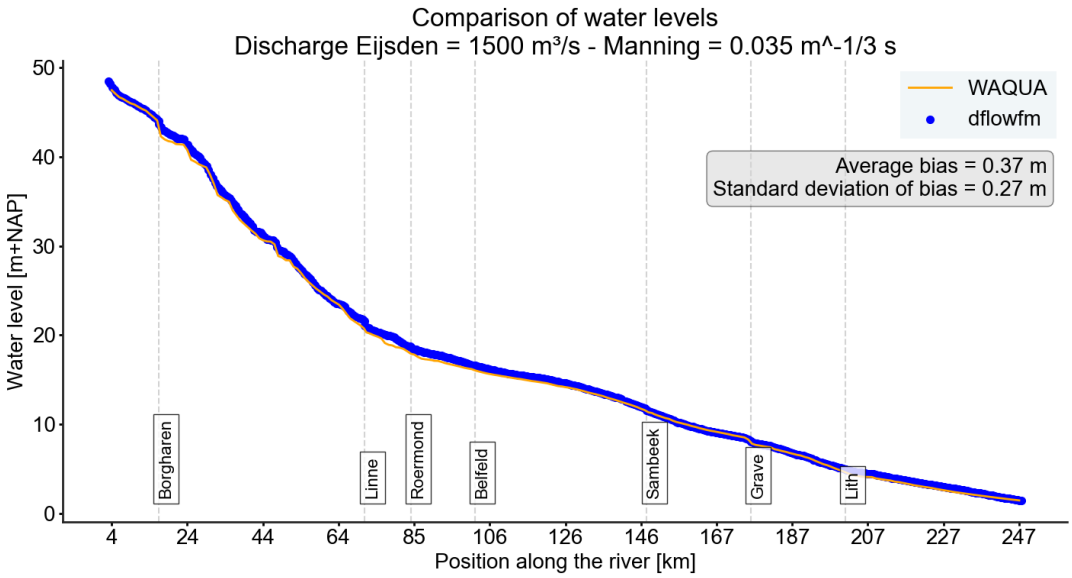

Figure E. 19 Final comparison of main channel flow discharge $Q_{Eijsden}$ = 1500 m³/s

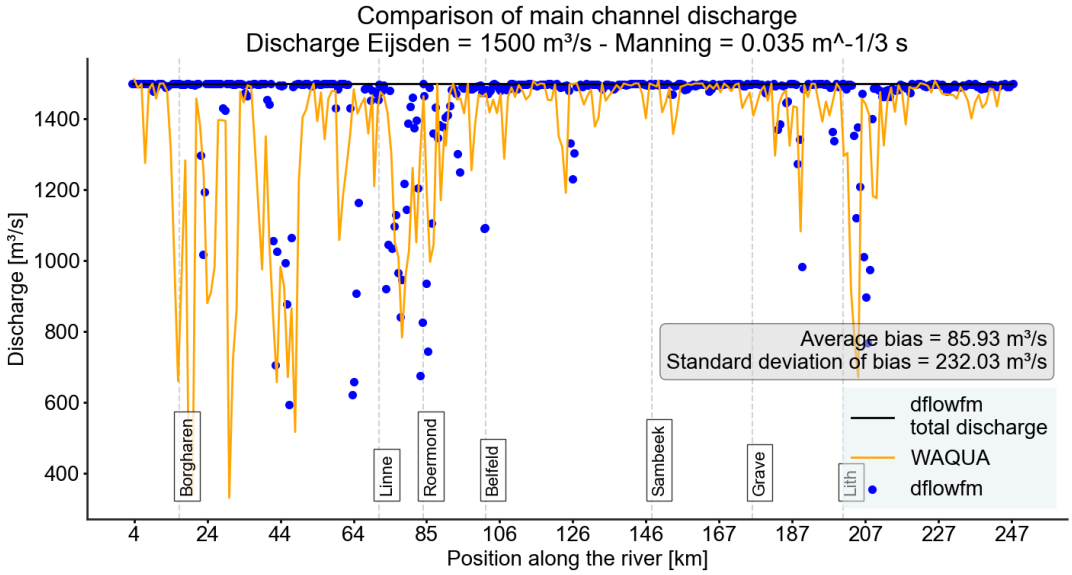

Figure E. 20 Final comparison of main channel flow discharge $Q_{Eijsden}$ = 1500 m³/s. The apparent variation in 2D is an artefact of how the main channel discharge is computed; see section 2.2.

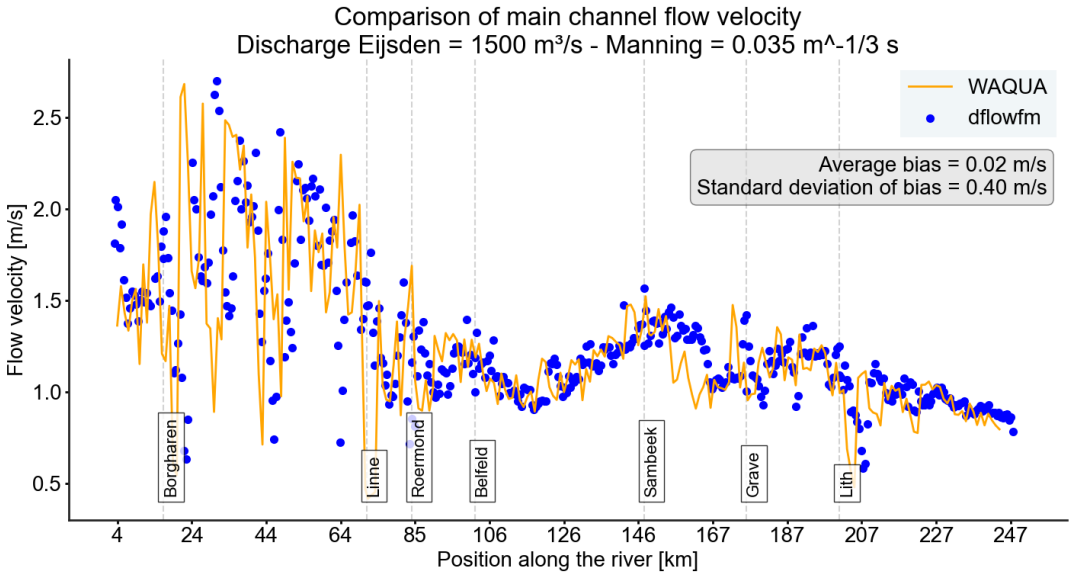

Figure E. 21 Final comparison of main channel flow velocity $Q_{Eijsden}$ = 1500 m³/s

E.2.4 Discharge Eijsden 2260 m³/s

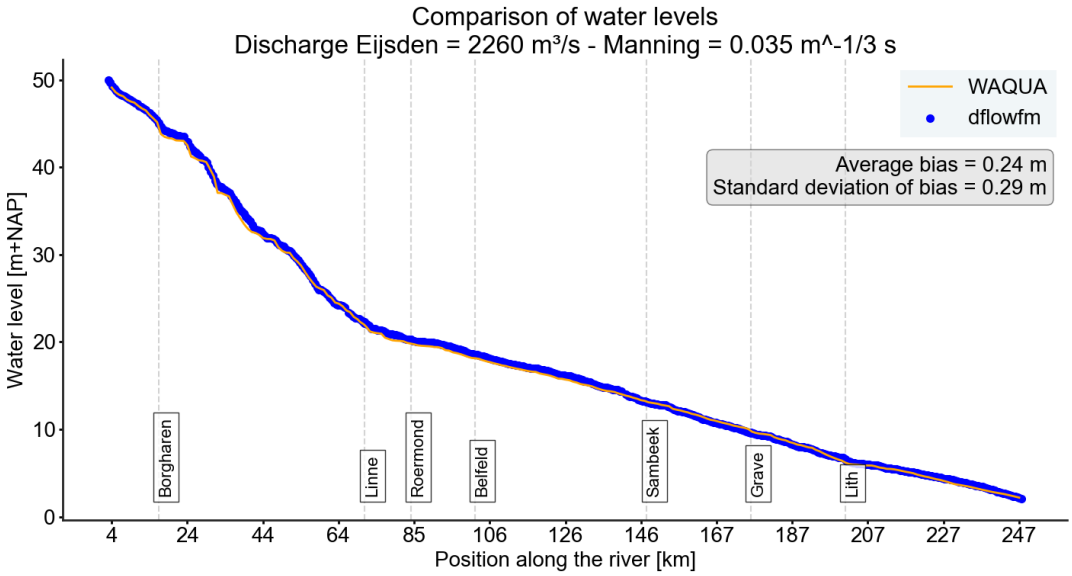

Figure E. 22 Final comparison of main channel flow discharge $Q_{Eijsden}$ = 2260 m³/s

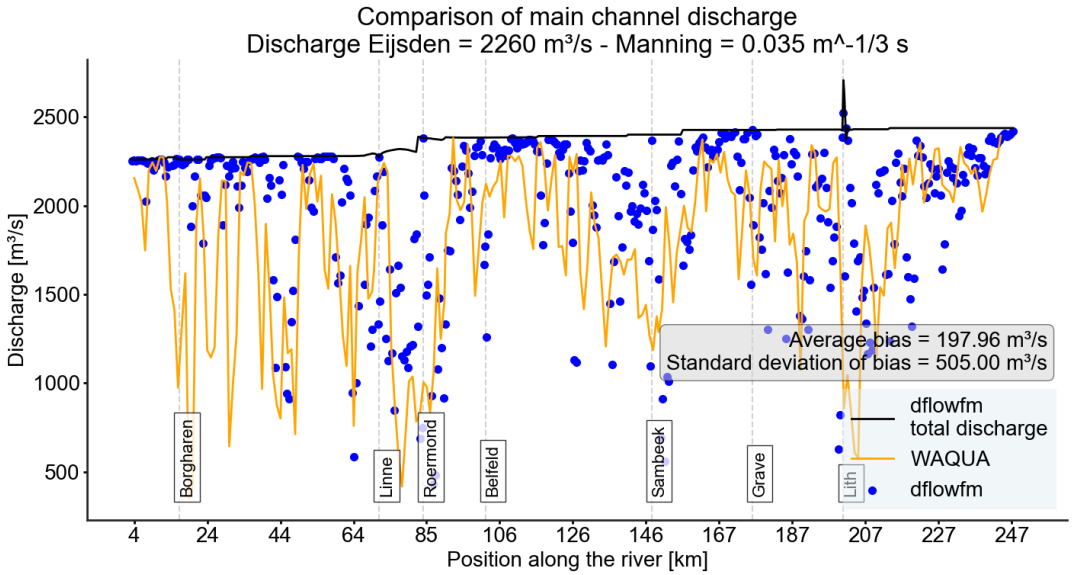

Figure E. 23 Final comparison of main channel flow discharge $Q_{Eijsden}$ = 2260 m³/s. The apparent variation in 2D is an artefact of how the main channel discharge is computed; see section 2.2.

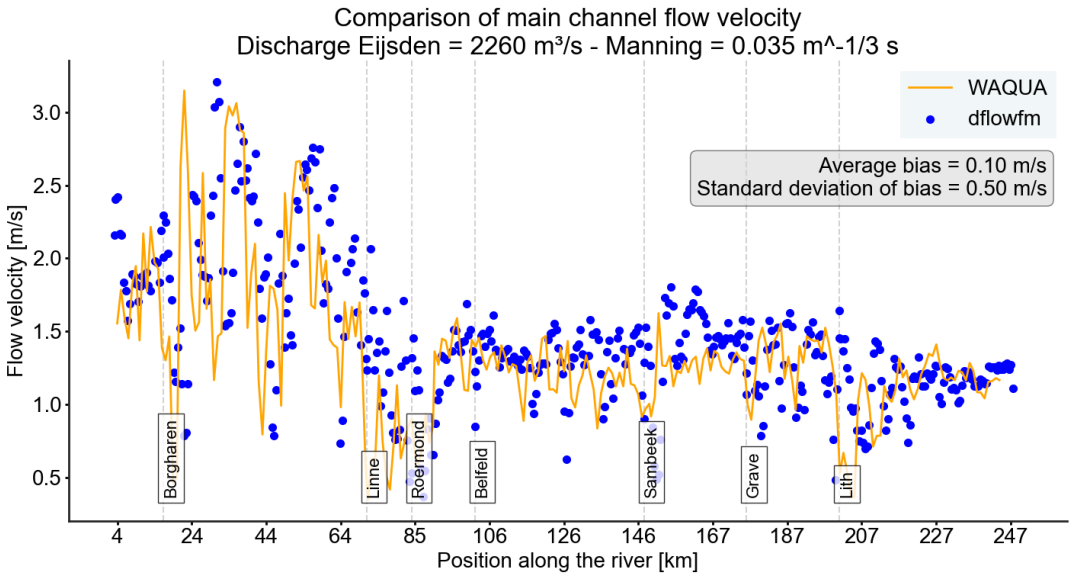

Figure E. 24 Final comparison of main channel flow velocity $Q_{Eijsden}$ = 2260 m³/s

F Results morphodynamic testing

F.1 Calibration 1995 - 2011

F.1.1 Meyer-Peter Müller (MPM)

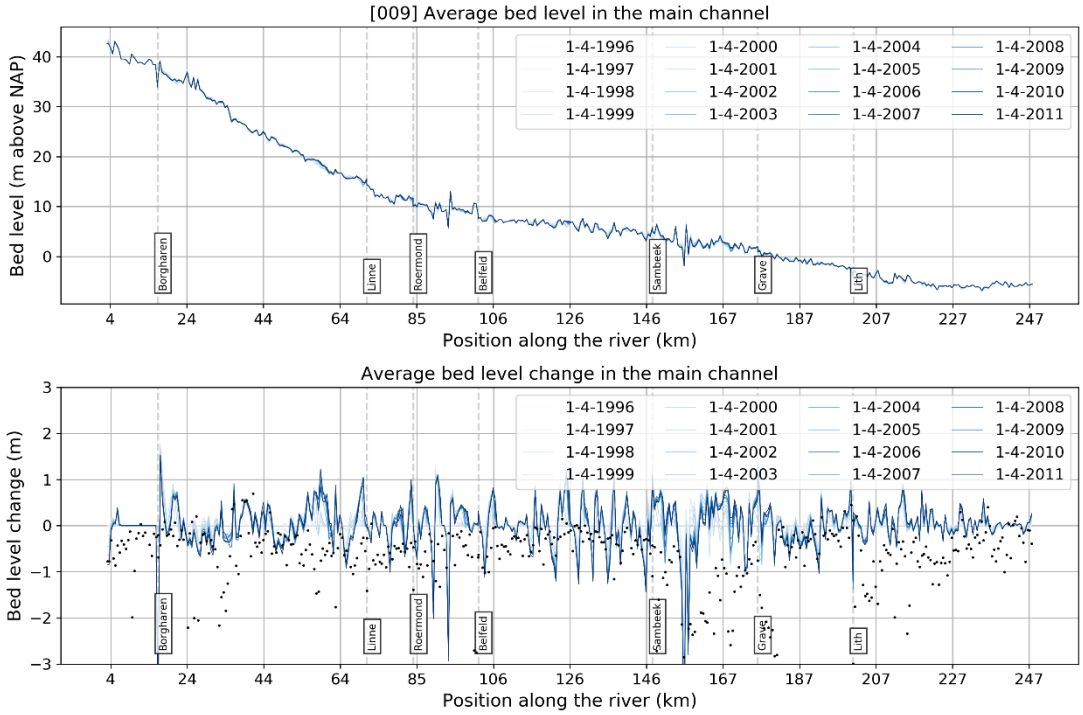

Figure F. 1 MPM – Main channel averaged bed level change

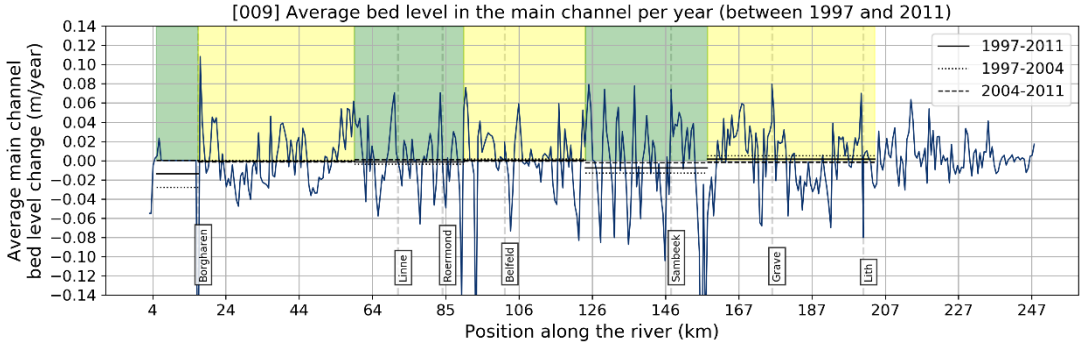

Figure F. 2 MPM – Main channel averaged bed level change per year

Figure F. 3 MPM – Temporal and spatial main channel averaged bed level change. The colour depicts the change in bed level.

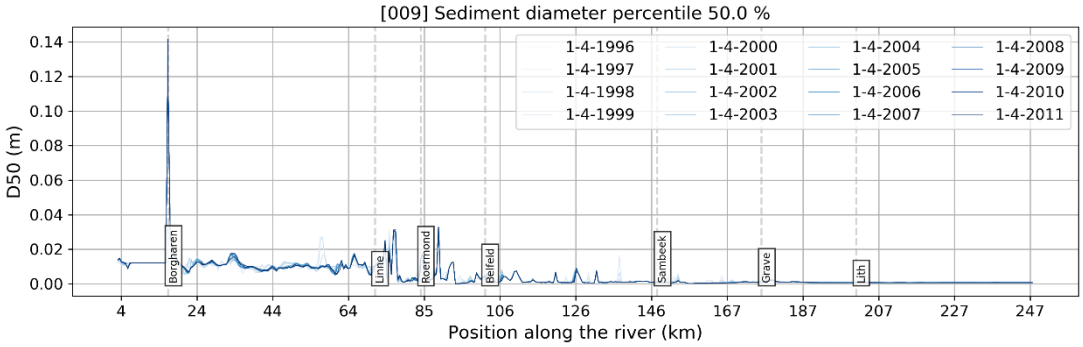

Figure F. 4 MPM – D50 in the top layer

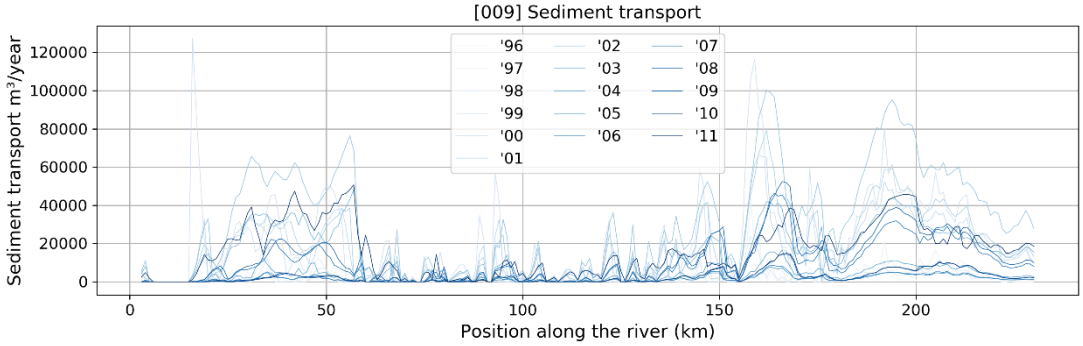

Figure F. 5 MPM – Sediment transport per year

F.1.2 Wilcock-Crowe (WC)

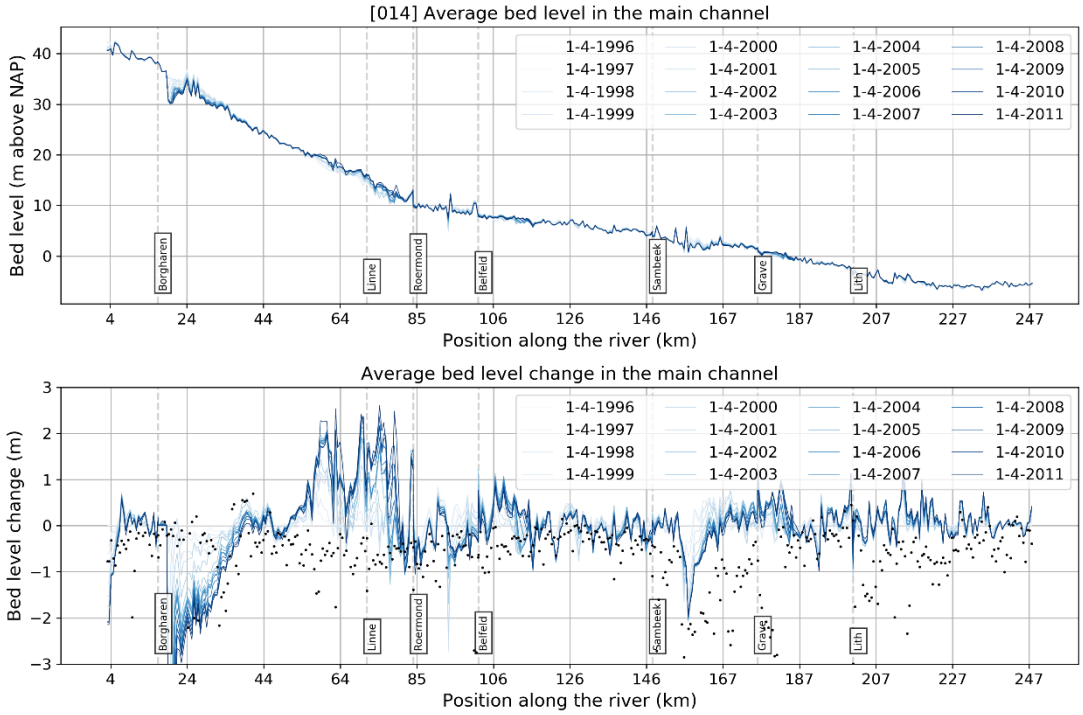

Figure F. 6 WC – Main channel averaged bed level change

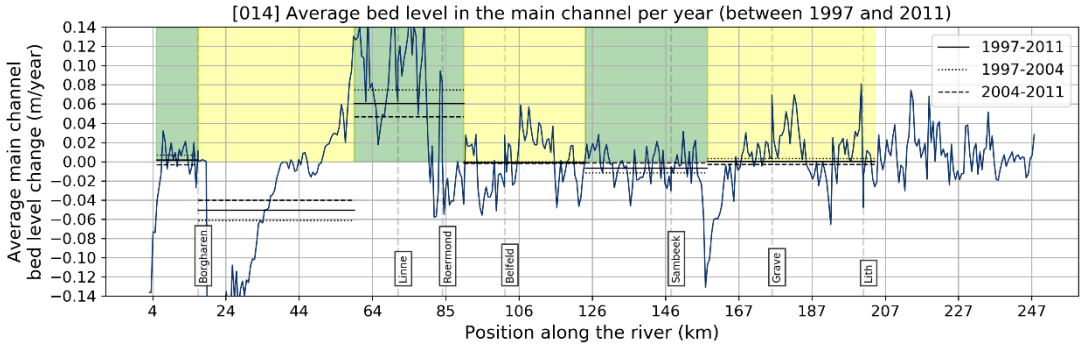

Figure F. 7 WC – Main channel averaged bed level change per year

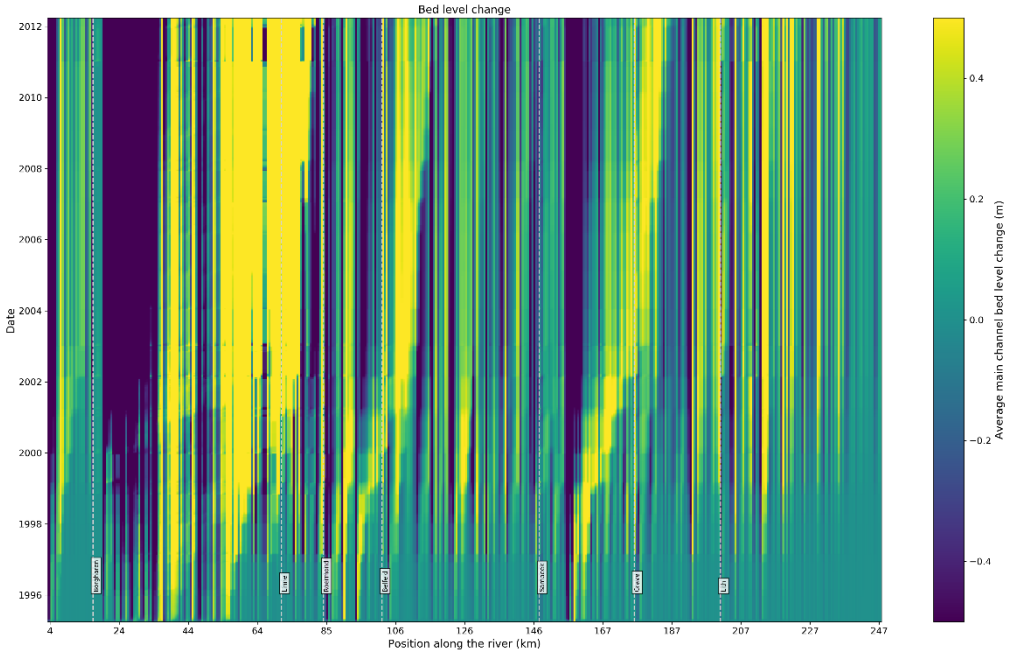

Figure F. 8 WC – Temporal and spatial main channel averaged bed level change. The colour depicts the change in bed level.

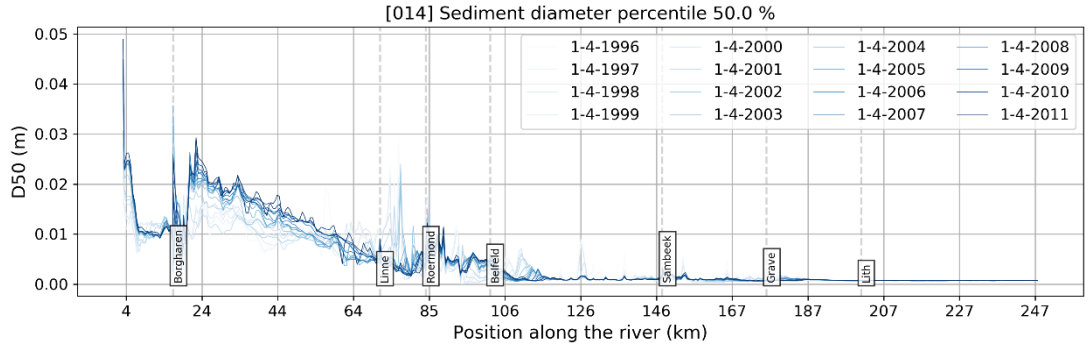

Figure F. 9 WC – D50 in the top layer

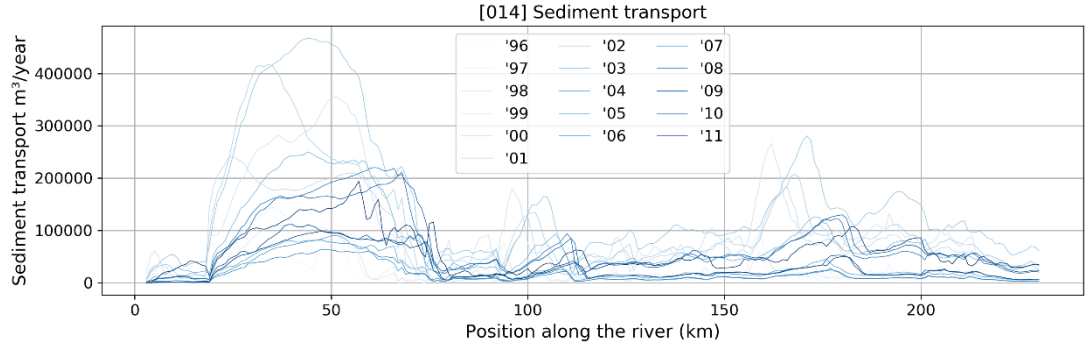

Figure F. 10 WC – Sediment transport per year

F.1.3 Combination of Meyer-Peter Muller and Engelund-Hansen (MPM+EH)

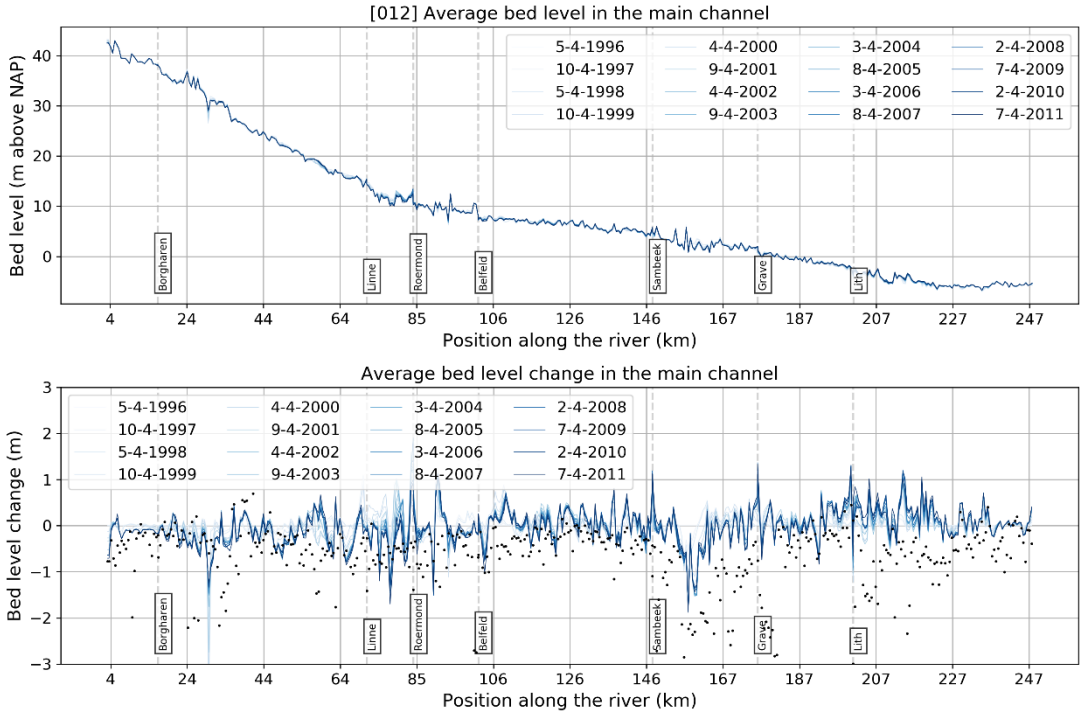

Figure F. 11 MPM+EH – Main channel averaged bed level change

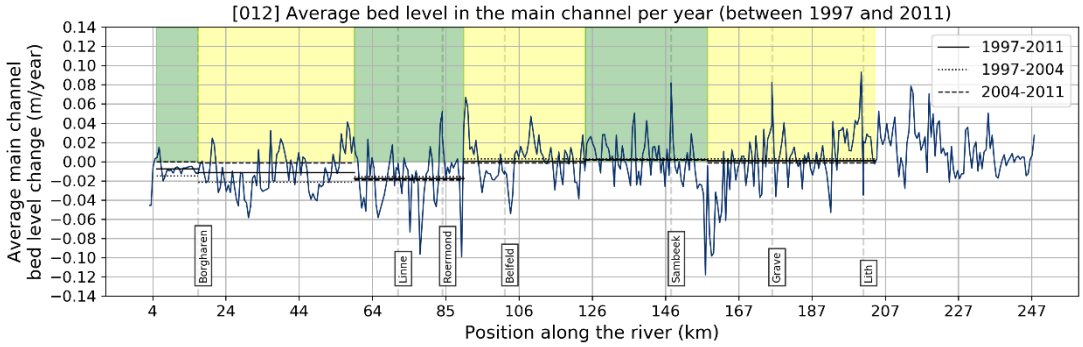

Figure F. 12 MPM+EH – Main channel averaged bed level change per year

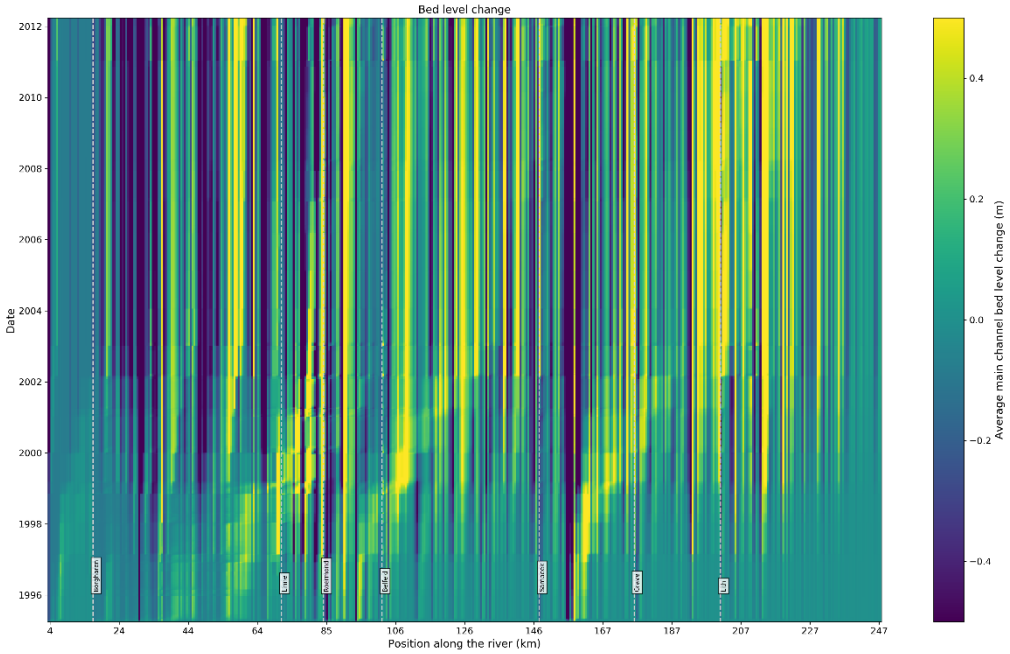

Figure F. 13 MPM+EH – Temporal and spatial main channel averaged bed level change. The colour depicts the change in bed level.

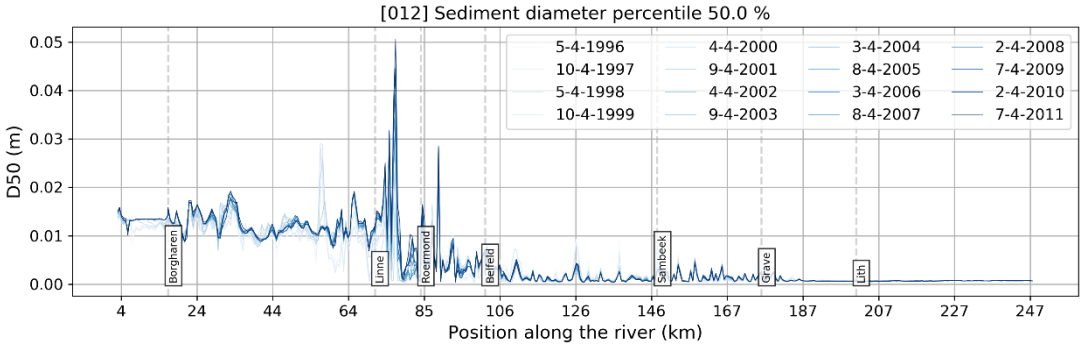

Figure F. 14 MPM+EH – D50 in the top layer

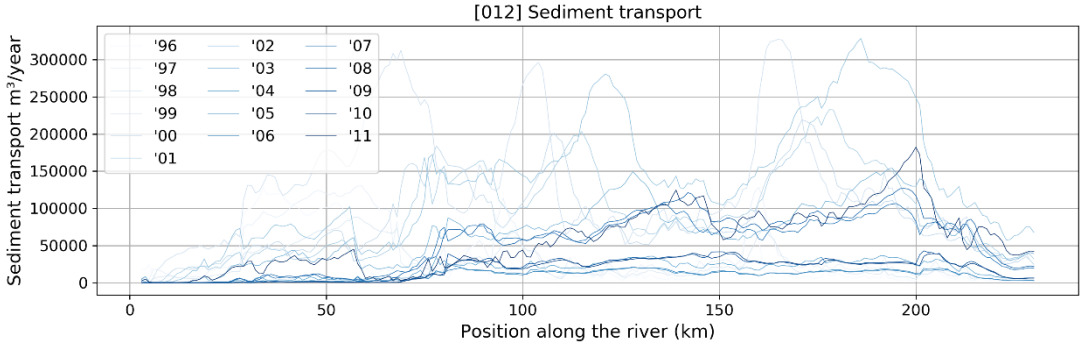

Figure F. 15 MPM+EH – Sediment transport per year

F.2 Validation 2011 - 2019

F.2.1 J11

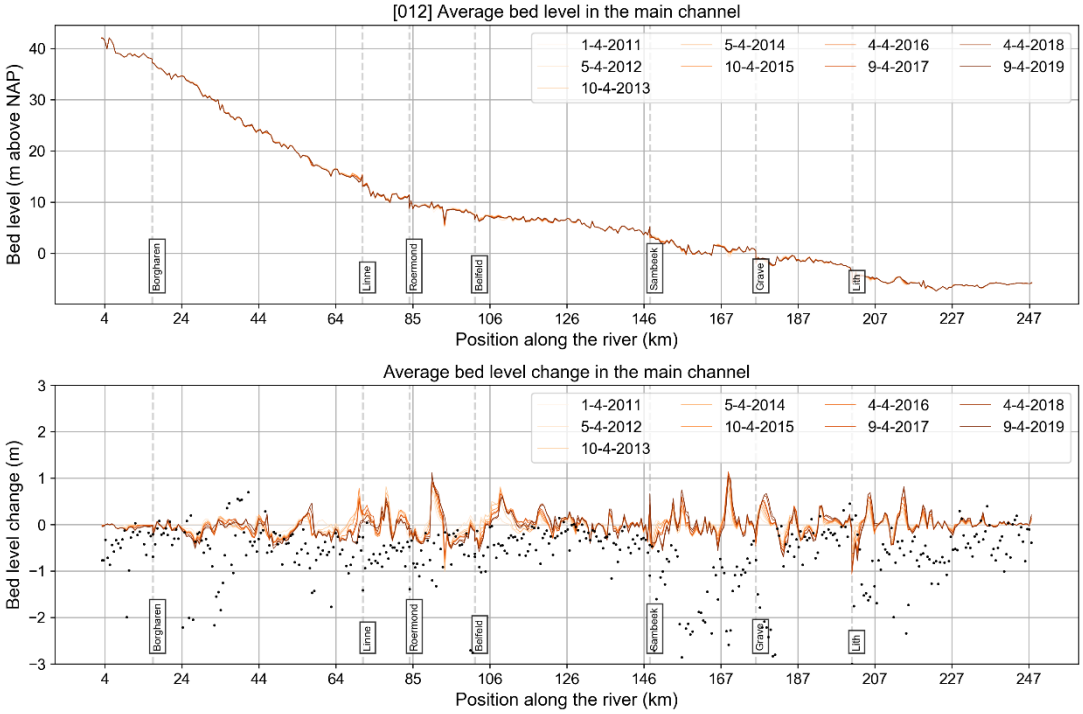

Figure F. 16 Validation j11 – Main channel averaged bed level change

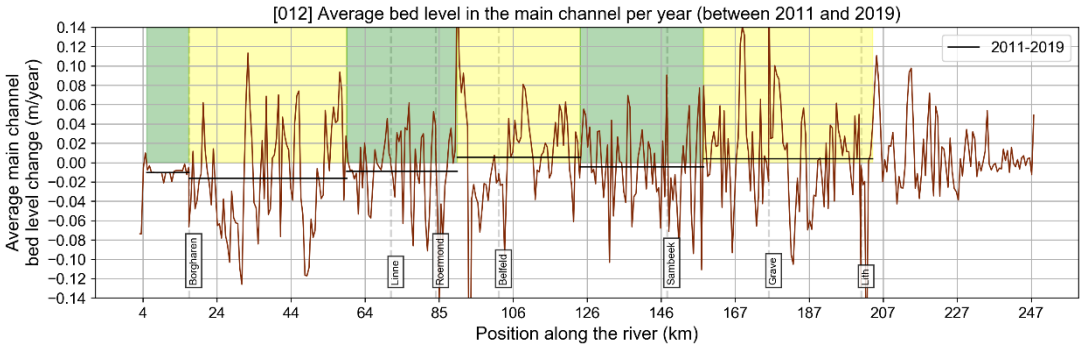

Figure F. 17 Validation j11 – Main channel averaged bed level change per year

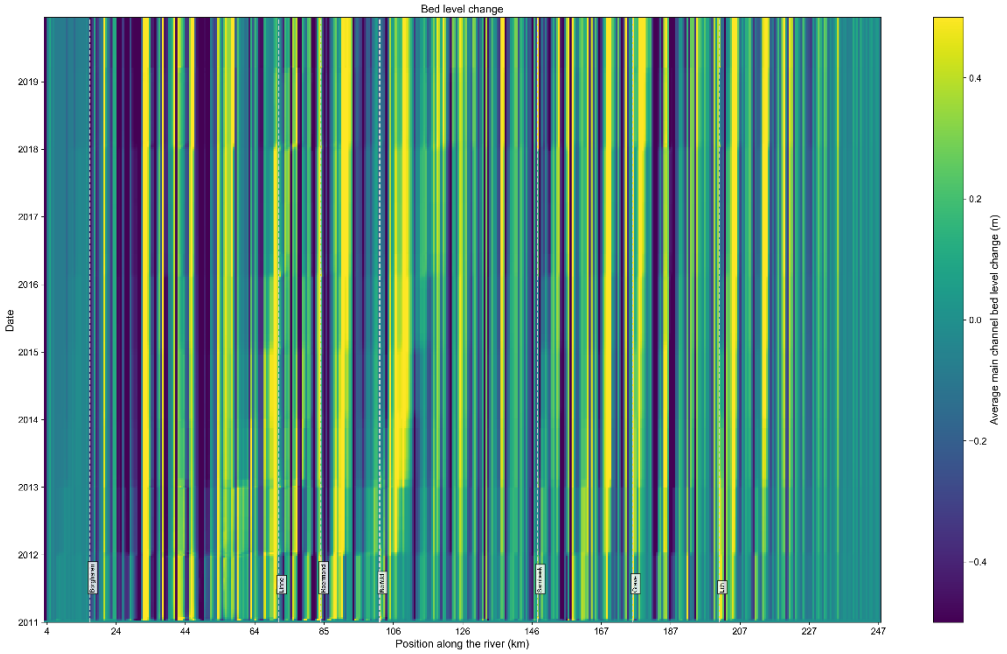

Figure F. 18 Validation j11 – Temporal and spatial main channel averaged bed level change. The colour depicts the change in bed level.

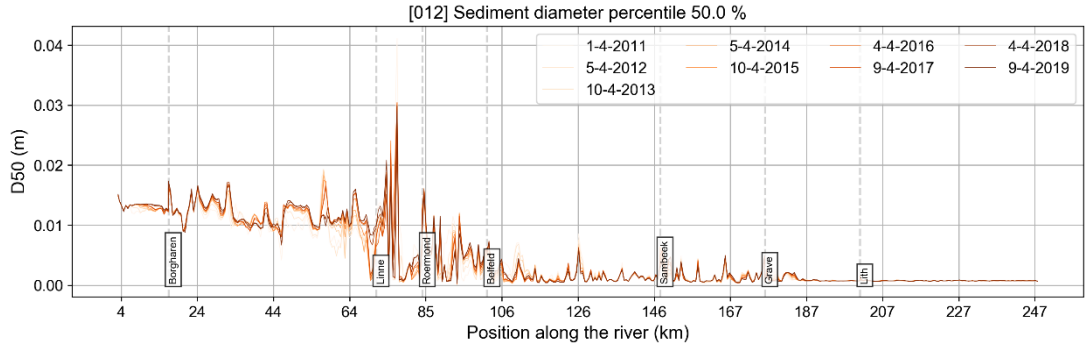

Figure F. 19 Validation j11 – D50 in the top layer

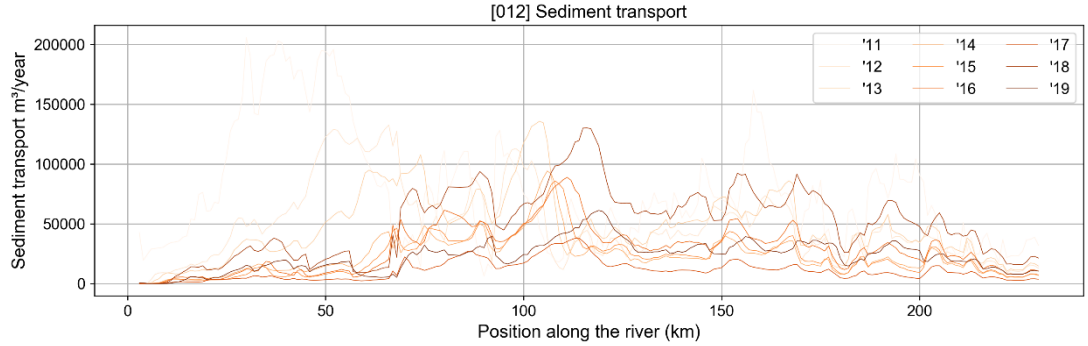

Figure F. 20 Validation j11 – Sediment transport per year

F.2.2 J19

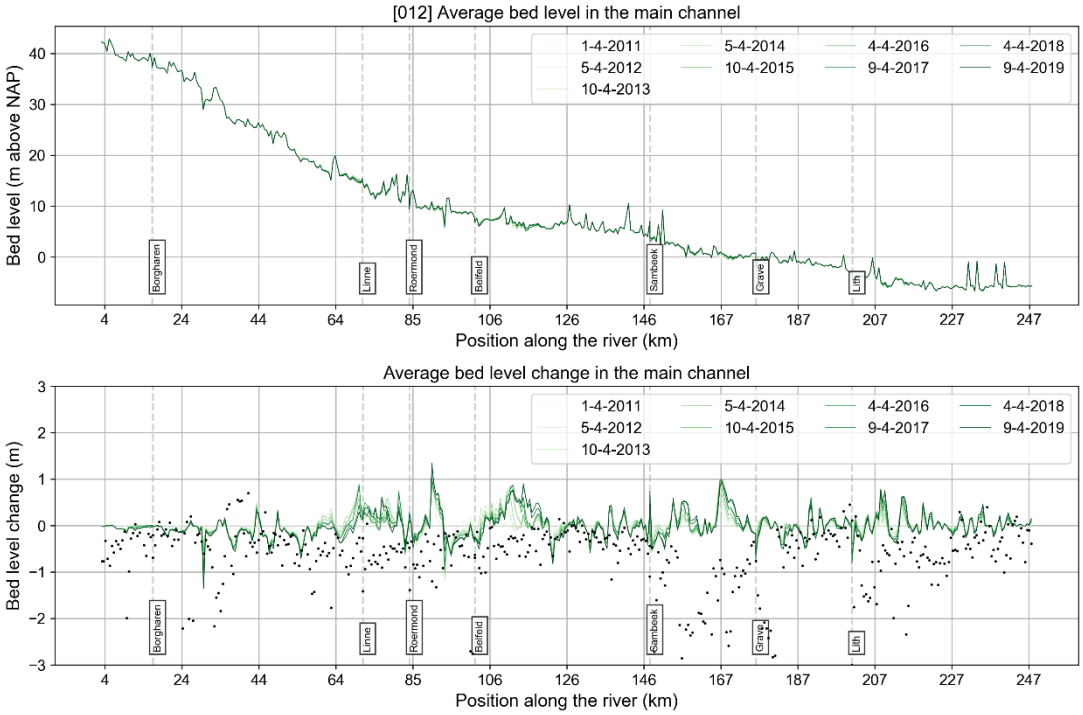

Figure F. 21 Validation j19 – Main channel averaged bed level change

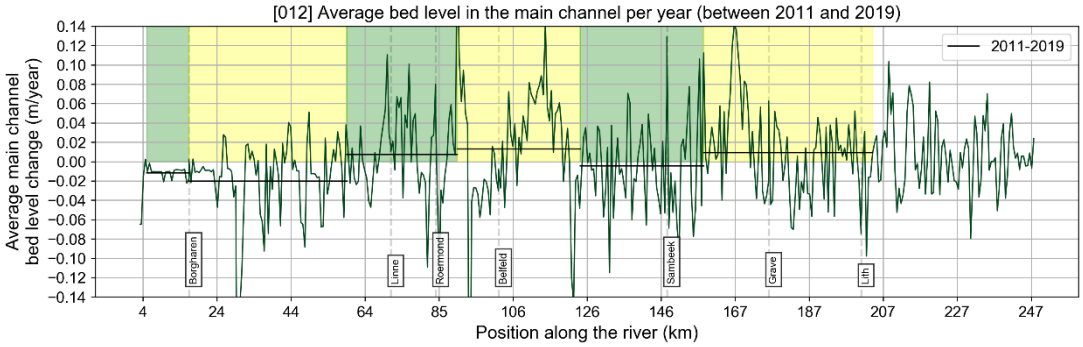

Figure F. 22 Validation j19 – Main channel averaged bed level change per year

Figure F. 23 Validation j19 – Temporal and spatial main channel averaged bed level change. The colour depicts the change in bed level.

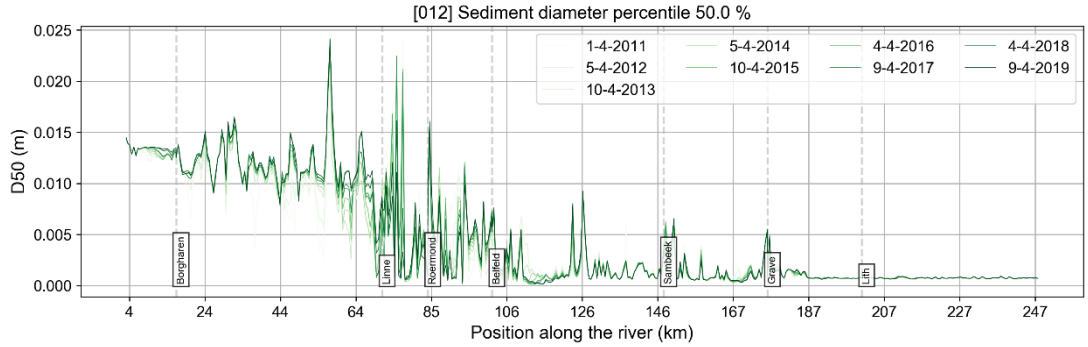

Figure F. 24 Validation j19 – D50 in the top layer

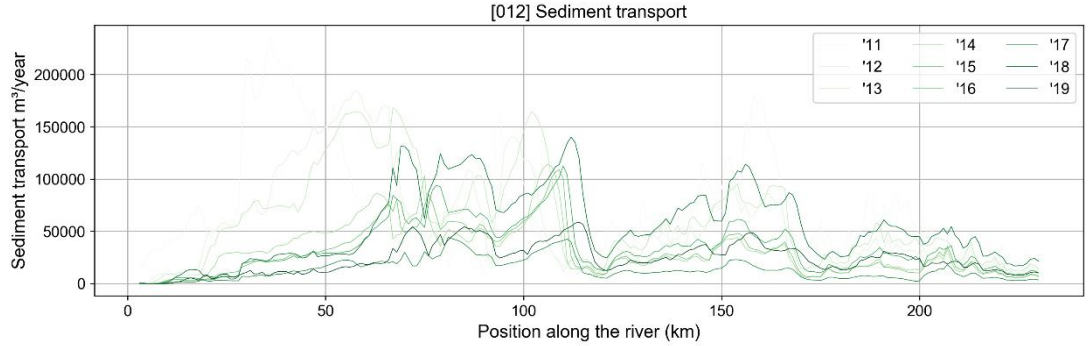

Figure F. 25 Validation j19 – Sediment transport per year

G Model software

G.1 Overview of Model development in 2020

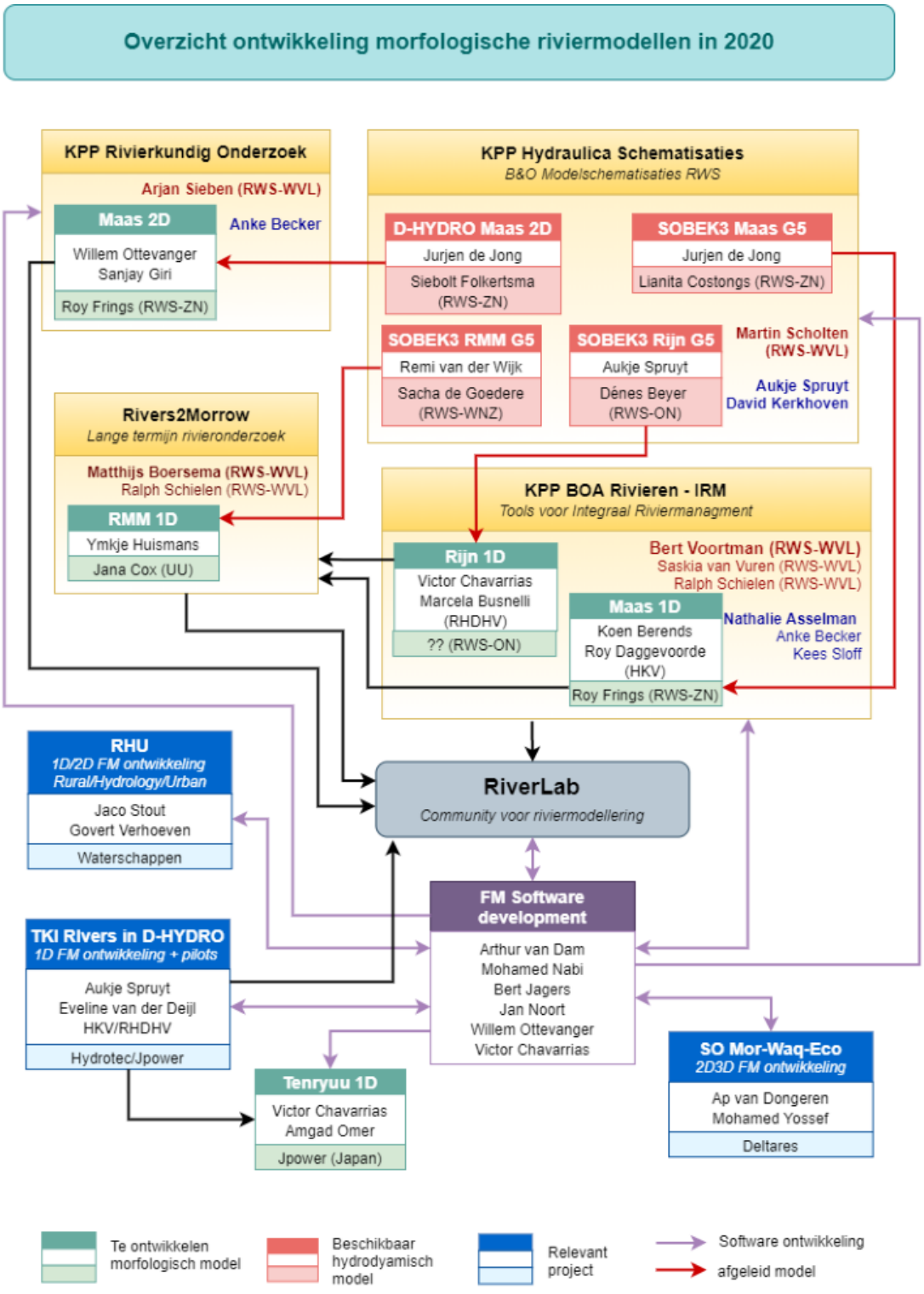

G.2 Overview of issues in software development

G.2.1 Completed issues

Issue number	Description
SOBEK-1900	Interpolation of SOBEK-3 profiles fixed
UNST-3458	Almost perfect restart (differences immediatetly after restart, but after some time rel abs error 10^(-8))
UNST-3459	Write average bed level in main channel to map file - fixed and added to map output
	Fix bobs at structures
UNST-3461	Dredging/dumping implemented - update to code after review has happened
UNST-3548	Supercritical flow case review - Review done, tests need to be added to testbench, last update to testcase description (Vi
UNST-3493	Add leveeTransitionHeight to Cross-section definition global input - Tests completed, still needs documentation for manual
UNST-3704	Orifice does not give the same result as SOBEK
	Implement output for morphologic area (mor_area)
	Implement output for morphologic cell width (mor_width_u)
UNST-1301	Implement former dll function Van Rijn and Kleinhans (2002) for Van Rijn 1984 with hiding exposure correction

G.2.2 In progress at time of writing

Issue number	Description
UNST-3460	Test long term evolution of nodal point relations - Wiggles are solved. Currently working on the new testcases by Schielen and Blom. First results look promising.
UNST-3463	Velocity/morphology at structures - Still opened.
UNST-3464	Implement Simulation Management Tool for FM1D and FM2D. First working version for Windows is available, bed update in progress, documentation still needs update
UNST-3650	Test morphodynamic boundary conditions 1 issue left regarding decreasing transport over time, which is not imposed/output correctly

G.2.3 Open issues at time of writing

Issue number	Description
UNST-3462	Assess bend effect
UNST-3506	Fix Rijn flow simulation case with more cross-sections than gridpoints - Pseudo code developed
	Check discharge Rijn model
UNST-3463	Possible workaround Velocity/morphology at structures - Fixed layer at structure

G.2.4 Issues solved by work-around

Issue number	Description
UNST-3462	Assess bend effect - Straightening script
UNST-3506	Fix Rijn flow simulation case with more cross-sections than gridpoints - Remove extra cross-sections script
UNST-3649	Test storage and conveyance - Tests for simple testcase show small differences (probably boundary location + hydraulic radius - check method computation of hyd. rad.), acceptable if also acceptable for Maas 1D model. Tests show this is related to advection in the model. For the IRM studies, storage is taken out of the domain.

H Model settings and run details

H.1 Model layout and boundary conditions

The model is shown on the next page in Figure H.2. The boundary conditions are described in paragraph 2.1.7. The upstream boundary is a discharge timeseries at Borgharen. (**Error! Reference source not found.** H.1). At the upstream boundary no sediment is provided to the model. The downstream boundary condition is a stage discharge relation at Keizersveer (Table H. 1). At the downstream boundary no bed level constraint is given for the bed development.

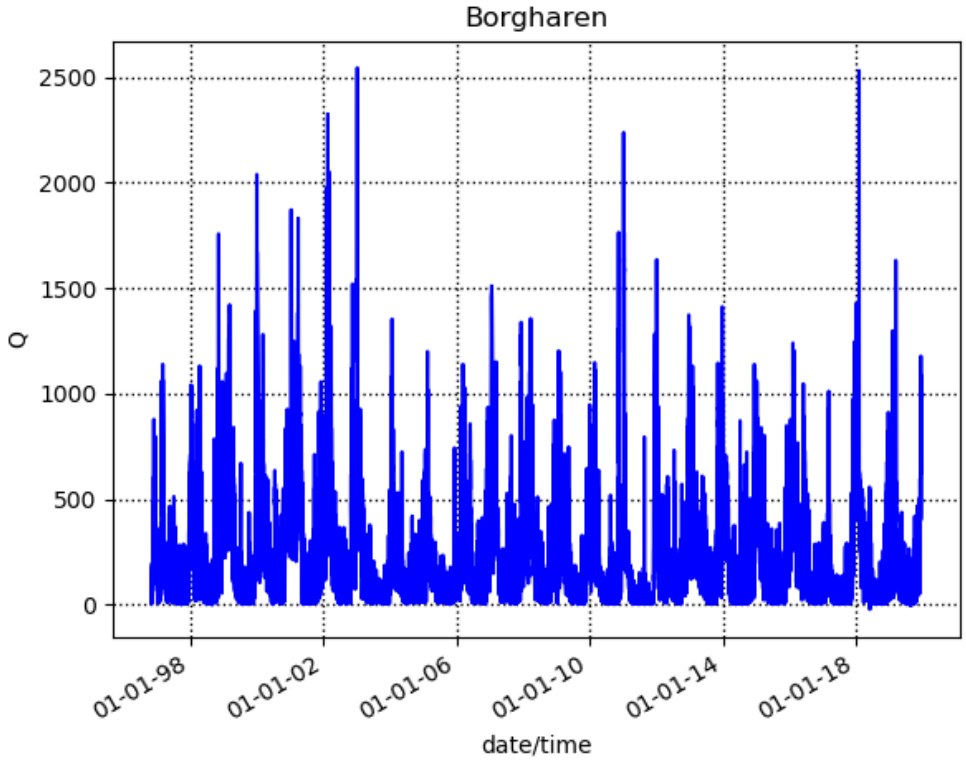

Figure H.1 Boundary condition Borgharen

Table H.1 Stage discharge relation at the downstream boundary "Keijzersveer"

Discharge (m^3/s)	Water level (m above NAP)
0.1	0.4
13	0.414
361	0.751
896	0.99
1357	1.329
1876	1.694
2530	2.091
3380	2.645
4191	3.203
4712	3.526
5204	3.778
6920	4.434

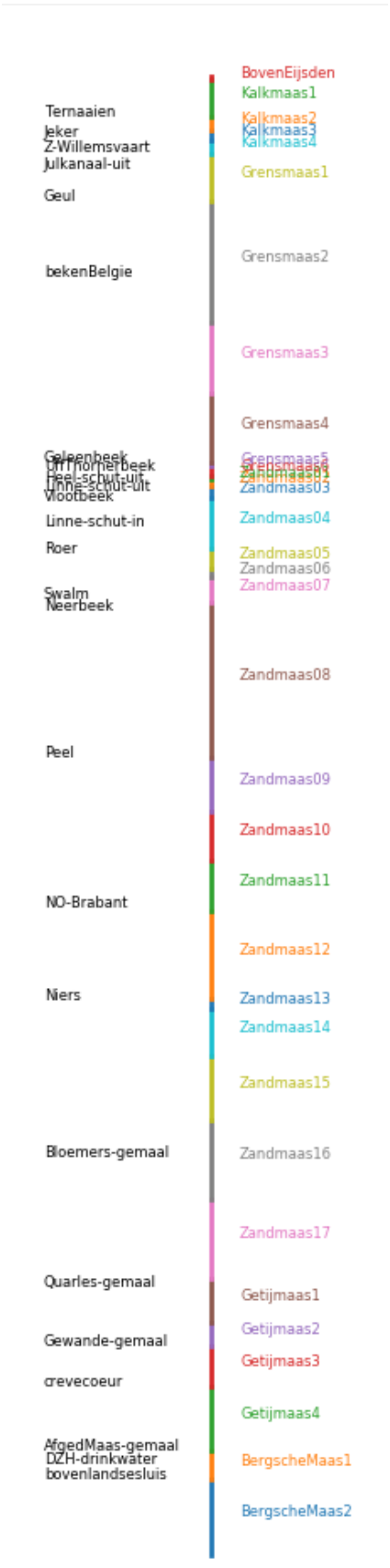

Figure H.2 Model layout, on the left the boundary locations, on the right the branch names. The colours of the branches coincide with the colours of the branch

H.2 Computational effort

On a standard laptop (Table H.2) the model runs 6208 days (17 years) in 7 hours.

Table H.2 Computer specifications

Property	Details
Processor	Intel® Core™ i5-7200 CPU @ 2.50 GHz 2.71GHz
Installed memory	16 GB (15.9 GB usable)
System type	64-bit Operation System, 64x-based processor

H.3 MDU

Item	Value	Explanation
Program	D-Flow FM	
fileVersion	1.09	File version (do not edit this)
fileType	modelDef	File type (do not edit this)
AutoStart	0	Autostart simulation after loading MDU (0: no, 1: autostart, 2: autostartstop)
NetFile	flow model_net.nc	Unstructured grid file *_net.nc
OneDNetworkFile		1d networkfile
BedlevelFile		street_level.xyz , Bedlevels points file e.g. *.xyz, only needed for bedlevtype not equal 3
DryPointsFile		Dry points file *.xyz (third column dummy z values), or dry areas polygon file *.pol (third column 1/-1: inside/outside)
IniFieldFile	initialFields.ini	Initial and parameter field file *.ini
LandBoundaryFile		Land boundaries file *.ldb, used for visualization
ThinDamFile		Polyline file *_thd.pli, containing thin dams
FixedWeirFile		Polyline file *_fxw.pliz, containing fixed weirs with rows x, y, crest level, left ground level, right ground level
Gulliesfile		Polyline file *_gul.pliz, containing lowest bed level along talweg x, y, z level
VertplizFile		Vertical layering file *_vlay.pliz with rows x, y, Z, first Z, nr of layers, second Z, layer type
ProflocFile		Channel profile location file *_proflocation.xyz with rows x, y, z, profile number ref
ProfdefFile		Channel profile definition file *_profdefinition.def with definition for all profile numbers
ProfdefxyzFile		Channel profile definition file _profdefinition.def with definition for all profile numbers
Uniformwidth1D	1.	Uniform width for channel profiles not specified by profloc
Uniformheight1D	1.	Uniform height for channel profiles not specified by profloc
ManholeFile		File *.ini containing manholes
PipeFile		File *.pliz containing pipe-based 'culverts'
ShipdefFile		File *.shd containing ship definitions
StructureFile	Structures.ini	File *.ini containing structures

Item	Value	Explanation
CrossLocFile	CrossSectionLocations.ini	Name and location of the file containing the locations of the cross sections
CrossDefFile	CrossSectionDefinitions.ini	Name and location of the file containing the definitions of the cross sections
frictFile	roughness-Main.ini;roughness-FloodPlain1.ini;roughness-FloodPlain2.ini	Name and location of the file containing the roughness data
WaterLevIni	-999.0	Initial water level at missing s0 values
BedlevUni	-5.	Uniform bed level used at missing z values if BedlevType > 2
BedlevType	1	Bathymetry specification
PartitionFile		Domain partition polygon file *_part.pol for parallel run
AngLat	0.	Angle of latitude S-N (deg), 0: no Coriolis
AngLon	0.	Angle of longitude E-W (deg), 0: Greenwich, used in solar heat flux computation.
Conveyance2D	-1	-1: R=HU,0: R=H, 1: R=A/P, 2: K=analytic-1D conv, 3: K=analytic-2D conv
Slotw2D	0.	-
CFLMax	0.7	Maximum Courant number
AdvecType	33	Advection type (0: none, 1: Wenneker, 2: Wenneker q(uio-u), 3: Perot q(uio-u), 4: Perot q(ui-u), 5: Perot q(ui-u) without itself)
TimeStepType	2	Time step handling (0: only transport, 1: transport + velocity update, 2: full implicit step-reduce, 3: step-Jacobi, 4: explicit)
Icoriolistype	5	0=No, 1=yes, if jsferic then spatially varying, if icoriolistype==6 then constant (anglat)
Limtypmom	4	Limiter type for cell center advection velocity (0: none, 1: minmod, 2: van Leer, 3: Kooren, 4: monotone central)
Limtypsa	4	Limiter type for salinity transport (0: none, 1: minmod, 2: van Leer, 3: Kooren, 4: monotone central)
TransportMethod	1	Transport method (0: Herman's method, 1: transport module)
Vertadvtypsal	6	Vertical advection type for salinity (0: none, 1: upwind explicit, 2: central explicit, 3: upwind implicit, 4: central implicit, 5: central implicit but upwind for neg. stratif., 6: higher order explicit, no Forester)
Vertadvtyptem	6	Vertical advection type for temperature (0: none, 1: upwind explicit, 2: central explicit, 3: upwind implicit, 4: central implicit, 5: central implicit but upwind for neg. stratif., 6: higher order explicit, no Forester)
Icgsolver	4	Solver type (1: sobekGS_OMP, 2: sobekGS_OMPthreadsafe, 3: sobekGS, 4: sobekGS + Saadilud, 5: parallel/global Saad, 6: parallel/Petsc, 7: parallel/GS)
Tlfsmo	0.	Fourier smoothing time (s) on water level boundaries
Slopedrop2D	0.	Apply drop losses only if local bed slope > Slopedrop2D, (<=0: no drop losses)
cstbnd	0	Delft-3D type velocity treatment near boundaries for small coastal models (1: yes, 0: no)
Epshu	1.d-4	Threshold water depth for wet and dry cells
jaupwindsrc	1	1st-order upwind advection at sources/sinks (1) or higher-order (0)

Item	Value	Explanation
jasfer3D	0	corrections for spherical coordinates
UnifFrictCoef	50	Uniform friction coefficient (0: no friction)
UnifFrictType	0	Uniform friction type (0: Chezy, 1: Manning, 2: White-Colebrook, 3: idem, WAQUA style)
UnifFrictCoef1D	50	Uniform friction coefficient in 1D links (0: no friction)
UnifFrictCoef1D2D	50	Uniform friction coefficient in 1D links (0: no friction)
UnifFrictCoefLin	0.	Uniform linear friction coefficient for ocean models (m/s) (0: no friction)
Vicouv	1.	Uniform horizontal eddy viscosity (m2/s)
Dicouv	1.	Uniform horizontal eddy diffusivity (m2/s)
Smagorinsky	0.	Smagorinsky factor in horizontal turbulence, e.g. 0.15
Elder	0.	Elder factor in horizontal turbulence
wall_ks	0.	Wall roughness type (0: free slip, 1: partial slip using wall_ks)
Rhomean	1000.	Average water density (kg/m3)
Ag	9.81	Gravitational acceleration
TidalForcing	1	Tidal forcing, if jsferic=1 (0: no, 1: yes)
SelfAttractionLoading	0	Self attraction and loading (0=no, 1=yes, 2=only self attraction)
Salinity	0	Include salinity, (0=no, 1=yes)
Temperature	0	Include temperature (0: no, 1: only transport, 3: excess model of D3D, 5: composite (ocean) model)
SecondaryFlow	0	Secondary flow (0: no, 1: yes)
ICdtyp		Wind drag coefficient type (1=Const; 2=Smith&Banke (2 pts); 3=S&B (3 pts); 4=Charnock 1955, 5=Whang 2005, 6=Wuest 2005, 7=Hersbach 2010 (2 pts)
Cdbreakpoints		Wind drag coefficient break points
Windspeedbreakpoints		Wind speed break points (m/s)
Rhoair		Air density (kg/m3)
PavBnd		Average air pressure on open boundaries (N/m2) (only applied if > 0)
Pavini		Average air pressure for initial water level correction (N/m2) (only applied if > 0)
RefDate	19950401	Reference date (yyyymmdd)
Tzone	0.	Time zone assigned to input time series
DtUser	3600.000	Time interval (s) for external forcing update
DtNodal	60.	Time interval (s) for updating nodal factors in astronomical boundary conditions
DtMax	600.	Maximal computation timestep (s)
Dtfacmax	1.1	Max timestep increase factor ( )

Item	Value	Explanation
DtInit		Initial computation timestep (s)
Timestepanalysis	0	0=no, 1=see file *.steps
Tunit	S	Time unit for start/stop times (D, H, M or S)
TStart	0.0	Start time w.r.t. RefDate (in TUnit)
TStop	536371200	Stop time w.r.t. RefDate (in TUnit)
RestartFile		Restart netcdf-file, either *_rst.nc or *_map.nc
RestartDateTime		Restart date and time (YYYYMMDDHHMMSS) when restarting from *_map.nc
ExtForceFile		Old format for external forcings file *.ext, link with tim/cmp-format boundary conditions specification
ExtForceFileNew	flow model.ext	New format for external forcings file *.ext, link with bc-format boundary conditions specification
OutputDir		Output directory of map-, his-, rst-, dat- and timings-files, default: DFM_OUTPUT_<modelname>. Set to . for current dir.
FlowGeomFile		Flow geometry NetCDF *_flowgeom.nc
ObsFile	ObservationPoints.ini	Points file *.xyn with observation stations with rows x, y, station name
CrsFile	ObservationPoints_crs.ini	Polyline file *_crs.pli defining observation cross sections
FouFile		Fourier analysis input file *.fou
HisFile		HisFile name *_his.nc
MapFile		MapFile name *_map.nc
HisInterval	43200.000 0. 0.	History output times, given as "interval" "start period" "end period" (s)
XLSInterval	0.	Interval (s) between XLS history
MapInterval	864000.000 0. 0.	Map file output, given as "interval" "start period" "end period" (s)
RstInterval	31536000. 0. 536371200.	Restart file output times, given as "interval" "start period" "end period" (s)
WaqInterval	0. 0. 0.	DELWAQ output times, given as "interval" "start period" "end period" (s)
StatsInterval	-900.	Screen step output interval in seconds simulation time, if negative in seconds wall clock time
TimingsInterval	0.	Timings statistics output interval
TimeSplitInterval	0X	Time splitting interval, after which a new output file is started. value+unit, e.g. '1 M', valid units: Y,M,D,h,m,s.
MapFormat	4	Map file format, 1: netCDF, 2: Tecplot, 3: netCFD and Tecplot, 4: NetCDF-UGRID
Wrihis_balance	1	Write mass balance totals to his file (1: yes, 0: no)
Wrihis_sourcesink	1	Write sources-sinks statistics to his file (1=yes, 0=no)
Wrihis_turbulence	1	Write k, eps and vicww to his file (1: yes, 0: no)
Wrihis_wind	0	Write wind velocities to his file (1: yes, 0: no)
Wrihis_rain	0	Write precipitation to his file (1: yes, 0: no)

Item	Value	Explanation
Wrihis_temperature	0	Write temperature to his file (1: yes, 0: no)
Wrihis_heatflux	0	Write heat flux to his file (1: yes, 0: no)
Wrihis_salinity	0	Write salinity to his file (1: yes, 0: no)
Wrimap_waterlevel_s0	0	Write water levels for previous time step to map file (1: yes, 0: no)
Wrimap_waterlevel_s1	1	Write water levels to map file (1: yes, 0: no)
Wrimap_velocity_component_u0	0	Write velocity component for previous time step to map file (1: yes, 0: no)
Wrimap_velocity_component_u1	1	Write velocity component to map file (1: yes, 0: no)
Wrimap_velocity_vector	1	Write cell-center velocity vectors to map file (1: yes, 0: no)
Wrimap_upward_velocity_componen t	0	Write upward velocity component on cell interfaces (1: yes, 0: no)
Wrimap_flow_flux_q1_main	1	Write flow flux in main channel to map file (1: yes, 0: no)
Wrimap_density_rho	0	Write flow density to map file (1: yes, 0: no)
Wrimap_horizontal_viscosity_viu	1	Write horizontal viscosity to map file (1: yes, 0: no)
Wrimap_horizontal_diffusivity_diu	1	Write horizontal diffusivity to map file (1: yes, 0: no)
Wrimap_flow_flux_q1	1	Write flow flux to map file (1: yes, 0: no)
Wrimap_spiral_flow	0	Write spiral flow to map file (1: yes, 0: no)
Wrimap_numlimdt	1	Write the number times a cell was Courant limiting to map file (1: yes, 0: no)
Wrimap_taucurrent	1	Write the shear stress to map file (1: yes, 0: no)
Wrimap_chezy	1	Write the chezy roughness to map file (1: yes, 0: no)
Wrimap_turbulence	0	Write vicww, k and eps to map file (1: yes, 0: no)
Wrimap_wind	0	Write wind velocities to map file (1: yes, 0: no)
Wrimap_tidal_potential	0	Write tidal potential to map file (1: yes, 0: no)
MapOutputTimeVector		File (*.mpt) containing fixed map output times (s) w.r.t. RefDate
FullGridOutput	0	Full grid output mode (0: compact, 1: full time-varying grid data)
EulerVelocities	0	Euler velocities output (0: GLM, 1: Euler velocities)
Wrirst_bnd	1	Write waterlevel, bedlevel and coordinates of boundaries to restart files
Writepart_domain	1	Write partition domain info. for postprocessing
SedimentmodelNr	4	Sediment model nr, (0=no, 1=Krone, 2=SvR2007, 3=E-H, 4=MorphologyModule)
MorFile	Maas1D.mor	Morphology settings file (*.mor)
MorCFL	0	Use CFL condition for morphologic updating
DzbDtMax	0.1	Maximum bed level change per time step
SedFile	Maas1D.sed	Sediment characteristics file (*.sed)

Item	Value	Explanation
DredgeFile		Dredging/dumping settings file (*.dad)
TransportVelocity	0	Velocities for sediment transport, 0=Lagr bed+sus, 1=Eul bed + Lagr sus, 2=Eul bed+sus
Nr_of_sedfractions	0	Nr of sediment fractions, (specify the next parameters for each fraction)
MxgrKrone	0	Highest fraction index treated by Krone
D50		Mean Sandgrain diameter (m), e.g. 0.0001
Rhosed		Mean Sandgrain rho (kg/m3) , e.g. 2650
InitialSedimentConcentration		Initial sediment concentration (kg /m3)
Uniformerodablethickness		Uniform erodable layer thickness (m)
Numintverticaleinstein	10	Number of vertical intervals in Einstein integrals ( )
Morfac	1.	Morphological acceleration factor (), bottom updates active for morfac > 0, 1d0=realtime, etc
TMorfspinup	0.	Spin up time for morphological adaptations (s)
Alfabed	1.	Calibration par bed load, default=1d0 ( )
Alfasus	1.	Calibration par suspende load, default=1d0 ( )
Crefcav	20.	Calibration par only in jased==3, default=20d0 ( )

H.4 MOR

Item	Value	Explanation
FileCreatedBy	Roy Daggenvoorde	
FileVersion	02.00	
FileCreationDate	17-3-2020	
EpsPar	False	Only for waves in combination with k-eps
IopKCW	1	Flag for determining Rc and Rw
MorFac	1	[-] Morphological scale factor
MorStt	30	[TUnits] Spin-up interval from TStart till start of morphological changes
Thresh	1.0	[m] Threshold sed thickness for reducing sed exchange
BedUpd	True	Update bathymetry during flow run
CmpUpd	True	
EqmBc	false	Equilibrium concentration at inflow boundaries
NeglectEntrainment	True	
DensIn	false	Include effect of sediment on density gradient
AlfaBs	1	[-] Longitudinal bed gradient factor for bedload transport
AlfaBn	1	[-] Transverse bed gradient factor for bedload transport

Item	Value	Explanation
Sus	1	[-] Multipl fac for suspended sed reference concentration
Bed	1	[-] Multipl factor for bedload transport vector magnitude
SusW	1	[-] Wave-related suspended sed. transport factor
BedW	1	[-] Wave-related bedload sed. transport factor
SedThr	0.1	[m] Minimum threshold depth for sediment computations
ThetSD	1.	[-] Fraction of erosion to assign to adjacent dry cells
IHidExp	3	hiding and exposure formulation number (1 integer
BcFil	TIJDELIJK_BCM.bcm	
AShld	0.85	
BShld	0.5	
CShld	0.0	
DShld	0.0	
IUnderLyr	2	[-] Flag for underlayer concept
IniComp	morlyr.ini	
TTLForm	1	[-] Transport layer thickness formulation
ThTrLyr	1	[m] Thickness of the transport layer
MxNULyr	40	[-] Number of underlayers (excluding final well mixed layer)
ThUnLyr	0.5	[m] Thickness of each underlayer
IBedCond	4	0 no bed level constraint
IBedCond	0	0 no bed level constraint
Percentiles	10 50 90	
HidExp	true	
WithPores	true	
VelocAtZeta	true	
VelocMagAtZeta	true	
VelocZAtZeta	true	
ShearVeloc	true	
BedTranspAtFlux	true	
SuspTranspAtFlux	false	
BedTranspDueToCurrentsAtZeta	true	
BedTranspDueToCurrentsAtFlux	true	
BedTranspDueToWavesAtZeta	false	

Item	Value	Explanation
BedTranspDueToWavesAtFlux	false	
SuspTranspDueToWavesAtZeta	false	
SuspTranspDueToCurrentsAtZeta	false	
SuspTranspDueToWavesAtFlux	false	
NearBedRefConcentration	true	
EquilibriumConcentration	true	
NearBedTranspCorrAtFlux	true	
SourceSinkTerms	true	
ReferenceHeight	true	
SettlingVelocity	true	
RawTransportsAtZeta	true	
Bedslope	true	
Taurat	true	
Dm	true	
Dg	true	
Dgsd	true	
Frac	true	
MudFrac	true	
SandFrac	true	
FixFac	true	
CumNetSedimentationFlux	true	
BedLayerSedimentMass	true	
BedLayerVolumeFractions	true	
BedLayerDepth	true	
BedLayerPorosity	true	
MainChannelAveragedBedLevel	true	

H.5 SED

Item	Value	Explanation
FileCreatedBy	Roy Daggenvoorde	
FileVersion	02.00	
FileCreationDate	19-3-2020	

Item	Value	Explanation
IopSus	1	Suspended sediment size is Y/N calculated dependent on d50
Cref	1.60e+03	[kg/m3] CSoil Reference density for hindered settling
Name	SedimentSand1	Name as specified in NamC in mdf-file
SedTyp	bedload	Must be "sand", "mud" or "bedload"
SedMinDia	8.00E-05	[m] Sand only: Minimum sediment diameter
SedMaxDia	0.000125	[m] Sand only: Maximum sediment diameter
RhoSol	2.65e+003	[kg/m3] Specific density
CDryB	1.6e+003	[kg/m3] Dry bed density
IniSedThick	morlyr.ini	Initial sediment layer thickness at bed (uniform value or filename)
TraFrm	1	[-] General formula (written like Meyer-Peter Mueller)
ACal	1	Calibration coefficient
RouKs	0.000	
SusFac	0.000	
Name	SedimentSand2	Name as specified in NamC in mdf-file
SedTyp	bedload	Must be "sand", "mud" or "bedload"
SedMinDia	0.000125	[m] Sand only: Minimum sediment diameter
SedMaxDia	0.00025	[m] Sand only: Maximum sediment diameter
RhoSol	2.65e+003	[kg/m3] Specific density
CDryB	1.6e+003	[kg/m3] Dry bed density
IniSedThick	morlyr.ini	Initial sediment layer thickness at bed (uniform value or filename)
TraFrm	1	[-] General formula (written like Meyer-Peter Mueller)
ACal	1	Calibration coefficient
RouKs	0.000	
SusFac	0.000	
Name	SedimentSand3	Name as specified in NamC in mdf-file
SedTyp	bedload	Must be "sand", "mud" or "bedload"
SedMinDia	0.00025	[m] Sand only: Minimum sediment diameter
SedMaxDia	0.001	[m] Sand only: Maximum sediment diameter
RhoSol	2.65e+003	[kg/m3] Specific density
CDryB	1.6e+003	[kg/m3] Dry bed density
IniSedThick	morlyr.ini	Initial sediment layer thickness at bed (uniform value or filename)
TraFrm	1	[-] General formula (written like Meyer-Peter Mueller)

Item	Value	Explanation
ACal	1	Calibration coefficient
RouKs	0.000	
SusFac	0.000	
Name	SedimentSand4	Name as specified in NamC in mdf-file
SedTyp	bedload	Must be "sand", "mud" or "bedload"
SedMinDia	0.001	[m] Sand only: Minimum sediment diameter
SedMaxDia	0.004	[m] Sand only: Maximum sediment diameter
RhoSol	2.65e+003	[kg/m3] Specific density
CDryB	1.6e+003	[kg/m3] Dry bed density
IniSedThick	morlyr.ini	Initial sediment layer thickness at bed (uniform value or filename)
TraFrm	4	[-] General formula (written like Meyer-Peter Mueller)
ACal	8	[-] Calibration factor
PowerB	0	[-] B Power
PowerC	1.5	[-] C Power
RipFac	0.7	[-] Ripple factor
ThetaC	0.047	[-] Dimensionless critical shear stress parameter
Name	SedimentSand5	Name as specified in NamC in mdf-file
SedTyp	bedload	Must be "sand", "mud" or "bedload"
SedMinDia	0.004	[m] Sand only: Minimum sediment diameter
SedMaxDia	0.008	[m] Sand only: Maximum sediment diameter
RhoSol	2.65e+003	[kg/m3] Specific density
CDryB	1.6e+003	[kg/m3] Dry bed density
IniSedThick	morlyr.ini	Initial sediment layer thickness at bed (uniform value or filename)
TraFrm	4	[-] General formula (written like Meyer-Peter Mueller)
ACal	8	[-] Calibration factor
PowerB	0	[-] B Power
PowerC	1.5	[-] C Power
RipFac	0.7	[-] Ripple factor
ThetaC	0.047	[-] Dimensionless critical shear stress parameter
Name	SedimentSand6	Name as specified in NamC in mdf-file
SedTyp	bedload	Must be "sand", "mud" or "bedload"
SedMinDia	0.008	[m] Sand only: Minimum sediment diameter

Item	Value	Explanation
SedMaxDia	0.016	[m] Sand only: Maximum sediment diameter
RhoSol	2.65e+003	[kg/m3] Specific density
CDryB	1.6e+003	[kg/m3] Dry bed density
IniSedThick	morlyr.ini	Initial sediment layer thickness at bed (uniform value or filename)
TraFrm	4	[-] General formula (written like Meyer-Peter Mueller)
ACal	8	[-] Calibration factor
PowerB	0	[-] B Power
PowerC	1.5	[-] C Power
RipFac	0.7	[-] Ripple factor
ThetaC	0.047	[-] Dimensionless critical shear stress parameter
Name	SedimentSand7	Name as specified in NamC in mdf-file
SedTyp	bedload	Must be "sand", "mud" or "bedload"
SedMinDia	0.016	[m] Sand only: Minimum sediment diameter
SedMaxDia	0.0315	[m] Sand only: Maximum sediment diameter
RhoSol	2.65e+003	[kg/m3] Specific density
CDryB	1.6e+003	[kg/m3] Dry bed density
IniSedThick	morlyr.ini	Initial sediment layer thickness at bed (uniform value or filename)
TraFrm	4	[-] General formula (written like Meyer-Peter Mueller)
ACal	8	[-] Calibration factor
PowerB	0	[-] B Power
PowerC	1.5	[-] C Power
RipFac	0.7	[-] Ripple factor
ThetaC	0.047	[-] Dimensionless critical shear stress parameter
Name	SedimentSand8	Name as specified in NamC in mdf-file
SedTyp	bedload	Must be "sand", "mud" or "bedload"
SedMinDia	0.0315	[m] Sand only: Minimum sediment diameter
SedMaxDia	0.063	[m] Sand only: Maximum sediment diameter
RhoSol	2.65e+003	[kg/m3] Specific density
CDryB	1.6e+003	[kg/m3] Dry bed density
IniSedThick	morlyr.ini	Initial sediment layer thickness at bed (uniform value or filename)
TraFrm	4	[-] General formula (written like Meyer-Peter Mueller)
ACal	8	[-] Calibration factor

Item	Value	Explanation
PowerB	0	[-] B Power
PowerC	1.5	[-] C Power
RipFac	0.7	[-] Ripple factor
ThetaC	0.047	[-] Dimensionless critical shear stress parameter
Name	SedimentSand9	Name as specified in NamC in mdf-file
SedTyp	bedload	Must be "sand", "mud" or "bedload"
SedMinDia	0.063	[m] Sand only: Minimum sediment diameter
SedMaxDia	0.1	[m] Sand only: Maximum sediment diameter
RhoSol	2.65e+003	[kg/m3] Specific density
CDryB	1.6e+003	[kg/m3] Dry bed density
IniSedThick	morlyr.ini	Initial sediment layer thickness at bed (uniform value or filename)
TraFrm	4	[-] General formula (written like Meyer-Peter Mueller)
ACal	8	[-] Calibration factor
PowerB	0	[-] B Power
PowerC	1.5	[-] C Power
RipFac	0.7	[-] Ripple factor
ThetaC	0.047	[-] Dimensionless critical shear stress parameter
Name	SedimentSand10	Name as specified in NamC in mdf-file
SedTyp	bedload	Must be "sand", "mud" or "bedload"
SedMinDia	0.1	[m] Sand only: Minimum sediment diameter
SedMaxDia	0.2	[m] Sand only: Maximum sediment diameter
RhoSol	2.65e+003	[kg/m3] Specific density
CDryB	1.6e+003	[kg/m3] Dry bed density
IniSedThick	morlyr.ini	Initial sediment layer thickness at bed (uniform value or filename)
TraFrm	4	[-] General formula (written like Meyer-Peter Mueller)
ACal	8	[-] Calibration factor
PowerB	0	[-] B Power
PowerC	1.5	[-] C Power
RipFac	0.7	[-] Ripple factor
ThetaC	0.047	[-] Dimensionless critical shear stress parameter

Deltares is an independent institute for applied research in the field of water and subsurface. Throughout the world, we work on smart solutions for people, environment and society.

Deltares

www.deltares.nl